



Annual Report 2012
Jahresbericht

Physikalisch-Meteorologisches Observatorium Davos und Weltstrahlungszentrum

Mission

Das PMOD/WRC

- dient als internationales Kalibrierzentrum für meteorologische Strahlungsmessinstrumente
- entwickelt Strahlungsmessinstrumente für den Einsatz am Boden und im Weltraum
- erforscht den Einfluss der Sonnenstrahlung auf das Erdklima.

Auftragerteilung

Das Physikalisch-Meteorologische Observatorium Davos (PMOD) beschäftigt sich seit seiner Gründung im Jahr 1907 mit Fragen des Einflusses der Sonnenstrahlung auf das Erdklima. Das Observatorium schloss sich 1926 dem Schweizerischen Forschungsinstitut für Hochgebirgsklima und Medizin Davos an und ist seither eine Abteilung dieser Stiftung. Auf Ersuchen der Weltmeteorologischen Organisation (WMO) beschloss der Bundesrat im Jahr 1970 die Finanzierung eines Kalibrierzentrums für Strahlungsmessung als Beitrag der Schweiz zum Weltwetterwacht-Programm der WMO. Nach diesem Beschluss wurde das PMOD beauftragt, das Weltstrahlungszentrum (World Radiation Center, WRC) zu errichten und zu betreiben.

Kerntätigkeiten

Das Weltstrahlungszentrum unterhält das Primärnormal für solare Bestrahlungsstärke bestehend aus einer Gruppe von hochpräzisen Absolut-Radiometern. Auf weitere Anfragen der WMO wurden 2004 das Kalibrierzentrum für Messinstrumente der atmosphärischen Langwellenstrahlung eingerichtet und 2008 das Kalibrierzentrum für spektrale Strahlungsmessungen zur Bestimmung der atmosphärischen Trübung. Seit 2007 wird auch das Europäische UV Kalibrierzentrum durch das Weltstrahlungszentrum betrieben. Das Weltstrahlungszentrum besteht heute aus vier Sektionen:

- Solare Radiometrie
- Infrarot Radiometrie
- Atmosphärische Trübungsmessungen (WORCC)
- Europäisches UV Kalibrierzentrum.

Die Kalibriertätigkeit ist in ein international anerkanntes Qualitätssystem eingebettet (ISO 17025) um eine zuverlässige und nachvollziehbare Einhaltung des Qualitätsstandards zu gewährleisten.

Das PMOD/WRC entwickelt und baut Radiometer, die zu den weltweit genauesten ihrer Art gehören und sowohl am Boden als auch im Weltraum eingesetzt werden. Diese Instrumente werden auch zum Kauf angeboten und kommen seit langem bei Meteorologischen Diensten weltweit zum Einsatz. Ein globales Netzwerk von Stationen zur Überwachung der atmosphärischen Trübung ist mit vom Institut entwickelten Präzisionsfilterradiometern ausgerüstet.

Im Weltraum und mittels Bodenmessungen gewonnene Daten werden in Forschungsprojekten zum Klimawandel und der Sonnenphysik analysiert. Diese Forschungstätigkeit ist in nationale, insbesondere mit der ETH Zürich, und internationale Zusammenarbeit eingebunden.

Table of Contents

3	Jahresbericht 2012
6	Introduction
7	Operational Services
7	Quality Management System and Instrument Sales
8	Calibration Services
9	Solar Radiometry Section (SRS/WRC)
10	Infrared Radiometry Section (WRC-IRS)
11	Atmospheric Turbidity Section (WRC-WORCC)
12	European Ultraviolet Calibration Center (EUVC)
13	Instrument Development
13	Spectroradiometer for Spectral Aerosol Optical Depth and Solar Irradiance Measurements
14	CSAR and MITRA
16	Heliostat
18	A World Radiometric Reference (WRR) to SI radiant power scale comparison with DARA
19	Space Experiments
21	Scientific Research Activities
21	Overview
22	Future and Past Solar Influence on the Terrestrial Climate (FUPSOL)
23	Further Development of the Chemistry-Climate Model SOCOL
24	Modulation of the Middle Atmospheric Response to Solar Irradiance Changes by Internal Variability
25	The Role of SSI Variability in the Evolution of the Middle Atmosphere during 2004–2009
26	Solar Variability and Climate Change during the First Half of the 20 th Century (SOVAC)
27	Evaluation of the Stratospheric Climate Change during the Dalton Minimum with AOCCM SOCOL-MPIOM
28	Development of the Sulfate Aerosol Module for the CCM SOCOL
29	Assessment of the Lifetime of Halogen Source Gases
30	Influence of a Carrington-Like Event on Atmospheric Chemistry, Temperature and Climate
31	Stratospheric Circulation under the Montreal Protocol Restrictions
32	Ground-Based Aerosol Optical Depth Time-Series at Three Swiss Sites
33	Spectral Aerosol Optical Depth from a Precision Spectroradiometer
34	Global Dimming and Brightening Trends at Davos
35	Development of a New High Resolution Extraterrestrial Spectrum
36	UV Measurements at Mountain Sites
37	Determination of Fractional Cloud Cover and Cloud Type Using Sky Cameras
38	Correlation of Spectral with Total Solar Irradiance on VIRGO
39	Spectral Solar Irradiance as Observed by PREMOS/PICARD
40	The PREMOS/PICARD Total Solar Irradiance (TSI) Time-Series
41	Modeling of the Spectral Solar Irradiance
42	Modeling of Variations in the EUV Spectral Irradiance
43	Physical Understanding of the Solar Irradiance at Radio Wavelengths
44	Modeling the Variability of Sun-Like Stars
45	Comparison of Stellar and Solar Variabilities
46	FP7 Space Project SOLID – First European Comprehensive SOLar Irradiance Data Exploitation
47	Publications
47	Refereed Publications
49	Other Publications
50	Administration
50	Personnel Department
52	Meeting Organisation
52	Public Seminars
53	Course of Lectures, Participation in Commissions
54	Modernization and Renovation of the PMOD/WRC Institute Building
55	PMOD/WRC Open Day Event
56	Bilanz 2012 inklusive Drittmittel
56	Erfolgsrechnung 2012 inklusive Drittmittel
58	Abbreviations

Jahresbericht 2012

Werner Schmutz

Dienstleistungsbetrieb Weltstrahlungszentrum

Die Anzahl Kalibrieraufträge nahm seit Jahren stetig zu. Im Berichtsjahr ist dieser Trend zum ersten Mal gebrochen worden und die Zahl der kalibrierten Instrumente ist gegenüber dem Vorjahr leicht zurückgegangen. Es bleibt die künftigen Jahre abzuwarten, um entscheiden zu können, ob dies nun eine Plafonierung der Kalibriertätigkeit bedeutet oder ob es sich nur um eine temporäre Fluktuation handelt. Die Unterscheidung der zwei Möglichkeiten ist für das Institut sehr wohl bedeutsam. Während eine stetig anwachsende Kalibriertätigkeit die Möglichkeiten des Weltstrahlungszentrums bald belasten und überfordern würde, wäre eine Stabilisierung der Kalibriertätigkeit passend für das Institut mit seiner derzeitigen Finanzierung und der neu renovierten Infrastruktur. Die Entwicklung muss verfolgt werden und unter Umständen braucht es eine entsprechende Anpassung der Grundfinanzierung für die Periode 2016–2019. Erfreulich ist, dass das Ultraviolett Kalibrierzentrum entgegen dem Gesamttrend wesentlich an Aufträgen zulegen konnte. Dies ist auf den Übergang eines Europäischen UV Zentrums auf ein Welt UV Zentrum zurückzuführen und zeigt, dass das Zentrum einem Bedürfnis entsprach. Die offizielle Ernennung der UV Sektion zum Weltkalibrierzentrum – World Ultraviolett Calibration Center – erfolgte zu Beginn des laufenden Jahres und somit ist nun das WUVCC die vierte Sektion des Weltstrahlungszentrums.

Parallel zu den Dienstleistungen als Weltstrahlungszentrum der Meteorologischen Weltorganisation ist das PMOD/WRC auch Unterzeichner der gegenseitigen Anerkennungs-Abkommen der Meterkonvention des Internationalen Büros für Mass und Gewicht. Von den verschiedenen Komitees des Büros ist das Konsultative Komitee für Photometrie und Radiometrie das für das PMOD/WRC mit seiner Aufgabe als Weltstrahlungszentrum relevante Gremium. Bisher konnte das Observatorium als designierte Organisation des Eidgenössischen Instituts für Metrologie an den Tagungen dieses Komitees teilnehmen. Zusätzlich zu dieser Möglichkeit ist nun das Observatorium Davos vom Internationalen Komitee für Mass und Gewicht als volles Komitee-Mitglied aufgenommen worden. Dieser neue Status wird es dem Institut erlauben, für seine anerkannten Messgrössen Vergleiche mit anderen Kalibrierlabors zu organisieren. Dies ist wichtig, da die Einhaltung der ISO Normen den Nachweis verlangt, dass die deklarierten Messgenauigkeiten in der Praxis auch erreicht werden.

Entwicklung und Bau von Experimenten

Die im Observatorium gebauten Weltraumexperimente sind das Aushängeschild der Forschungsaktivität des Institutes. Die relativ neuen aktiven Experimente LYRA/PROBA2 und PREMOS/PICARD, die 2009 bzw. 2010 gestartet wurden, sowie das langjährige VIRGO/SOHO, das seit 1996 die Sonneneinstrahlung misst, laufen alle bestens. Leider hat die Französische Weltraumagentur CNES beschlossen, den Satelliten PICARD im Verlauf von 2013 auszuschalten. Zugleich

wird auch erwartet, dass der Amerikanische Satellit SORCE wegen Batterieproblemen seine Messungen einstellen muss. Da SORCE wie PICARD Experimente zur Überwachung der solaren Einstrahlung enthält, kann davon ausgegangen werden, dass bald die zwei wichtigsten Systeme zur Überwachung einer für das Erdklima zentralen Grösse, der Totalen einfallenden Einstrahlung, fehlen werden. Es ist daher dringend erforderlich, dass Nachfolgemissionen geplant und realisiert werden, damit die Messreihe nicht abbricht. In diesem Zusammenhang ist es daher sehr erfreulich, dass in direkter Zusammenarbeit mit Norwegen ein PMOD/WRC Radiometer-Experiment auf dem Norwegischen NORSAT-1 realisiert werden kann. Das Davoser Experiment CLARA wird ein äusserst willkommener Beitrag zu den weltweiten Bemühungen zur Überwachung eines der wichtigsten natürlichen Klimaeinflüsse sein.

Zur Charakterisierung von Strahlungsmessinstrumenten ist es vorteilhaft einen Heliostat zur Verfügung zu haben, der es erlaubt Sonnenlicht ins Labor zu bringen. Die Planung und Vorbereitungen des neuen Heliostaten für das Observatorium machten 2012 wesentliche Fortschritte und dieser wird nun dieses Jahr installiert werden. Die Charakterisierung von CLARA für NORSAT-1 wird zu den ersten Aufgaben gehören, die mit der neu erstellten Einrichtung angegangen werden.

Die wichtigste Institutsaktivität bezüglich bodengebundener Instrumentierung ist die Entwicklung eines robusten Spektroradiometers. Das Ziel ist ein Instrument, das auch unter ändernden Umwelteinflüssen im Freien stabile Messwerte liefert. Ein Prototyp des neuen Instrumentes ist entwickelt worden und die ersten Tests, über die in diesem Jahresbericht berichtet wird, sehen sehr vielversprechend aus. Wenn auch der Bau einer ersten Kleinserie erfolgreich gelingt, und das neue Instrument genügend kostengünstig angeboten werden kann, könnte dieses Instrument eventuell die Filterradiometer ersetzen, die sich im vergangenen Jahrzehnt recht gut verkaufen liessen.

Klimaforschung

Das Rückgrat der Klimaforschung am PMOD/WRC ist das FUPSOL Projekt (Future and Past Solar Influence on the Terrestrial Climate). Diese Zusammenarbeit mit vier weiteren Schweizer Instituten im Rahmen eines SINERGIA Programms des Schweizerischen Nationalfonds geht nun in die letzte Phase seiner dreijährigen Laufzeit. Viele weitere Projekte hängen direkt oder indirekt mit dem Ziel zusammen, die natürlichen Klimaeinflüsse der letzten 500 Jahre zu verstehen, um daraus den zukünftigen Anteil eines natürlichen Einflusses auf die kommende Erderwärmung abzuschätzen. Es ist dabei nicht nur die variable Sonneneinstrahlung relevant, sondern auch die Effekte der Teilchen die von der Sonne kommen. Besonders auf kürzeren Zeitskalen als diejenigen von Klimaänderungen, was heutzutage als Weltraumwetter bezeichnet wird, kann ein sogenannter Sturm von solaren Protonen bemerkenswerte Auswirkungen

haben. Würde die Erde von einem ähnlich grossen Ereignis wie 1859 dem berühmten «Carrington-Ereignis» betroffen, dann könnte das Chemiegleichgewicht in unserer Atmosphäre mit entsprechenden Auswirkungen auf Wetter und Satellitendienste für mehrere Monate verändert werden.

Die wissenschaftliche Literatur beschreibt, dass es im letzten Jahrhundert längere Phasen gab während denen weniger Sonnenstrahlung die Erdoberfläche erreichte. Die Phasen mit abnehmender Einstrahlung werden Globale Verdunkelung und die Phasen mit zunehmender Helligkeit Globale Aufhellung genannt. Eine Doktorarbeit am PMOD/WRC untersuchte, ob Strahlungswerte, die in den letzten 100 Jahren in Davos gemessen wurden, helfen könnten, die Ursachen für diese Änderungen zu ergründen. Man fand, dass die Trübung der Atmosphäre über Davos nicht stark änderte. Zugleich zeigen aber die in Davos gemessenen globalen Strahlungswerte die beschriebenen Schwankungen. Es müssen daher andere Faktoren als eine Trübung der Atmosphäre für die Einstrahlungsschwankungen verantwortlich sein, wie möglicherweise die Art oder Häufigkeit der Bewölkung. Immerhin, eine geringe Zunahme der Einstrahlung seit den 1990ern könnte mit einer klareren Atmosphäre erklärbar sein.

Die Resultate der Untersuchungen der Langzeitreihe werden durch die direkten Messungen der atmosphärischen Trübung mit Sonnenphotometern bestätigt. Trübungsmessungen sind in Davos seit den 1990er Jahren verfügbar und diese immer noch relativ kurze Datenreihe zeigt keine offensichtlich signifikanten Trends. Eine geringe Abnahme der Trübung, wie oben diskutiert, liegt aber innerhalb der Unsicherheiten der Trendanalysen.

Ein Institutsprojekt, das durch einen Schweizer Beitrag zum Global Atmosphere Watch Programm der Meteorologischen Weltorganisation finanziert wird, fokussiert auf die Erfassung von Wolken und möchte deren Einfluss auf das terrestrische Energiegleichgewicht quantifizieren. Die direkten Ziele des Projekts sind die automatische Erfassung des Wolkenanteils und eine Klassifizierung der Wolkentypen, basierend auf hemisphärischen Himmelsbildern, die von automatisierten Kameras geliefert werden. Im Rahmen einer erfolgreich abgeschlossenen Dissertation waren automatische Auswertungen schon sehr erfolgsversprechend. Obwohl für ein vollkommen automatisches System noch substantielle weitere Entwicklungsarbeit und Praxistests benötigt werden, scheint immerhin die prinzipielle Machbarkeit eines automatischen Wolkenbestimmungssystems nachgewiesen.

Sonnenphysik

Es ist nach wie vor eine von den Fachleuten umstrittene offene Frage, ob die Variationen der Totalen und Spektralen solaren Einstrahlung gross genug sind, um das Erdklima wesentlich beeinflussen zu können. In einer wichtigen Arbeit haben Haigh

und ihre Mitautoren 2010 gezeigt, dass wenn die spektralen Variationen so verlaufen, wie es vom Wissenschaftler Team um das SIM/SORCE Experiment propagiert wurde, dies dann einen messbaren Einfluss auf das Erdklima zur Folge haben würde. Die Besonderheiten der SIM/SORCE Variationen sind, dass diese im UV wesentlich grösser wären als früher angenommen und im visuellen Spektralbereich durch Variationen in anti-phase zur solaren Aktivität kompensiert werden. Wir haben nun die 17-jährige Datenreihen der Filterradiometer des PMOD/WRC Experiments VIRGO/SOHO analysiert, um die SIM/SORCE Ergebnisse zu überprüfen. Basierend auf elf Jahre Daten von 2002–2012 konnten wir zeigen, dass der grüne Kanal bei 500 nm in Phase mit der solaren Aktivität variiert, was im Widerspruch zu den SIM/SORCE Resultaten steht.

Die Quantifizierung der Variationen der Spektralen solaren Einstrahlung ist eine extrem wichtige Herausforderung für die weltweite Wissenschaftler Gemeinschaft. Dieser Aufgabe stellt sich das Konsortium des SOLID Projekts – First European SOLar Irradiance Data. Das erste Ziel des FP7 Projektes ist die kritische Inventarisierung aller existierenden Messungen der solaren Einstrahlung, inklusive einer Beurteilung der Messunsicherheiten. Der zweite ebenso ambitionöse Schritt ist die Absicht, bestehende Lücken sowohl in Zeit als auch Wellenlängen-Bereich mit Hilfe von Modellrechnungen zu füllen. SOLID wurde von PMOD/WRC Wissenschaftlern initiiert und das letzten Dezember gestartete Projekt wird vom Observatorium geleitet.

Personelles

Gegen Ende Jahr verliessen zwei langjährige Mitarbeiterinnen das Observatorium. Frau Sonja Degli Esposti, Leiterin der Administration, und die Institutssekretärin Stephanie Ebert zogen in die Nähe von Zürich. Ihr fast gleichzeitiger Weggang lässt eine Administration zurück, die ohne ihre langjährige Erfahrung auskommen muss. Niemand ist unersetzlich aber ohne Zweifel waren die meisten Sachen wesentlich einfacher mit der Unterstützung eines erfahrenen und eingespielten Teams. Frau Sandra Kissling, die neue Leiterin der Administration, begann im Dezember und sie wird seit Jahresbeginn von der Sekretärin Frau Seraina Egartner unterstützt. Wir sind sehr froh, dass die beiden neuen engagierten Kräfte zu uns gestossen sind und wir wünschen ihnen eine interessante und erfüllte Arbeit an unserem Institut.

Infrastruktur

Das Jahr 2012 brachte einschneidende Änderungen: Am 17. August, nach eineinhalb Jahren in den Provisorien, konnten alle wieder zurück ins Alte Schulhaus ziehen. Es ist ein gutes Gefühl wieder im angestammten Institutsgebäude zu sein. Aber noch wichtiger ist, dass die Zeit der räumlichen Trennung der Departemente vorbei war und wieder alle unter einem Dach vereint arbeiten können. Die Einweihung des neuen Seminarraums fand am 26. Oktober 2012 mit einer Aufführung

der Kabarettistin Michaela Maria Drux statt. Am folgenden Tag, Samstag 27. Oktober 2012 öffneten wir das ganze Institut für die Davoser Öffentlichkeit, die wir zu einem Tag der offenen Tür eingeladen hatten. Die Gäste kamen in Scharen und sie waren vom modernisierten Gebäude und den neuen technischen Einrichtungen beeindruckt. Gleichzeitig kann man auch dem Architekten gratulieren, der das Ambiente des ehemaligen Schulhauses trotz der Renovation zu bewahren wusste.

Dank

Allen Personen die zur geglückten Renovation des Institutes beitrugen und denjenigen, die den Betrieb auch unter erschwerten Bedingungen aufrecht hielten, möchte ich ganz herzlich meinen Dank aussprechen. Sehr viele haben dazu beigetragen, dass wir nun eine optimale Infrastruktur in einem attraktiven Gebäude zur Verfügung haben. All das wäre ohne die verschiedensten Unterstützungen und Hilfen nicht möglich gewesen. Der Umbau

des Alten Schulhauses hat eine stattliche Summe gekostet und wir sind dem Bund zu grossem Dank verpflichtet, dass er diese Investition in die Zukunft des Weltstrahlungszentrums möglich gemacht hat. Ich danke dem Bund, dem Kanton und der Gemeinde Davos für ihre sehr positive Haltung gegenüber dem Observatorium Davos.

Den Mitgliedern des Ausschusses des Stiftungsrates und den Mitgliedern der Aufsichtskommission des Weltstrahlungszentrums verdanke ich herzlich ihre stete Unterstützung und Begleitung der Anliegen des PMOD/WRC. Dieses Mal möchte ich einen ganz speziellen Dank dem abtretenden Präsidenten der Aufsichtskommission, Herr Gerhard Müller, aussprechen. Ohne seine vielfache Unterstützung im Hintergrund und manchem direkten Eingreifen bei Verhandlungen wären die nach aussen sichtbaren Leistungen des Observatoriums nicht möglich gewesen.

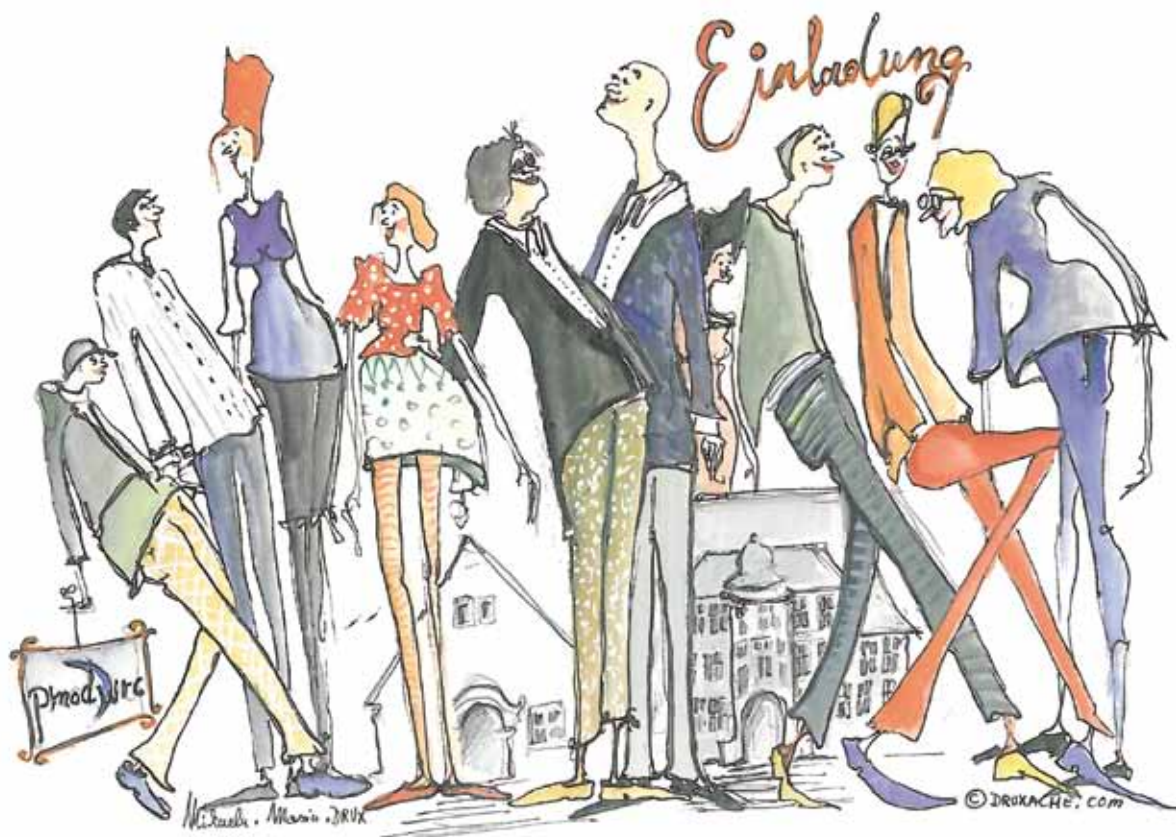


Bild 1. Einladung zur Einweihung des neuen Seminarraums am 26. Oktober 2012. Gezeichnet von Michaela Maria Drux, 2012, Wasserfarben auf Papier, 29.7 cm x 21 cm.

Werner Schmutz

The year 2012 brought several profound changes. After one and a half years, on August 17, 2012, there was the move from the provisional accommodation back to the 'old school house', the fully renovated PMOD/WRC building. It felt good to be back in our original home but more importantly, it brought back all departments under one roof. We inaugurated our new seminar room with a performance by a cabaret artist, Michaela Maria Drux, on October 26, 2012. On the following day we invited the public to an Open-Day event. People came in large numbers and all were impressed at how well the building had been modernized but at the same time that the architect had managed to retain the buildings ambience with a touch of the former schoolhouse.

An important occurrence towards the end of last year was the departure of two long time staff members. Sonja Degli Esposti, head of administration and human resources, and the institute secretary, Stephanie Ebert, moved on to live close to Zürich. Their almost simultaneous departure left the administrative department without their vast long-term experience. Nobody is irreplaceable but many things were definitely much easier with their comprehensive support and know-how. The new head of administration, Sandra Kissling, started in December and Seraina Egartner, the new secretary, began working at the beginning of the year. We are glad that they joined us and we wish them an interesting and fulfilling time at our institute.

In contrast to previous years, the demand for calibration services offered by the World Radiation sections did not increase but slightly decreased for the first time. We will have to see whether this reflects an end of the trend in the last years or whether it is just a temporary effect. The outcome of either scenario has important implications for the institute. On the one hand, a further increasing trend will soon strain and overburden the PMOD/WRC. On the other hand, a stabilization of the calibration demand would allow us to cope with the operational services given the current funding and renovated facilities. The development needs to be assessed in the coming years and the funding requests for the next funding period 2016–2019 will have to be adjusted accordingly. A closer analysis of each operational service shows that despite the declining overall trend, the calibration demands of the Ultraviolet center have increased significantly. This reflects the UV center changing from a European to a World UV Calibration Center (WUVCC), as newly mandated by the World Meteorological Organization. The WUVCC is now the fourth section of the World Radiation Center since the beginning of this year.

In parallel to the activities as a calibration laboratory for the World Meteorological Organization, the PMOD/WRC is also a signatory of the mutual recognition agreement of the International Committee for Weights and Measures. As an additional step in the recognition of the PMOD/WRC, the institute was admitted as a full member of the Consultative Committee for Photometry and Radiometry in 2012. This new status allows the institute to organize comparisons in its recognized calibration and measurement capabilities.

The space experiments built in-house are at the center of the institute's research. The two relatively recent LYRA/PROBA2 and PREMOS/PICARD experiments, launched in 2009 and 2010, respectively, as well as the long-term VIRGO/SOHO experiment, which was launched in 1996, are all performing very well. Unfortunately, the French space agency CNES decided to switch off PICARD during the course of 2013. It is also expected that during the current year the American SORCE satellite will cease operation because of problems with its batteries. As SORCE comprises experiments observing the solar irradiance, as well as PREMOS/PICARD, it is anticipated that two experiments monitoring the Total Solar Irradiance (TSI) will soon be lost. A follow-on mission to measure TSI therefore becomes urgent. At the time of writing it appears very promising that a PMOD/WRC experiment named CLARA will fly on bilateral terms on the Norwegian NORSAT-1 satellite. This would be a welcome contribution to the worldwide efforts to ensure the continuity and stability to monitor one of the key natural parameters that influences the terrestrial climate.

In order to characterize instruments it is important to have a facility that brings sunlight into the optical laboratory. A crucial upgrade has been the development of the heliostat during last year, which is now under construction. One of the first tasks with the new facility will be to characterize instruments for the new space CLARA experiment on NORSAT-1.

Regarding the institute's commercial activities, the development of a robust outdoor spectroradiometer is an important investment in the future. The prototype has been developed and built, and first tests as reported in this annual report look very promising. Given successful completion of the development phase the instrument could eventually replace the Precision Filter Radiometer, which has sold well in the past years.



Figure 1. Conversation during the inauguration of the seminar room on 26 October 2012, as seen by the artist Michaela Maria Drux, watercolor, 29.7 cm x 21 cm.

Quality Management System

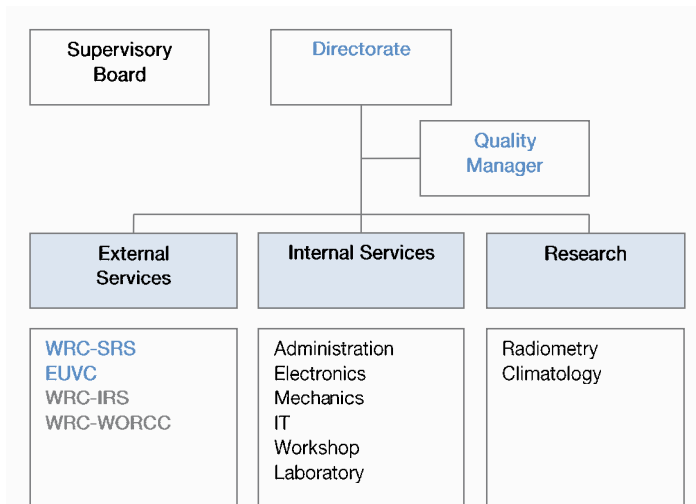


Figure 1. Organizational chart of the PMOD/WRC Quality Management System. The WRC Solar Radiometry Section and the EUVC section perform calibrations according to the EN ISO/IEC standard 17025.

PMOD/WRC QMS

Since 2006 the PMOD/WRC has maintained an approved Quality Management System (QMS, see Fig. 1) based on the general requirements for the competence of testing and calibration laboratories (EN ISO/IEC 17025).

The QMS covers the WRC-SRS and the EUVC Sections.

During 2012 the preparation for the re-evaluation of the QMS was done. The re-evaluation will be at the EURAMET TC-Q Meeting in March 2013.

Quality Management System Activities

Two calibration and measurement capabilities (CMC) are listed in the database of the 'Bureau International des poids et mesures' (BIPM): Responsivity, direct and global solar irradiation. The CMC 'Responsivity, global solar irradiance weighted (UV (280–400 nm), UVB (280–315 nm), UVA (315–400 nm), Erythema CIE)' was submitted to the inter-RMO in 2010 and is in the review process.

Instrument Sales

In 2012, we sold three PMO6-cc absolute radiometers (1 Mexico, 1 Japan and 1 Spain). One single Precision Filter Radiometer (PFR) was sold to Estonia.

This is a remarkable decrease compared to the previous years, as illustrated in Fig. 2.

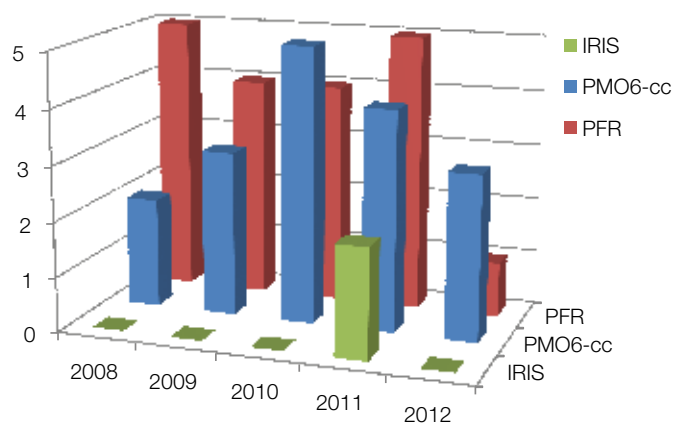


Figure 2. Instrument Sale Statistic 2008–2012.

Calibration Services

Manfred Gyo, Wolfgang Finsterle, Julian Gröbner, and Christoph Wehrli

During the whole calibration season of 2012, the laboratories were in temporary buildings. All laboratories moved back into the institute building towards the end of Autumn 2012. A big thank you to the calibration team is in order who kept up the same quality of work during this difficult period. All are happy with the new infrastructure and their place of work.

In 2012, we saw an overall decrease in the number of calibrations to 203 see Fig. 1. One reason might be that when a customer implements his own calibration facility, only a reference instrument is sent to PMOD/WRC.

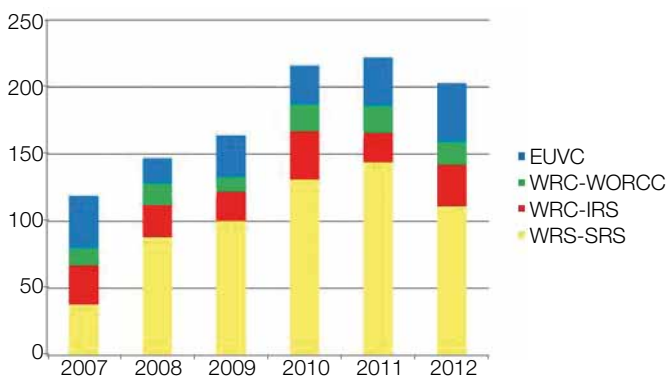


Figure 1. Statistics of instrument calibrations at PMOD/WRC 2007–2012.

Solar Radiometry Section (WRC-SRS)

The biggest decrease in the number of calibrations occurred in the SRS section which was down from 144 in 2011 to 111 in 2012.

Infrared Radiometry Section (WRC-IRS)

The WRC-IRS Section saw an increase in the number of calibrations from 22 in 2011 to 31 in 2012. Twenty nine pyrgeometer and 2 IRIS radiometers were calibrated. The new roof platform is seen in Fig. 2.

Atmospheric Turbidity Section (WRC-WORCC)

The World Optical depth Research and Calibration Center calibrated 17 filter radiometers against the WORCC Triad standard. This is less than in 2011.

European Ultraviolet Calibration Center (EUVC)

The Ultraviolet Calibration Center of the PMOD/WRC calibrated 4 spectroradiometers at their respective field sites using the QASUME traveling reference spectroradiometer. Seventeen UVB, 3 UVA, 2 UV-Global and 2 dual channel (UVA/UVB) broadband radiometers, one UV dosimeter and 2 pyranometers were calibrated at PMOD/WRC. The QASUME irradiance scale was transferred to 9 standard lamps at two European and one Canadian Institutes.

In July 2012, 9 Brewer spectrophotometers were calibrated relative to the QASUME spectroradiometer during the 7th RBCC-E campaign at Arosa, Switzerland.



Figure 2. New Roof Platform for WRC-IRS.

Solar Radiometry Section (SRS/WRC)

Wolfgang Finsterle

The Solar Radiometry Section of the WRC (SRS/WRC) is responsible for maintaining and disseminating the World Radiometric Reference (WRR). The WRR is the primary reference for short-wave solar irradiance measurements world-wide. In 2012, the SRS/WRC participated in three regional, sub-regional, and national pyrheliometer comparisons with three transfer standards. Apart from validating the traceability of solar irradiance measurements world-wide, such inter-laboratory comparisons of standards also serve a key role in maintaining the WRR's status as a primary reference according to the ISO 17025 quality management system. Other milestones include the publication of results from the fourth WRR to SI radiometric scale comparison, and the relocation of the World Standard Group (WSG) back to its original site after the completion of renovation work at PMOD/WRC.

Pyrheliometer comparison campaigns

The year 2012 was quite busy for the SRS/WRC staff with three pyrheliometer comparisons. The Japanese Regional Radiation Center of WMO Regional Association II (RRC RA-II) and the National Radiation Center (NRC), USA, again organized Regional and National Pyrheliometer Comparisons (RPC and NPC), respectively (Figure 1). While the NPC are held annually, the RPC of RA-II are organized every five years after the International Pyrheliometer Comparisons (IPC) in order to disseminate the IPC results within Asian countries. In addition to these well-established events, the Swedish RRC has for the first time organized the sub-regional Baltic Region Pyrheliometer Comparison (BRPC). Apart from the pyrheliometer comparison, the BRPC also incorporated a comparison of pyranometers, including the determination of thermal offsets by a capping-and-extrapolating method developed at the Swedish Meteorological and Hydrological Institute (SMHI). The results from the latter are particularly interesting because they show substantial differences between different types of pyranometers and heating/ventilation units.

All three comparisons ensured the WRR traceability of solar irradiance measurements in the participating countries and confirmed the stability of the WRR. Experience was shared between experts during seminar presentations and discussions. This building and sharing of knowledge during instrument comparison campaigns is a huge added value (as opposed to calibration orders). Such inter-laboratory comparisons are also mandated by the ISO 17025 quality management system for calibration and testing laboratories.



Figure 1. Participants get ready for another chilly day on the slopes of Japan's Mt. Tsukuba during the 3rd Regional Pyrheliometer Comparison (RPC-III) of the WMO Regional Association II (RA-II).

The WRR and SI radiometric scales

The WRR was originally established in 1977 based on the average reading of 15 absolute cavity Electrical Substitution Radiometers (ESR). Since then the WRR scale is maintained by the WSG. The uncertainty of the WRR with respect to the SI scale (W/m^2) was estimated at 0.3%. The cryogenic radiometers developed in the 1980s allowed radiant power to be measured with a much higher accuracy than with ambient temperature ESRs. However, until recently cryogenic radiometers were not technically suitable for solar irradiance measurements. The WSG instruments (and thus the WRR scale) could only be indirectly compared to the SI scale as established by cryogenic radiometers. Such comparisons were conducted in 1990, 1995, and 2005 and have shown no significant differences between both scales, however with relatively large uncertainties. With the construction of the Cryogenic Solar Absolute Radiometer (CSAR) and the commissioning of dedicated laboratory facilities such as the TSI Radiometer Facility (TRF) at the University of Colorado in Boulder, USA., the uncertainty levels of WRR-to-SI scale comparisons as well as the diagnostic capabilities have improved to the point where a significant difference in both scales can be detected. According to Fehlmann et al. 2012, solar irradiance measurements yield a 0.34% (± 0.18) higher value on the WRR scale than on the SI scale.

Relocation of the WSG

After renovation of the PMOD/WRC building was finished, the WSG was moved from its temporary location to its original site on the solar tracking platform. On this occasion the data acquisition system DAQ10, which began operation during IPC 2010, was finally commissioned for calibration under ISO 17025. It was not feasible to use the DAQ10 at the temporary WSG location in the container buildings because of logistical difficulties. The efforts to adapt and re-validate the DAQ10 for operation with the temporary solar tracker would have been prohibitive.

References: Fehlmann A., Kopp G., Schmutz W., Winkler R., Finsterle W., Fox N.: 2012, *Metrologia* 49, S34–S38.

Infrared Radiometry Section (WRC-IRS)

Julian Gröbner, Stephan Nyeki, and Stefan Wacker

The Infrared Radiometry Section of the WRC maintains and operates the World Infrared Standard Group of Pyrometers (WISG) which represents the world-wide reference for atmospheric long-wave irradiance measurements.

The new measurement platform on the PMOD/WRC roof was inaugurated in September 2012 with the installation of the whole infrared infrastructure from its temporary location on the containers. Access to and operation of the radiometers has therefore been significantly improved as shown in the figure on page 12 (EUVC section).

A comprehensive report describing the calibration procedure of pyrometers as performed at the PMOD/WRC was reviewed by experts in the community and can be found at ftp://ftp.pmodwrc.ch/pub/julian/Pyrometer_calibrationsV3.pdf. This document describes the calibration process, the selection process of the measurement data based on ancillary data and the retrieval of the calibration factor with the respective uncertainty. The most noteworthy feature is the use of the integrated atmospheric water vapour (IWV) as a criterion for the data selection: Measurements during previous years have in fact shown significant discrepancies between some pyrometers, the IRIS Radiometers (see below) and the WISG when calibrated during the winter or summer seasons at Davos. In order to homogenise calibrations until the observed discrepancies are understood in detail, it was decided to limit outdoor calibrations to the March to November period, when IWV is larger than about 10 mm and these discrepancies are not apparent.

The Infrared Integrating Sphere Radiometer IRIS

Measurements from more than 180 clear nights since January 2010 were compared to the WISG. As shown in Figure 1, the average WISG difference to the IRIS radiometers shows a clear dependence on IWV. Indeed, changes in the spectrum are suspected of being responsible for observed differences between various types of pyrometers. These findings were presented at the most recent International Radiation Symposium, held in Berlin in July 2012 and were published in the IRS proceedings (<http://proceedings.aip.org>). Furthermore, differences between the WISG and IRIS Radiometers for IWV contents larger than 10 mm show a clear offset of approximately -4 W/m^2 , the WISG reading lower. At IWV below 10 mm, the measurements of the WISG increase with respect to the wet conditions by about 0.45 W/m^2 per mm IWV. This leads to a seasonal variation between the WISG and the IRIS radiometers between winter and summer of about 4 W/m^2 .

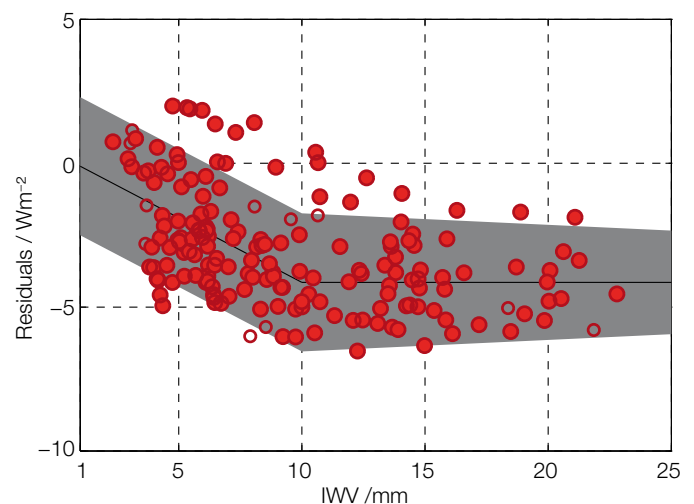


Figure 1. Residual average night differences from 182 clear nights between the mean of the WISG and the two IRIS Radiometers since 2010 (WISG-IRIS). The shaded area represents the estimated IRIS uncertainty.

Additional studies, including a direct comparison between IRIS radiometers and the absolute cavity pyrometer developed by NREL, are scheduled for Fall 2013 to confirm these observations.

Atmospheric Turbidity Section (WRC-WORCC)

Christoph Wehrl, Stephan Nyeki, and Natalia Kouremeti

The Atmospheric Turbidity Section of WRC maintains a standard group of 3 Precision Filter Radiometers that serve as a reference for Aerosol Optical Depth measurements within WMO. WORCC also operates the global GAW-PFR AOD network.

The extent of the GAW-PFR network has stabilized at 23 global stations. A description of all GAW-PFR stations can be found at www.pmodwrc.ch/worcc. Graphs of daily and monthly time-series aerosol optical depth are available, and are updated each month to allow the early detection of potential trends.

In 2012, nine instruments of the extended GAW-PFR network were calibrated against the reference Triad at Davos, and four instruments were calibrated by the Langley method at their respective sites. The Cimel radiometer at Davos that serves as a link to AERONET was re-calibrated by the Laboratoire d'Optique Atmosphérique of the University Lille1 and its quality assured data were updated to October 2012.

Annual quality assured data from 9 GAW-PFR stations (total of 13 station years) were updated to 2011 and submitted to WDCA. Daily AOD results from 24 stations are submitted in (quasi) near real time. These data are available through <http://www.gaw-wdca.org>.

The PFR at the GAW station Cape Point, South Africa (see Fig. 1) was replaced with a refurbished system during a station audit in September. As part of the WORCC calibration programme, a second PFR was installed at Izaña (Spain) to facilitate routine Langley calibrations for WORCC Triad instruments.

This PFR was calibrated at WORCC, and then by the Langley method at Izaña. Both calibrations agree to within less than 0.5% except for a difference of 0.8% in the 412nm channel.

An intercomparison between 7 instruments affiliated with the PolarAOD network and the WORCC Triad was held at Davos in February (see Fig. 2). All participating instruments showed RMS differences to the group mean of less than 0.01 optical depths and were thus well within GAW uncertainty.



Figure 1. PFR at Cape Point, South Africa. View towards the North showing the marine location. The black baffle tube protects the window from contamination by mineral dust and salt spray under high wind conditions.

In collaboration with the Institute of Atmospheric Sciences and Climate, Bologna and the Earth System Research Laboratory of NOAA, we modified a PFR instrument for Moon-photometry. Given successful testing in spring 2013, this prototype will be installed at Ny-Ålesund to observe AOD during the polar night, to complement co-located Lidar measurements and to validate satellite observations in the Arctic.

A fourth GAW-PFR Newsletter was distributed in March, and is available at http://www.pmodwrc.ch/worcc/GAW-PFR_Newsletter_Nr4.pdf.



Figure 2. Two robotic SPTA filter radiometers (Dr. Schulz & Partner) participating in the PolarAOD intercomparison 2012 at Davos.

European Ultraviolet Calibration Center (EUVC)

Julian Gröbner, Gregor Hülsen, and Luca Egli

The Global Atmosphere Watch (GAW) Ultraviolet (UV) calibration center aims to improve data quality in the European GAW UV network and to harmonise the results from different stations and monitoring programs in order to ensure representative and consistent UV radiation data on a European scale.

Thanks to the generous financial support of the Kanton of Graubünden and the support of the WMO, we are expanding the activities of the EUVC from being a regional GAW Center for Europe to becoming a World Calibration Center for UV, within the next four year period, 2012–2015. Towards this goal, development of a second transportable reference spectroradiometer, QASUME II has begun which we hope to put into operation in 2013. It has also been decided to expand our laboratory infrastructure with a dedicated spectral responsivity and transfer standard calibration facility based on an Acton DM500 double monochromator combined with a custom made 1000 W Xenon radiation source.

The new 'Optic II' laboratory dedicated to EUVC activities, was built as part of the overall PMOD/WRC renovation and could be used for all calibration activities as of 2012. In addition, a new and more accessible roof platform for the absolute outdoor calibrations was constructed (Fig. 1) on which the UV instrumentation was installed in September 2012.

As part of the implementation of the ISO 17025 Quality System at the EUVC, an external audit by the Swiss national metrology Institute (METAS) was organized in September 2012, which confirmed the high level of expertise and competence of the EUVC.

The EMRP project ENV03 'Traceability of spectral solar ultraviolet radiation' entered its second year of activities, including a dedicated session at the International Radiation Symposium in Berlin in July, gathering more than 70 participants. Following this conference, a two-day project meeting was held at the PTB in order to review and discuss the status of the project. While most activities are progressing according to plan, minor delays occurred due to participant's administrative procedures. Current highlights of the project include: 1) the construction of a high resolution extraterrestrial spectrum in the range 290 to 500 nm based on a ground-based FTIR solar spectrum from Kitt-Peak, combined with the low-resolution composite solar spectrum by Thullier et al (2004) and corrected by comparison with three ground-based spectroradiometers; 2) a guideline document for operating array spectroradiometers, including a sensitivity study to determine the uncertainties of measured solar spectra weighted with several standard action spectra, and 3) the assessment of new technologies useful for reducing the stray-light of array spectroradiometers. Additional information and ongoing activities can be found at the project website: <http://projects.pmodwrc.ch/env03/>.

The transportable reference spectroradiometer QASUME was used during quality assurance site visits to measure alongside spectroradiometers located at the University of Reading (UK, operated by the Univ. of Manchester) and at the Health Protection Agency in Chilton (UK) in June. In addition, the 7th calibration campaign in the frame of the RBCC-E was organized in Arosa in Switzerland with the participation of QASUME as UV reference for all 9 participating Brewer Spectrophotometers. Results of all the QASUME site audits can be found at the EUVC website: http://www.pmodwrc.ch/euvc/euvc.php?topic=qasume_audit.

References: Thullier G., Floyd L., Woods T., Cebula R., Hilsenrath E., Herse M., Labs D.: 2004, Solar irradiance reference spectra for two solar active levels, *Advances in Space Research*, 34, 256–261.



Figure 1. The new platform on the PMOD/WRC roof used for all outdoor EUVC measurements.

Instrument Development

Spectroradiometer for Spectral Aerosol Optical Depth and Solar Irradiance Measurements

Julian Gröbner, Natalia Kouremeti, Etienne de Coulon, Fabian Dürig, Manfred Gyo, Ricco Soder, and Diego Wasser

The radiative forcing of atmospheric aerosols represents one of the largest uncertainties in the Earth radiative budget. Global networks of surface based sunphotometers such as the GAW-PFR network operated by PMOD/WRC measure the aerosol optical depth at several distinct wavelength channels between the ultraviolet and the infrared. A precision solar array spectroradiometer has been developed in order to complement and eventually replace the four-channel precision filter sunphotometer currently in use.

A new generation of solar spectroradiometers, the Precision Solar Spectroradiometer (PSR), has been developed at PMOD/WRC to eventually replace current filter based sunphotometers (see Figure 1). It is based on a temperature stabilized grating spectroradiometer with a 1024 pixel Hamamatsu diode-array detector, operated in a hermetically sealed nitrogen flushed enclosure. The spectroradiometer is designed to measure the solar spectrum in the 320 to 1040 nm wavelength range with a spectral resolution of approximately 1.5 to 3 nm (at full width at half maximum). The optical bench made of a carbon alloy is optimized to minimize the temperature dependence of the solar measurements to less than 0.1 % K⁻¹ for ambient temperatures ranging between -20 °C to +40 °C. A dual-level Peltier temperature regulation system stabilizes the overall temperature to ±10 K, while the detector is stabilized to better than 1 K with a dedicated Peltier circuit.

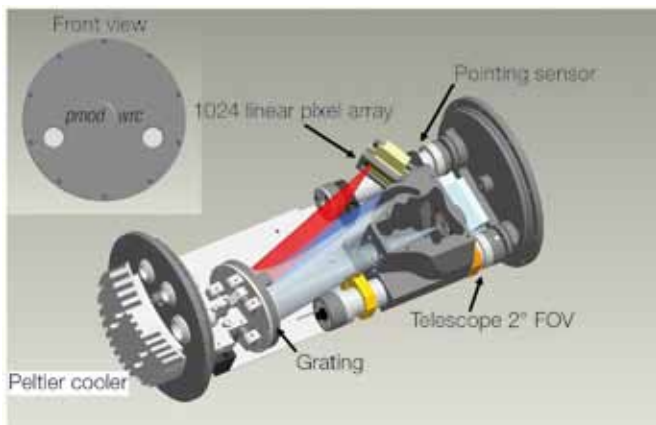


Figure 1. Schematic layout of the Precision Spectroradiometer.

The PSR design benefits from the experience gained from successive generations of the successful Precision Filter Radiometers (PFR), which includes: an in-built solar pointing sensor, an ambient pressure sensor and several temperature sensors to provide routine quality control information which will allow autonomous operation at remote sites using an internal web-based server interface for instrument control and data retrieval.

A prototype of the instrument has been in continuous operation since April 2012, specifically during the Direct Normal Irradiance sensor intercomparison field campaign at Payerne, Switzerland.

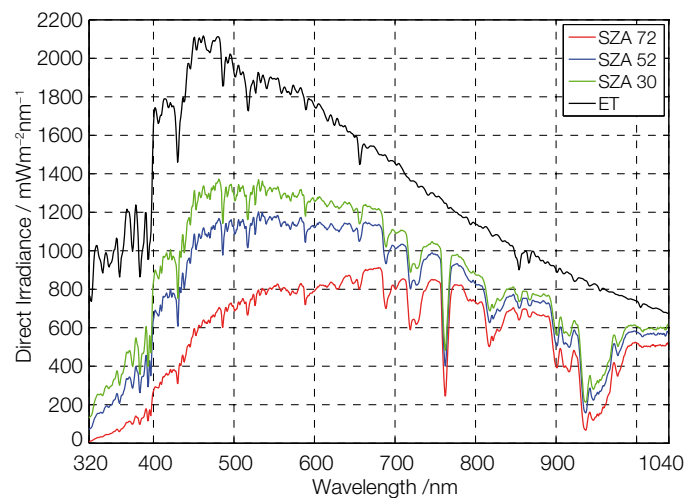


Figure 2. Solar spectra at three solar zenith angles measured on 30 May 2012 at Payerne, Switzerland during the DNI campaign.

Indeed, measurements of direct normal spectral solar irradiance are a crucial parameter required by the photovoltaic industry to optimise current multi-junction photo cells. Figure 2 shows example solar spectra retrieved during this campaign.

Noteworthy was the stability of the PSR during this 5 month period, which included transportation and installation at a remote site. The absolute calibration is shown in Figure 3, and was performed before and after the field campaign in May and October respectively.

The design of the PSR has now been finalized and a commercial version of the instrument is being constructed, with first units ready by Autumn 2013.

An extraterrestrial solar spectrum is shown for comparison. Atmospheric absorption features such as water vapor bands are clearly visible.

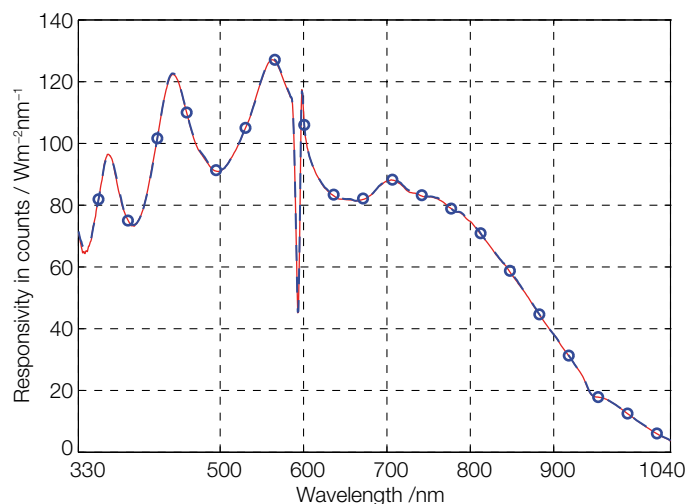


Figure 3. Spectral responsivity of the PSR determined on 5 June 2012 (red curve), and on 25 October 2012 (blue curve) using a spectral irradiance reference traceable to PTB.

CSAR and MITRA

André Fehlmann

The Cryogenic Solar Absolute Radiometer (CSAR) currently stays at the National Physical Laboratory (NPL) in Teddington, UK, where new cavities are built into the instrument. Thus we have no new measurement results from this instrument. The Monitor to measure the Integral Transmittance of windows (MITRA) experiment still shows measurement fluctuations that are larger than the desired accuracy of 0.1% in absolute transmission. Problems in the manufacturing process were identified as possible causes and solutions will be investigated.

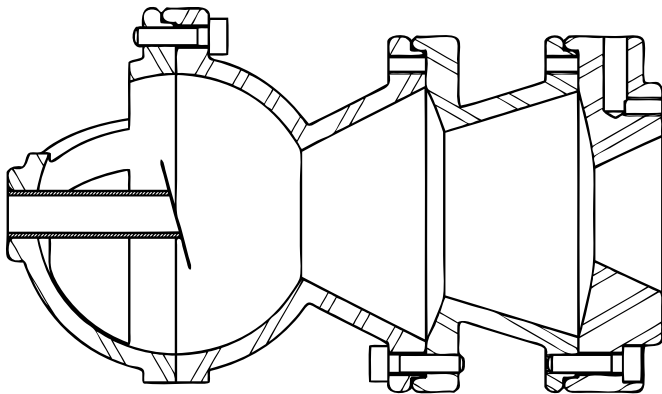


Figure 1. Schematic of the CSAR radiant power cavity which is made from electroformed copper and will be gold-coated to reduce radiative energy transfer. The active detector area is the small, inclined disc sitting on the post on the left-hand side of the figure. The 'Christmas tree' shape of the detector housing reduces the reflection losses to a minimum.

During 2012, renovation of the PMOD/WRC building made it impossible to use the solar tracking platform for most of the time. However, as all instruments had been removed from the platform, the technical department was able to modify the platform by reinforcing it with preloaded springs. The platform should now be able to operate in the most extreme altitude and azimuth positions even with heavy instruments mounted, e.g. the CSAR instrument weights 100 kg.

Throughout 2012, CSAR remained at the National Physical Laboratory (NPL) in Teddington, UK where our partners disassembled the instrument and started to integrate the radiant power cavities. Once these detectors are installed, CSAR will be able to measure the power level of monochromatic radiation up to 1mW with an anticipated accuracy of 0.1%. Figure 1 shows a schematic of the CSAR radiant power cavity. After completion of the upgrade and successful testing, CSAR will be reinstalled on the solar tracking platform in Davos to perform long-term stability tests.

To measure the integral transmittance of the CSAR window the MITRA instrument uses a passive operation principle where two detectors observe the sun in parallel. First, the detector signal ratio is determined with no window in place, which serves as the reference value. Second, the sunlight to one detector is obstructed by the window under investigation, to obtain a measurement detector ratio. The integral transmittance of the window is then calculated by dividing the measurement ratio by the reference value.

The instrument optimizations completed last year include: 1) reducing the number of thermal contacts in the measurement circuit, 2) replacing a damaged precision aperture, 3) enlarging the entrance aperture which might have caused stray light. MITRA was then tested in the optical laboratory and by the end of 2012 on the solar tracking platform.

Once more the dark measurements performed to investigate the thermal stability yielded a detector ratio which is stable within 100 parts per million. However, as soon as the cavities are illuminated by either a stabilized split laser beam or the Sun, the detector ratio starts to fluctuate on the percent level. Although the temperature rise measurements of the two cavities seem highly correlated, small differences cause large fluctuations when the detector ratio is calculated (c.f. Figure 2).

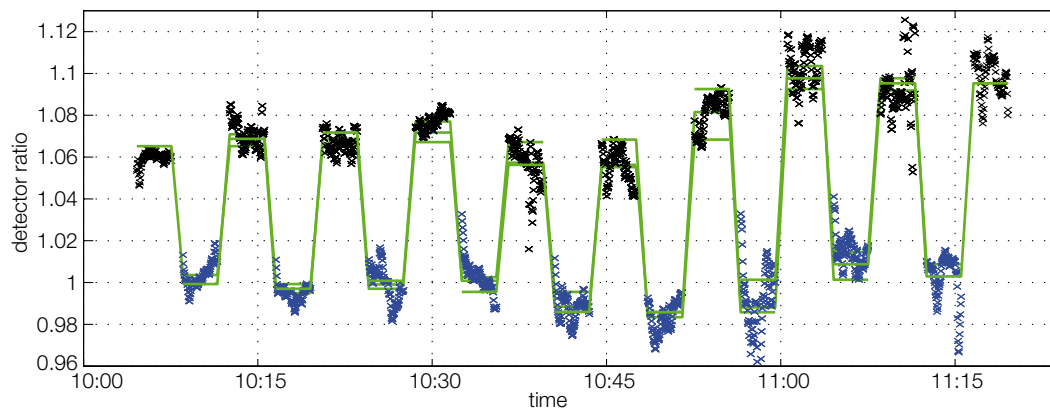


Figure 2. MITRA detector ratio time-series measurements in front of the Sun. The black data points represents the measurements without a window in the beam path. The blue ones are with the window obstructing the path to the left detector. The black reference ratio would be constant for perfectly symmetric detectors. Thermal drifts of the heat sink however cause variations in the reference measurements, indicating that the two MITRA cavities are not yet perfectly balanced. The green line shows the fitting curve used to determine the offset between the two sets, i.e. the transmittance of the window.

Because the dark measurements, where the detectors have to respond to slowly varying ambient temperature changes, are stable and the irradiance measurements, where the detectors have to respond to quick changes, are unstable, we conclude that the observed fluctuations are due to persistent small differences between the two detectors. These include: 1) The thermal capacity of the hand-wound copper coil thermometer around the cavities may differ due to a length difference of the applied wire or due to the amount of glue used to fix the coil, 2) The thermal contact between thermometer and cavity depends on the tension applied to the copper wire during fixation as well as the number of coil layers.



Figure 3. Copper coil thermometer glued to a MITRA detector. The amount of applied glue is hard to control which affects the thermal capacity of the detector.

All these issues affect the thermal relaxation time constants of the detectors differently and thus can cause fluctuations of the detector ratio. Figure 3 shows the copper coil thermometer glued to a MITRA cavity.

To overcome these possible human-influenced deviations in the manufacturing process we are now investigating the use of vapor deposited resistance thermometers. By applying this established technique we can avoid the use of glue and would be able to match the resistance value by a laser trimming method. In this manner we hope to obtain the best thermal equivalence of the two detectors and thus stable measurements required to achieve MITRAS's goals.

- References:
- Fehlmann A.: 2011, Metrology of Solar Irradiance, PhD Thesis, University of Zürich.
 - Winkler R.: 2012, Cryogenic Solar Absolute Radiometer – a potential replacement for the World Radiometric Reference, PhD Thesis, University College London.

Heliostat

Markus Suter

When the old heliostat system, which was part of the old clean room facility, was removed as part of the renovation of the institute building, in 2011 the planning of a new heliostat began. After planning, fundraising, and basic design studies in 2011 (see Annual report 2011), the heliostat was designed in detail in 2012, and manufacturing of the mounting and mirrors, as well as testing of the motion control began.

While the old system was used to test instrument functionality in the clean room, the new system will provide a solar beam of much higher quality. This beam will allow sensitive radiometric experiments to be carried out in a controlled laboratory environment. The beam can also be optionally feed into the new clean-room.

The Final Design

The mounting pan for the mirrors was designed in-house and optimized for low weight and high stiffness. The pan that holds the mirror has an outer dimension of 770 mm and was milled out of a solid block of aluminium. The mounting pans of the mirrors were among the first parts to be manufactured. Figure 2 shows such a mounting pan.

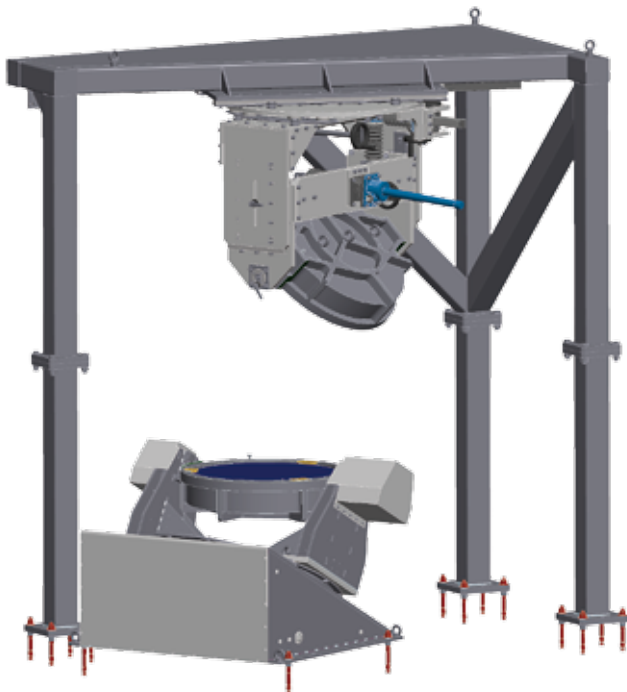


Figure 1. Mechanical Design of the Heliostat: The Heliostat consists of the tracking system (lower mirror) and the mounting for the secondary mirror (top). The tracking mirror is motorised and tracks the motion of the sun, while the secondary mirror is in a fixed position to direct the light into the laboratory. The secondary mirror can be adjusted with hand wheels to put it in its required position.



Figure 2. Markus Suter with the mounting pan for the heliostat mirror.

As a first step, the tracking system of the primary mirror was designed in-house, and is currently being manufactured by G+P Engineering in Sargans. The mounting construction for the secondary mirror pan was designed by the same company. The design process was finished by November 2011 and soon afterwards the construction began. Figure 1 shows the final heliostat design.

The Mirrors: Manufacturing and Self-Gravity Compensation

Both heliostat mirrors have a diameter of 650 mm and a thickness of 100 mm, and are made of Zerodur, a ceramic glass with virtually no thermal expansion. The coatings are aluminium with a protective layer. The mirrors were manufactured and delivered towards the end of 2012 by Thales-Seso, a company located in Southern France.

To ensure a good quality light beam, these mirrors need to be extremely flat. They are polished to an rms error of less than 25 nm.

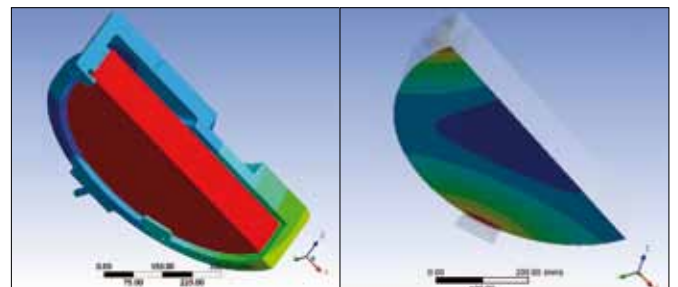


Figure 3. The left image shows the deformation of the mounting pan under gravity load. The pan is optimised for low deformation while keeping the weight as low as possible. The right image shows the deformation of the secondary mirror due to gravity. The area in blue is highly displaced (around 300nm), while the red areas have low displacement (position of the bearings).

To prevent mirror deformation due to self-gravity the primary mirror is mounted in a way so that at 9 well-defined points the mirror is supported with equally distributed force.

On the other hand the secondary mirror is already polished to compensate for self-gravity deformation in the mounting position. The self-gravity deformation of the mirror (Figure 3) was determined in an in-house study, and details were sent to the manufacturer in Summer 2012.

The Drive and Control Concept

The heliostat tracking system has two movable axes. The primary (pseudo azimuth) axis is inclined by 27 degrees to the vertical and the secondary axis (pseudo elevation) is perpendicular to the primary axes. The concept allows a relatively continuous movement and the dynamic range of the drive can be kept low. It is a compromise between an alt-azimuth and an equatorial mount. The advantage over an equatorial mount is that the incidence angle on the mirrors is steeper which thus takes better advantage of the mirror size. The advantage over an alt-azimuth mount is that the motion is more continuous.

The device is driven by two stepper motors, with micro stepping capability. Attached to the motors is a backlash-free harmonic drive gearbox with a transmission ratio of 1:160.

For exact positioning each axis is equipped with an 18-bit rotary encoder. This allows the sun to be tracked in a passive mode to a precision of less than 0.01 degrees, which will be satisfactory for radiometer experiments. In addition, an optical tracking sensor will be installed to allow a tracking accuracy close to several arc seconds.

All sensor/actor devices are connected through a CAN-bus system and controlled by a standard PC. A test-stand has been built where a motor/gearbox/encoder combination has been set up to test the components and the software (Figure 4).

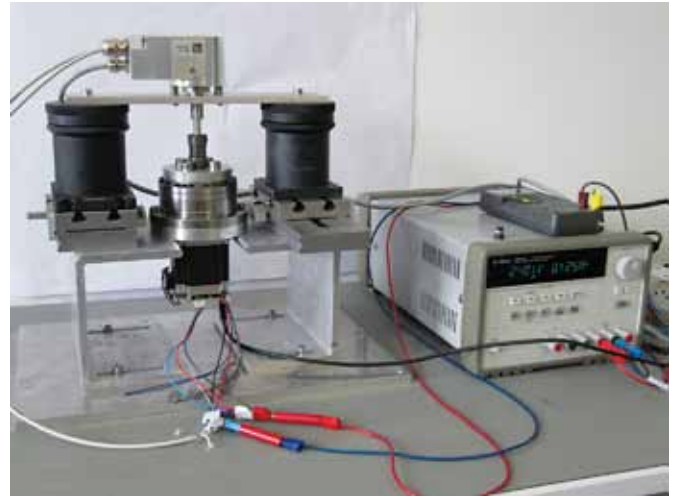


Figure 4. Motor/Encoder Test Stand.

Schedule for 2013

The installation on the prepared platform (Figure 4) at PMOD is scheduled for the end of April 2013. After a commissioning phase the heliostat is planned to be operational in the second half of 2013. It will then first be used for the characterisation of the DARA instrument.

Construction of the heliostat is supported by the Swiss National Science Foundation Grant No. 206021_139119 and Grant No. 200021_132553.



Figure 5. Foundation for the Heliostat at the south-east face of the institute building.

A World Radiometric Reference (WRR) to SI radiant power scale comparison with DARA

Markus Suter

Four Comparisons between the WRR (SI Scale for Solar Irradiance) and the SI radiant power scale have been performed in the past. The first three comparisons showed good agreement between the scales, within the uncertainties of the comparison. However, the fourth comparison in 2010 found a significant difference of 0.34 % between the two scales. In 2012 a fifth comparison was made, using the DARA instrument.

The WRR scale is the WMO and SI reference scale for Solar Irradiance that is officially used in meteorological measurements. The WRR standard is realized by a conventional standard, the World Standard Group (WSG) of pyrhelimeters operated at PMOD/WRC. On the other hand there is the SI radiant power scale that is directly linked to the basic SI units. This scale is realized with cryogenic laboratory radiometers by the national metrology institutes. These instruments are regularly compared against each other in key comparisons.

Four comparisons between WRR and SI radiant power scales, using PMO6-radiometers, have been conducted in the 1990 to 2010 period. In the first three comparisons the scales agreed well within the stated uncertainties of the comparison. However, the most recent comparison in 2010 suggested that the WRR scale is significantly higher (0.34 % \pm 0.18) than the SI radiant power scale. Unlike earlier measurements that were conducted in power mode (under filled aperture) this comparison was carried out in irradiance mode e.g. using a beam that overfills the radiometric aperture. This was made possible by the new TSI Radiometer Facility (TRF) at LASP, Boulder, USA. Fehlmann et al. (2012) explain a part of the difference of the results with the underestimation of stray light effects in PMO6-Radiometers.

A 5th WRR to SI comparison in 2012 was carried out with DARA, our new prototype instrument for a space experiment on PROBA3. DARA is a digitally controlled absolute radiometer, with a different aperture geometry than PMO6-Radiometers. This will reduce stray light that was a major source of uncertainty in the earlier comparisons.

The DARA instrument was calibrated against a cryogenic radiometer at the Total Solar Irradiance Radiometer Facility (TRF) in 2011 (Annual Report 2011). The TRF is located at the Laboratory for Atmospheric and Space Physics (LASP) at the University of Colorado in Boulder, USA, and allows indoor irradiance calibrations for solar radiometers to be conducted with a high accuracy (Kopp et al 2007). The PMO6-PREMOS flight unit and the PMO6-VIRGO flight spare radiometers were also calibrated at the TRF in the past. The TRF facility provides a 7.3 mm diameter beam that overfills the aperture of the instrument.

This allows calibrations in irradiance mode (overfilling all apertures). The DARA instrument and the TRF cryogenic radiometer are alternately exposed to the beam that is also monitored by a silicon diode. Both instruments are operated inside a vacuum chamber.

The DARA instrument has been compared to the World Standard Group (WSG) at PMOD, where the WSG represents the WRR standard for radiometric measurements. These measurements were conducted in February 2012. The reference (PMO2) and the DARA instruments measured the solar irradiance side-by-side at PMOD. Four data runs, each lasting a full day, were performed.

While the TRF calibration is performed in vacuum at a single wavelength, the WRR calibration is performed at ambient pressure with the sun as a source. Two transfer factors therefore need to be introduced to compare both calibrations. One of these factors is the air-to-vacuum ratio which describes the different instrument sensitivity in air and vacuum. The second transfer factor is a diffraction correction as the diffraction at the 532 nm laser wavelength produces a slightly different effect than the solar beam. This also needs to be corrected. While the air-to-vacuum ratio is determined experimentally, the diffraction transfer factor is calculated numerically.

Comparing the results from the calibrations against the WRR and the cryogenic radiometer at the TRF, it is found that the WRR scale is 0.3 % higher than the SI scale. With an uncertainty of \pm 0.1 % (2 Sigma) all three cavities agree on this value. This result is in good agreement with those of Fehlmann et al. (2012) who found a scale difference of 0.34 %. It supports the 2010 result with a different transfer instrument, while avoiding the stray light effects of PMO6 radiometers.

- References:
- Fehlmann A.: 2011, Metrology of Solar Radiometry, PhD-Thesis, Universität Zürich.
 - Fehlmann A., Kopp G., Schmutz W., Winkler R., Finsterle W., Fox N.: 2012, Fourth World Radiometric Reference to SI radiometric scale comparison and implications for on-orbit measurements of the total solar irradiance, *Metrologia* 49, S34–S38.
 - Kopp G., Heuermann K., Harber D., Drake G.: 2007, The TSI Radiometer Facility: absolute calibrations for total solar irradiance instruments. In: Society of Photo-Optical Instrumentation Engineers (SPIE) Conference Series, volume 667.
 - Suter M., Finsterle W., Kopp G.: 2012, WRR to SI comparison with DARA, WMO-TECO 2012 Bruxelles: http://www.wmo.int/pages/prog/www/IMOP/publications/IOM-109_TECO-2012/Programme_TECO-2012.html.

Space Experiments

Manfred Gyo, Dany Pfiffner, Fabian Dürig, Valeria Büchel, Markus Suter, Wolfgang Finsterle, and Werner Schmutz

PREMOS

The PREMOS experiment, a payload aboard the French micro satellite PICARD.

The PMO6 radiometers on PREMOS/PICARD are the only TSI instruments in space with unbroken traceability chains to the ground-based standards for SI radiant power (NIST), and solar irradiance (WRR). The extensive pre-launch calibration efforts not only resolved the cause for the offset between different TSI instruments in space but also allowed the WRR and SI scales to be compared with unprecedented accuracy (Fehlmann et al., 2012, Metrologia, 49). Because of the unprecedented absolute accuracy of the PMO6/PREMOS TSI measurements the ISSI international team, with the working title 'An Assessment of the Accuracies and Uncertainties in the Total Solar Irradiance Climate Data Record', agreed during its 2012 meeting to anchor a new TSI composite to the PMO6/PREMOS absolute value.

Overall the PREMOS experiment performed excellent during 2012 with only one single event upset. The instrument was fully functional after an instrument re-start and software re-load. This good news contrasts some bad news received towards the end of 2012: CNES has announced that PICARD will be switched off in 2013.

SuMo

DARA (Digital Absolute Radiometer) is a prototype for the SuMo (Sun Monitor) experiment on the PROBA-3 satellite. DARA has a completely new cavity and electronics design.

During 2012, the DARA prototype was mounted on the Sun Tracker at PMOD/WRC and numerous measurements were conducted.

The calibration measurements within the on-going PhD project to characterize the new DARA/SUMO radiometer design for absolute solar irradiance measurements in space and on ground confirmed the results found earlier with the PMO6/PREMOS radiometers. In particular, the PMO6 problems with internal stray light were confirmed and eliminated in the DARA/SUMO optical design (Suter et al., 2012; http://www.wmo.int/pages/prog/www/IMOP/publications/IOM-109_TECO-012/Session4/O4_05_Suter_WRR_SI_Comparison_to_DARA.pdf).

A detailed description of the DARA/SUMO project can be found in a dedicated section in this report.

EUI

The experiment Extrem UV Imager (EUI) is a payload aboard ESA/NASA Solar Orbiter Mission. PMOD/WRC is leading the Swiss hardware contribution.

In 2012, the preliminary design of the optical bench was completed and phase B was successfully finished with the preliminary design review (PDR) in April (see Fig. 1.).

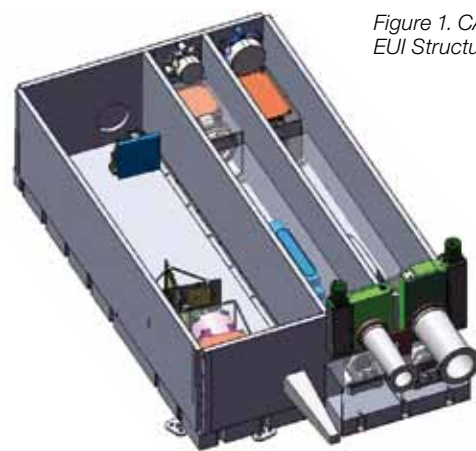


Figure 1. CAD Model of EUI Structure.

After the PDR the tender process for Phase C/D (critical design phase and manufacturing of the instrument) starts. It takes a long time to obtain an industry contract, however, a contract with APCO Technologies was completed in November 2012 by ESA, and the critical design phase started shortly afterwards.

The infrastructure in the PMOD/WRC laboratories was set-up to conduct the baking-out procedure during manufacturing.

A vacuum oven for small parts and a heat case (Fig. 2) for the large elements of the optical bench were constructed. The heat case helps to handle the structural elements within the big vacuum recipient, to heat them during bake-out and to hold the parts purged during the entire procedure.

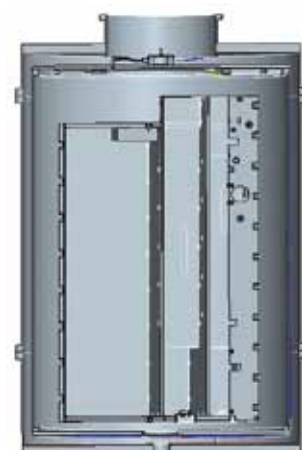


Figure 2. Heat Case.

SPICE

The SPICE experiment is a payload aboard ESA/NASA Solar Orbiter Mission. PMOD/WRC is leading the Swiss hardware contribution.

In 2012, industry contracts for the preliminary mechanism design were completed. A successful PDR finished the preliminary design of all three components: The low voltage power supply (LVPS), the slit change mechanism and the SPICE door mechanism.

Low Voltage Power Supply

During the preliminary design phase the design was improved and a bread-board was built. First EMC and thermal vacuum tests to correlate with the thermal simulation were conducted (Fig. 3).

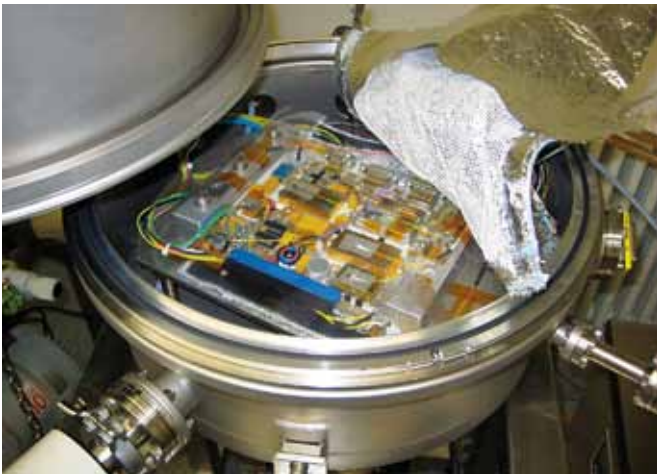


Figure 3. LVPS preparation for thermal vacuum test.

Slit Change Mechanism

A blade design was established as a baseline design together with ALMATECH who is our industry partner for manufacture of the slit mechanism. The design fulfils the requirements for positioning accuracy of the slits, and cleanliness.

The tender process began after the PDR in order to have an industry contract ready for phase C/D. ESA released the Invitation to Tender (ITT) in late December.

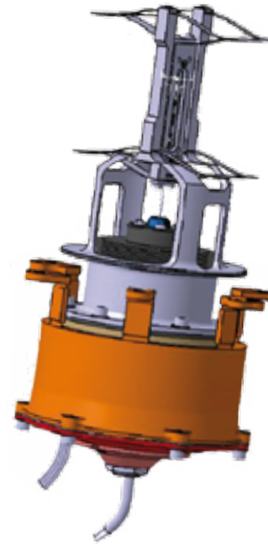


Figure 4. Model of Slit Change Mechanism.

SPICE Door Mechanism

The preliminary design of the SPICE Door Mechanism was completed with APCO Technologies. The door is designed to prevent the instrument from being contaminated during ground operation and during non-measurement phases in orbit.

Similar to the Slit Change Mechanism, the ITT for Phase C/D was released in late December by ESA.

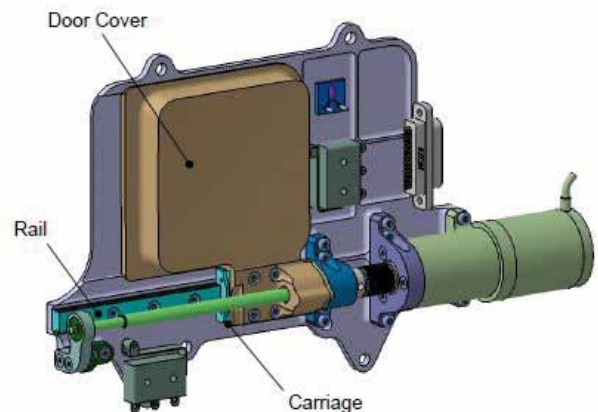


Figure 5. Model of SPICE Door Mechanism.

Projects at PMOD/WRC are related to solar radiation. We address questions regarding the radiation energy budget in the terrestrial atmosphere as well as problems in solar physics to understand the mechanisms concerning the variability of solar irradiance. Hardware projects at our institute are part of investigations into Sun-Earth interactions by providing measurements of solar irradiance.

The choice of projects to be conducted at the institute is governed by the synergy between the know-how obtained from the operational services of the World Radiation Center and other research activities. Basically, the same instruments are built for space-based experiments as are utilized for ground-based measurements.

The research activities can be grouped into three themes:

- Climate modeling
- Terrestrial radiation balance
- Solar physics

Research activities are financed through third party funding. Last year, we were supported by the Swiss National Science Foundation (7 projects), MeteoSwiss (1 project), the seventh European Framework Program FP7 (2 projects), and the European Metrology Research Program (2 projects). Hardware development of space experiments is paid by the ESA PRODEX program (3 projects). These funding sources have supported 4 PhD Theses, of which two were completed last year, and 6 postdoctoral positions. The institute's PRODEX projects paid for the equivalent of four technical department positions.

The backbone of climate research at PMOD/WRC is the FUPSOL project (Future and Past Solar Influence on the Terrestrial Climate), which is a collaborative multi-institute research with partners from the EAWAG, IAC ETHZ, Bern University, and Oeschger Centre for Climate Change Research. Several other PMOD/WRC projects directly or indirectly relate to the goal of understanding and reproducing natural climate change of the past 500 years as well as forecasting the contributions from natural influences to future climate change. Not only are variations in solar irradiance of importance but the effects of particles are also relevant. In particular, on a shorter time-scale than climate time-scales, i.e. where space weather has an influence, so-called Solar Proton Events can have remarkable effects. If the Earth were to be hit by a strong event similar to the famous 1859 Carrington event, our simulations show that it could have an impact on the chemical state of the terrestrial atmosphere that lasts for several months.

It has been reported in the literature that the past century experienced phases when less solar irradiance reached the terrestrial surface which lasted several decades. The phases with decreasing irradiance have been termed global dimming, and the phases when the irradiance increased, are named global brightening. A PhD Thesis at PMOD/WRC investigated whether the data collected at the observatory in Davos for the past 100 years could

shed more light on the cause of these changes. It was found that atmospheric transmission over Davos did not change by a sufficient amount to explain the reported dimming. Factors other than atmospheric transparency, such as the type or amount of cloud cover, are probably responsible for the dimming measured by pyranometer instruments (ie global irradiance) in Davos. However, a slight brightening since about 1990 could be the effect of a cleaner, less polluted atmosphere.

The result of the long-term analysis is supported by measurements of aerosol optical depth (AOD) obtained with sun-photometers. AOD time-series are available for Switzerland since the early 1990s. These still relatively short data series exhibit no obvious trends at present. A slight decrease of AOD, as required by a brightening discussed above, is within the measurement uncertainties.

The PMOD/WRC CLASS project, which is supported by the Swiss contribution to the Global Atmosphere Watch Programme of the World Meteorological Organization, will eventually deliver the tools to record and estimate the effect of clouds on the radiative energy budget. The aim is an automated measurement of the cloud fraction and a classification of cloud types, based on hemispherical sky images obtained by automated cameras. First results obtained by a successfully completed PhD Thesis are very promising and an automated system seems to be feasible, although we are still far from having a fully operational system. Further research and development of the necessary algorithms and field tests will be needed.

Whether variations in Total Solar Irradiance (TSI) and/or Spectral Solar Irradiance (SSI) are large enough to be relevant to the terrestrial climate is still a topic of keen debate among experts. In an important paper, Haigh et al. (2010) pointed out that if SSI variations as reported by the SIM/SORCE team were correct, then solar variations would influence the terrestrial climate. The peculiarity of the SIM/SORCE variations is that the UV variations are larger than previously assumed and are compensated by an out-of-phase variation of the visual spectral range. We have now analyzed filter radiometer data from VIRGO/SOHO, which is a PMOD/WRC space experiment that has been running for 17 years. Based on the 2002 – 2012 VIRGO time-series, the 500 nm channel was shown to be in-phase with TSI rather than out-of-phase, as claimed by SIM/SORCE.

Reliably quantifying SSI variations is an important ongoing task that is being addressed by several groups world-wide. In this respect, the SOLID project – First European SOLAR Irradiance Data – will make an important contribution. The goal of this FP7 project is a critical inventory of existing solar irradiance measurements, including an assessment of the measurement uncertainties. A second ambitious aim of SOLID is to fill observational gaps in either time or in wavelength coverage by model calculations. The project was initiated by the PMOD/WRC and is being led by the observatory.

Future and Past Solar Influence on the Terrestrial Climate (FUPSOL)

Werner Schmutz (PI), Eugene Rozanov (project manager) and Alexander Shapiro in collaboration with teams from EAWAG, IAC ETHZ, KUP and GIUB of University of Bern, and Oeschger Centre for Climate Change Research

FUPSOL is a Swiss collaboration project involving partners from the Institute for Atmosphere and Climate Sciences of the ETH Zürich (IAC ETH), the Swiss Federal Institute of Aquatic Science and Technology, Dübendorf (EAWAG), the Physics Institute (KUP) and Institute of Geography (GIUB) of the University of Bern and the Oeschger Centre for Climate Change Research. It aims to quantify solar forcing and its influence on the Earth's atmosphere and climate.

The main efforts during the second year of the FUPSOL project were aimed at developing 1) the natural and anthropogenic forcing scenarios covering 2000–2100, 2) simulations of the 20th and 21st century's climate with the atmosphere-ocean-chemistry-climate model (AOCCM) SOCOL-MPIOM using several scenarios for the evolution of the solar activity and 3) analysis of the results obtained for the Dalton minimum (DM). We completed all planned sensitivity runs for Dalton minimum conditions and analyzed the contribution of different factors. We show that for the reproduction of the cold climate during the DM a combination of both volcanic eruptions and reduction in solar irradiance is needed (see science page describing DM results). The climate simulations which started during the first year of the project have reached year 2000 and the results of this experiment have been prepared for the analysis. Figure 1 presents global annual mean total column ozone (TCO) simulated by the AOCCM SOCOL-MPIOM for two (mean and minimum strength) scenarios of SSI evolution as proposed by Shapiro et al. (2011). The TCO dependence on the solar, volcanic and anthropogenic activities is evident. The TCO is low during the Maunder and Dalton minima as well as around 1900. The magnitude of these minima clearly depends on the strength of the applied solar forcing. Due to smoothing, the influence of volcanic eruptions is not so visible except for two extremely powerful events during the DM. The ozone decline caused by the increased halogen loading due to anthropogenic activity is clearly visible during the last 40 years of the 20th century. The difference between two applied solar forcing data sets is small during this period, therefore the TCO behavior does not depend on the applied solar forcing. Further detailed analysis of the obtained results including the response of the tropospheric circulation and surface temperature is in progress.

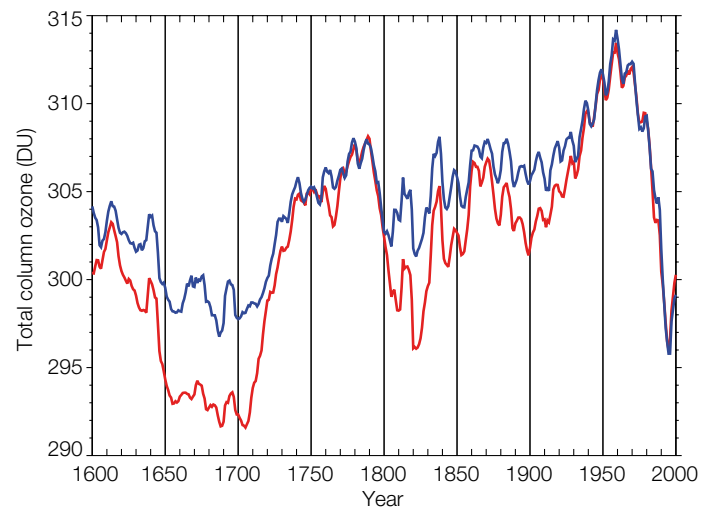


Figure 1. Global annual mean total column ozone (DU) simulated by AOCCM MPIOM for mean (red) and minimum (blue) strength scenarios of SSI evolution as proposed by Shapiro et al., (2011). The results are smoothed by a 7-year running average.

The next phase of the project implementation will be devoted to projections of the future climate and ozone layer. On the basis of the spectral analysis of the solar activity behavior in the past we predict its steady decrease in the future, reaching approximately the level of the DM in the year 2100 (Steinhilber and Beer, 2012). From this time-series we have derived the evolution of the energetic electron precipitation (EEP) and Galactic Cosmic Rays (GCR) as well as the spectral solar irradiance (SSI) for 1600–2100. We have also produced model boundary conditions for the 21st century, including a novel, detailed stratospheric aerosol data set. The prepared set of forcing data has been used to drive climate simulations from 2000 to 2100. The simulation of the future climate driven by this forcing data are ongoing for several scenarios including the cases of stable and declining solar activity and the results of these experiments will allow us to estimate the contribution of changes in solar activity to the future greenhouse warming and ozone recovery.

References: Shapiro A.I., Schmutz W., Rozanov E., Schoell M., Haberreiter M., Shapiro A.V., Nyeki S.: 2011, A new approach to the long-term reconstruction of the solar irradiance leads to large historical solar forcing, *A&A*, 529, A67.

Steinhilber F., Beer J.: 2012, Prediction of solar activity for the next 500 years. submitted to *Astronomy and Astrophysics*.

Further Development of the Chemistry-Climate Model SOCOL

Eugene Rozanov, Timofei Sukhodolov in collaboration with J. Anet, A. Stenke, and T. Peter, IAC ETH, Zurich

We continue the development of the chemistry-climate model (CCM) SOCOL. The third version of the model has been further improved to better represent the solar related forcing such as spectral solar irradiance (SSI) and energetic particle precipitation (EPP). We have also extended the previous simulations to evaluate the model behavior during the last decade.

Compared to the previous version, SOCOL v.3.0 exhibits a more realistic distribution of atmospheric trace gases and some advanced features of dynamics (Stenke et al., 2012). However, a number of model deficiencies still remain and this makes it necessary to continue the improvement of the model. The main direction of recent model improvements has been related to the parameterizations of heating rates due to absorption of solar irradiance and ionization rates caused by the precipitation of different energetic particles.

The original radiation scheme of the model uses the six bands model of Cagnazzo et al. (2007) which does not contain oxygen absorption and hence underestimates heating rates in the mesosphere and upper stratosphere. Moreover, the original radiation code highly underestimates the response of the heating rates in the middle stratosphere to variability in the solar spectral irradiance. We have solved this problem by applying additional parameterizations of heating rates by oxygen absorption in the Lyman- α line and Schumann-Runge band and by ozone absorption in the Hartley and Huggins bands (Zhu, 1994).

Parameterizations of the galactic cosmic rays, solar proton events and energetic electron precipitation were implemented into the model. Rozanov et al. (2012) showed that these particles can noticeably affect the stratospheric ozone and temperatures over the high latitudes.

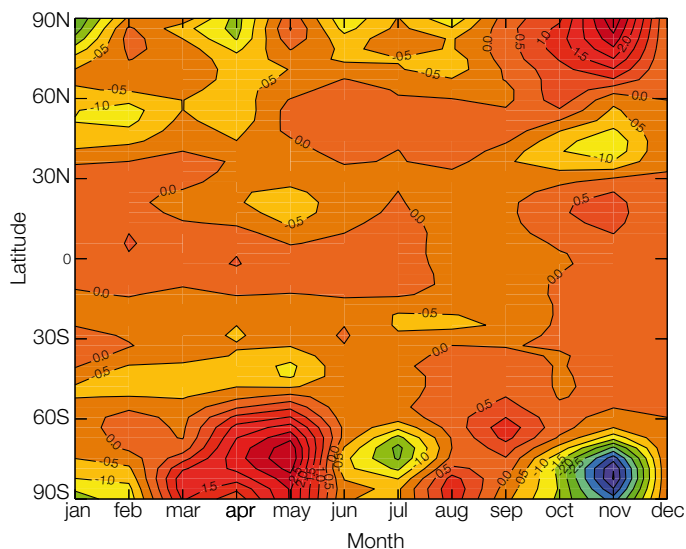


Figure 1. Linear trend (DU/year) of the zonal mean total column ozone as a function of latitude and month.

The existent transient simulation analysed by Stenke et al. (2013) was repeated with a new model version and extended from 2001 to 2010. The simulation includes several natural and anthropogenic forcings, of which the main effects during the considered period were represented by a decrease in solar activity and halogen loading as well as by a continuous increase in greenhouse gases. The linear trend in the zonal mean total column ozone is illustrated in Figure 1 as a function of latitude and month.

The model results show that the decade under consideration was marked by an intensification of polar ozone depletion of up to 3.2 Dobson units (DU) per year over the South Pole in November and up to 2.5 DU/year over the North Pole in January. On the other hand, a positive trend (2.5 DU/year) in total column ozone during the polar nights is found in the high latitudes of both hemispheres. Reasons for these effects are under investigation because of the complexity of dynamical and chemical processes in Polar Regions.

Decreasing halogen loading leads to less intensive ozone, but on the other hand it activates nitrogen radicals. Lower solar activity leads to less ozone production via oxygen photolysis but modulates the active nitrogen and hydrogen production by energetic particles followed by some ozone changes especially in the Polar Regions. This increase in active nitrogen can cause additional destruction of ozone via the nitrogen catalytic cycles, but can also deactivate active chlorine and hydrogen radicals, and hence can reduce the ozone destruction rate. The changes in nitrogen oxide content could affect the formation of the polar stratospheric clouds, which play an important role in the polar ozone pattern.

A complete understanding of the obtained ozone changes requires a number of additional sensitivity runs to elucidate the mechanisms responsible for the trends.

References: Cagnazzo C., Manzini E., Giorgetta M.A., Forster P.M.D., Morcrette J.J.: 2007, Impact of an improved short-wave radiation scheme in the MAECHAM5 General Circulation Model, *Atmos. Chem. Phys.*, 7(10), 2503–2515, doi:10.5194/acp-7-2503-2007.

Rozanov E., Calisto M., Egorova T., Peter T., Schmutz W.: 2012, Influence of the Precipitating Energetic Particles on Atmospheric Chemistry and Climate, *Surveys in Geophysics*, Volume 33, Issue 3–4, pp. 483–501.

Stenke A. et al.: 2012, The SOCOL version 3.0 chemistry-climate model: description, evaluation, and implications from an advanced transport algorithm, *Geosci. Model Dev. Discuss.*, 5, 3419–3467.

Zhu X.: 1994, An accurate and efficient radiation algorithm for the middle atmosphere model, *JAS*, 51, 24, 3593–3614.

Modulation of the Middle Atmospheric Response to Solar Irradiance Changes by Internal Variability

Anna Shapiro, Eugene Rozanov, Alexander Shapiro, and Tatiana Egorova in collaboration with IAC ETH, Zurich

We studied the internal variability of the atmosphere and its possible influence on the middle atmospheric response to the 27-day solar irradiance variability. We applied the Chemistry-Climate Model (CCM) SOCOL to simulate the atmospheric evolution from 2000 to 2006. We found that the atmospheric state can be strongly affected by the Madden Julian Oscillation (MJO).

The variability of the middle atmosphere state is affected by a number of external (e.g. solar variability) and internal (e.g. sea surface temperature changes, Quasi Biennial Oscillation) processes, which are characterized by different periodicities. Internal processes can modulate the effects of the 27-day solar irradiance variability rendering the extraction of the solar signal very difficult. We have performed four 7-year long (2000–2006) ensemble runs with CCM SOCOL to study the main features of the ozone variability on a daily time scale. Figure 1 presents the power spectrum of the zonal mean ozone mixing ratio at 45 km for one of the ensemble runs. It shows strong ozone variability around the solar rotational period (25–35 days), however, spectral power at longer periods is also significant.

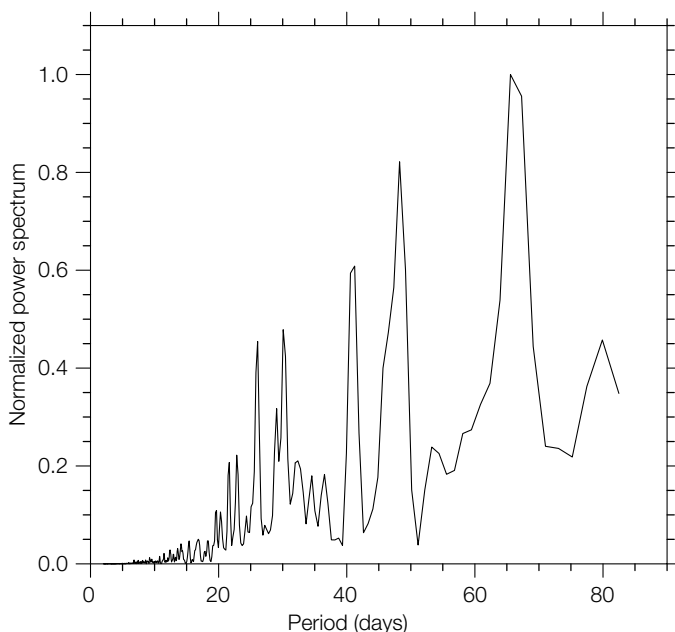


Figure 1. The normalized power spectrum of O3 at about 45 km.

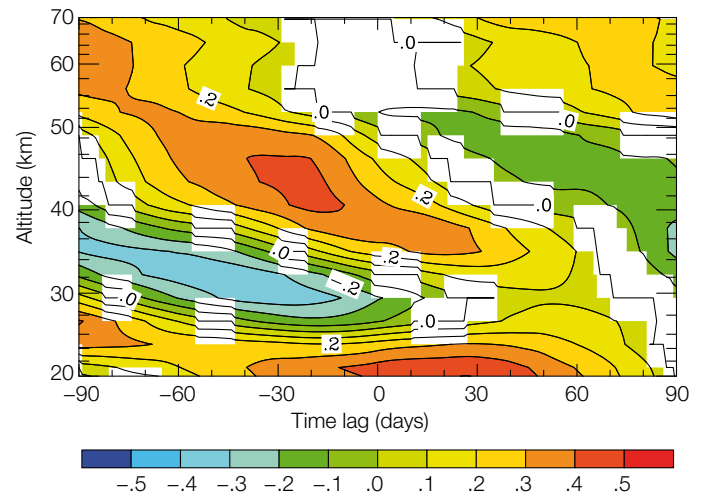


Figure 2. Cross-correlation functions between O3 and zonal wind at 850 hPa. The colored areas correspond to a significance level better than 99%.

The ozone variability with a 30–90 day period could be caused by MJO, which is an eastward propagating anomaly in the tropospheric tropical zonal wind and rainfall with an approximately 30–90 day period. Weare (2010) has found MJO in tropospheric and lower stratospheric wind, temperature and ozone. To check the influence of the internal variability on the middle atmosphere we performed six additional 7-year long (2000–2006) ensemble runs with CCM SOCOL. For these experiments the model was driven by the same set of forcings but we kept the solar irradiance constant. Figure 2 shows the cross-correlation functions between the tropical ozone mixing ratio and the tropical zonal wind at 850 hPa (proxy for the MJO) obtained from the sensitivity runs. The results reveal significant correlations (up to 0.4) at 60 km that propagates to lower altitudes. At 30–40 km the correlation is significant and negative.

We interpret this result as a connection between MJO and stratospheric ozone variability. Thus the tropospheric dynamical variability might strongly influence the stratospheric composition and affect the middle atmospheric response to the solar irradiance variability.

References: Weare B.C.: 2010, Madden Julian Oscillation in the tropical stratosphere, *J. Geophys. Res.*, 115, D17113, doi: 10.1029/2009JD013748.

The Role of SSI Variability in the Evolution of the Middle Atmosphere during 2004–2009

Anna Shapiro, Eugene Rozanov, Alexander Shapiro, Tatiana Egorova and Werner Schmutz in collaboration with Thomas Peter (IAC ETH, Zurich), Jerry Harder (LASP, Boulder, USA), Anne Smith (ACD NCAR, Boulder, USA) and Mark Weber (IUP, Bremen, Germany)

We analyzed the response of the middle atmosphere to the different Spectral Solar Irradiance (SSI) datasets using 1-D and 3-D Chemistry-Climate Models (CCM). We compared CCM SOCOL results with atmospheric observations. The comparison showed good agreement between the measurements and results of the model runs driven by SIM and SOLSTICE SSI.

The recent SSI data observed by the Spectral Irradiance Monitor (SIM) and SOLar STellar Irradiance Comparison Instrument (SOLSTICE) on-board the Solar Radiation and Climate Experiment (SORCE) satellite show that ultraviolet (UV) variability is higher than previously observed or calculated with theoretical models (e.g. NRL SSI, see Lean et al., 2005). Figure 1 illustrates this disagreement showing measured and calculated SSI changes between 05.2004 and 02.2009. The SSI variabilities measured by SIM and SOLSTICE in their common part of the spectrum (210–290nm) are also different.

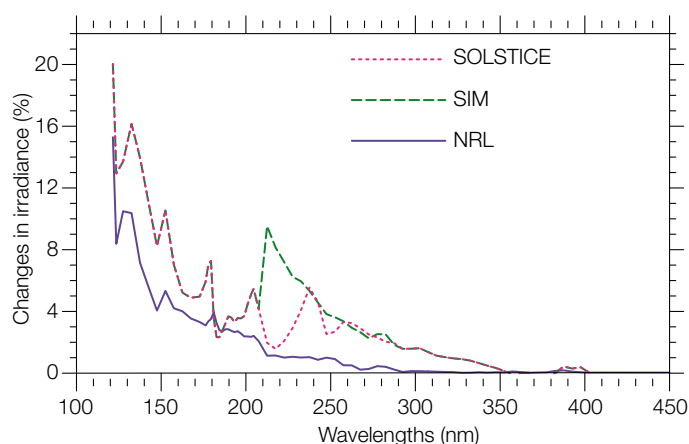


Figure 1. SSI changes between May 2004 and February 2009.

Radiation in the 210–290 nm spectral range strongly affects the middle atmospheric state and composition. To estimate the influence of the difference in the SSI variability on the middle atmosphere we applied the CCM SOCOL model and simulated atmospheric time-series using four different SSI data sets: constant SSI (NO SUN runs), NRL SSI and two composites (SIM and SOLSTICE runs). The first composite was based on SOLSTICE data from 121 to 290 nm and SIM data from 290 to 750 nm. The second composite contains the SOLSTICE SSI from 121 to 210 nm and the remaining part of the used spectrum (210–750 nm) was covered by the SIM irradiance.

We compared the simulated changes with available atmospheric measurements to define which SSI data set gives the best agreement between the modeled and measured evolution of the atmospheric state. For the ozone we used the observations by SBUV/NOAA, SABER/TIMED and SCIAMACHY/ENVISAT.

Figure 2 demonstrates that the simulated O₃ changes between July 2004 and July 2008 are smaller in general than the measured values. On the other hand the ozone changes simulated with SIM and SOLSTICE are closer to measured values. A paper about this investigation is in press (Shapiro et al. (2013)).

We compared the simulated changes with the available atmospheric measurements to define which SSI data set gives the best agreement between the modeled and measured evolution of the atmospheric state. For the ozone we used the observations by SBUV/NOAA, SABER/TIMED and SCIAMACHY/ENVISAT. Fig. 2 demonstrates that the simulated O₃ changes between July 2004 and July 2008 are smaller in general than the measured values. On the other hand the ozone changes simulated with SIM and SOLSTICE are closer to measured values. A more detailed comparison of changes in the middle atmosphere can be found in Shapiro et al. (2013).

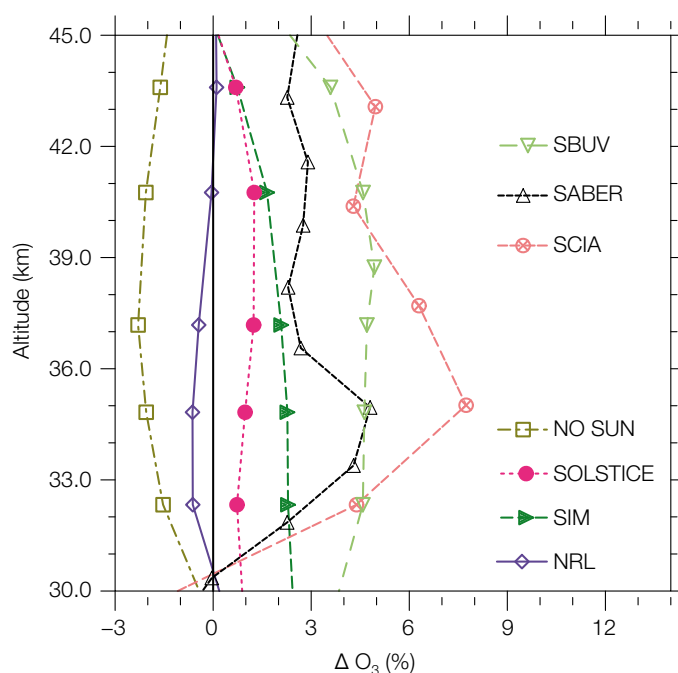


Figure 2. Comparison of the modeled O₃ changes with the changes measured by SBUV, SABER and O₃.

References: Lean J., Rottman G., Harder J., Kopp G.: 2005, SORCE contributions to new understanding of global change and solar variability, *Solar Phys.* 230, 27–53.

Shapiro A.V., Rozanov E.V., Shapiro A.I., Egorova T.A., Harder J., Weber M., Smith A.K., Schmutz W., Peter T.: 2013, The role of the solar irradiance variability in the evolution of the middle atmosphere during 2004–2009, *J. Geophys. Res.*, 118, 1–13, doi:10.1029/2012JD018624.

Solar Variability and Climate Change during the First Half of the 20th Century (SOVAC)

Tatiana Egorova, Eugene Rozanov, and Werner Schmutz in collaboration with FUPSOL team (PMOD/WRC, EAWAG, IAC ETHZ, Bern University and Oeschger Centre for Climate Change Research)

In the SOVAC project we intend to elucidate the causes of observed climate warming during the first half of the 20th century. To address this question we will simulate the climate evolution from 1880 to 1950 using our atmosphere-ocean-chemistry-climate model (AOCCM) SOCOL-MPIOM and the updated reconstructions of all known climate forcings.

Most of the models that participated in the IPCC AR4 experiment failed to reproduce a statistically significant global warming in the first half of the 20th century as well as typical features of its space pattern like e.g., the warming over the continental US and over the Arctic. This problem remains important and should be reinvestigated given the noticeable recent progress in modeling and understanding of past solar irradiance variations.

We will investigate on a series of multi-year ensemble runs of the AOCCM SOCOL-MPIOM driven by all known anthropogenic and natural forcings taken in different combinations to elucidate the effects of anthropogenic factors as well as natural phenomena such as solar spectral irradiance, energetic particle precipitation and volcanic aerosol loading. The seasonal and geographical patterns of the climate change during the considered period will be compared to observational data and reanalysis products to establish the robustness of the obtained climate behavior. The analysis of the sensitivity runs will allow disentangling the contribution of different forcing mechanisms, which are responsible for climate change. The results will have implications for the forecast of future climate change due to the combined effects of anthropogenic and natural factors.

The main modeling tool of the proposed project is AOCCM SOCOL-MPIOM which is a combination of the GCM MA-ECHAM5, dynamic ocean model MPIOM (Marsland et al., 2003) and the chemistry module MEZON. The chemistry-climate part of the model with prescribed sea surface temperature and sea ice concentration has been described and evaluated by Stenke et al. (2012).

The SOVAC project is in the first phase. According to the plan we have installed the model on PMOD/WRC in-house workstations. All necessary forcing and initialization fields for the 1880–1950 model runs including three different scenarios for volcanic and solar irradiance forcing have been prepared. The observational data and statistical tools for the analysis of the results are in preparation.

We have also analyzed the model results for 1850–1960 obtained in the framework of the FUPSOL project to evaluate the behavior of the model driven by a standard set of anthropogenic and natural forcings, which is a necessary step before the start of sensitivity simulations. The climate evolution has been simulated with two 2-member ensemble runs using intermediate and strong solar irradiance forcing as recommended by Shapiro et al. (2011). The anomalies of the surface air temperature during the cold period (November–April) averaged over 20°–60°N are shown in Figure 1.

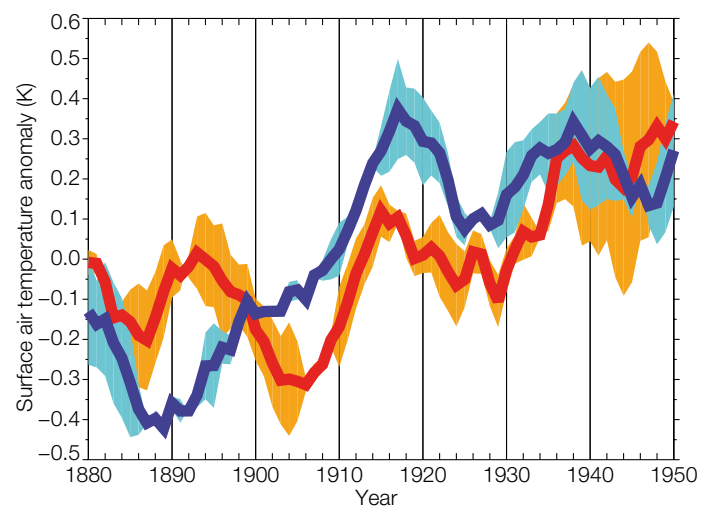


Figure 1. Surface air temperature anomalies during the boreal cold season averaged over 20°–60°N obtained from SOCOL-MPIOM runs driven by intermediate (blue) and strong (red) solar irradiance forcing. The shading indicates the scatter between ensemble members.

The presented results reveal the increase in the surface air temperature from 1900 to 1940 and smaller changes afterwards in general agreement with observations presented by Brönnimann (2009). It is interesting to note some non-homogeneity in the temperature behavior, which will be investigated during the intended sensitivity runs.

References: Brönnimann S.: 2009, Early twentieth-century warming, *Nature Geoscience*, v.2, p.735.

Marsland S.J., Haak H., Jungclaus J.H., Latif M., Roeske F.: 2003, The Max-Planck Institute global ocean/sea ice model with orthogonal curvilinear coordinates, *Ocean Modelling*, 5, 91–127.

Shapiro A., et al.: 2011, A new approach to the long-term reconstruction of the solar irradiance leads to large historical solar forcing, *A&A*, 529.

Stenke A., Schraner M., Rozanov E., Egorova T., Luo B., Peter T.: 2012, The SOCOL version 3.0 chemistry-climate model: description, evaluation, and implications from an advanced transport algorithm, *Geosci. Model Dev. Discuss.*, 5, 3419–3467.

Evaluation of the Stratospheric Climate Change during the Dalton Minimum with AOCCM SOCOL-MPIOM

Eugene Rozanov and Julien Anet in collaboration with FUPSOL team (PMOD/WRC, EAWAG, IAC ETHZ, Bern University, and Oeschger Centre for Climate Change Research)

The SNF-supported FUPSOL project aims to evaluate the solar variability impact on climate and the ozone layer. We analyse the results of experiments with the Atmosphere–Ocean–chemistry–climate model (AOCCM) SOCOL-MPIOM to elucidate the climate response to spectral solar irradiance, volcanic eruptions, and energetic particle precipitation variability during the Dalton Minimum.

The SNF-Sinergia project ‘Future and Past Solar Influence on the Terrestrial Climate’ (FUPSOL) investigates the response of the Earth’s climate to changes in solar spectral irradiance and ionization by different energetic precipitating particles (EPP) for the period 1600 to 2100. Using the AOCCM SOCOL-MPIOM, we successfully performed the first part of our modelling studies, focusing on the Dalton Minimum (DM). This solar activity minimum lasted from around 1790 to 1830 and is characterized by a substantial decrease in solar spectral irradiance (Shapiro et al., 2011), an increase in galactic cosmic ray (GCR) intensity and decrease in solar proton and auroral electron precipitation intensity. During the DM two major volcanic eruptions occurred: an unknown volcano in 1809 ejecting 50 Mt of SO₂ and the Tambora volcano in 1815, ejecting 100 Mt of SO₂ into the atmosphere. To be able to discern among all these climate impacting factors, we perform six 20-year long (1805–1825) runs using different combinations of forcings: (i) all forcings are fixed on the 1805 level, (ii) all forcings are evolving, (iii) only solar UV irradiance is changing, (iv) only solar visible and infrared irradiance is changing, (v) volcanic eruptions are switched on, and (vi) EPP is changing.

Figure 1 shows the ozone change caused by the effect of all considered factors on ozone. The combined effect leads to a significant gain in ozone over the tropics due to the volcanic eruptions. However, in the rest of the atmosphere ozone is depleted due to a decrease in UV radiation – except at the mesospheric poles where a reduced UV irradiance is destroying less ozone. The ozone changes have significant impacts on stratospheric temperatures. Figure 2 illustrates that volcanic aerosols are warming up the lower tropical stratosphere while an overall cooling of up to 5 K is found in the remaining parts of the stratosphere due to a decrease in UV radiation. The cooling in the troposphere is attributed to the decrease in solar visible and infrared irradiance.

Such results might be of great interest when looking towards the next possible future solar minimum (Abreu et al. 2010). Although the current understanding and modelling results predict a recovery of the ozone layer due to decreasing halogen loading during this century, a decrease in UV might partially compensate this gain in ozone. The second, ongoing part of FUPSOL is devoted to the future climate evolution.

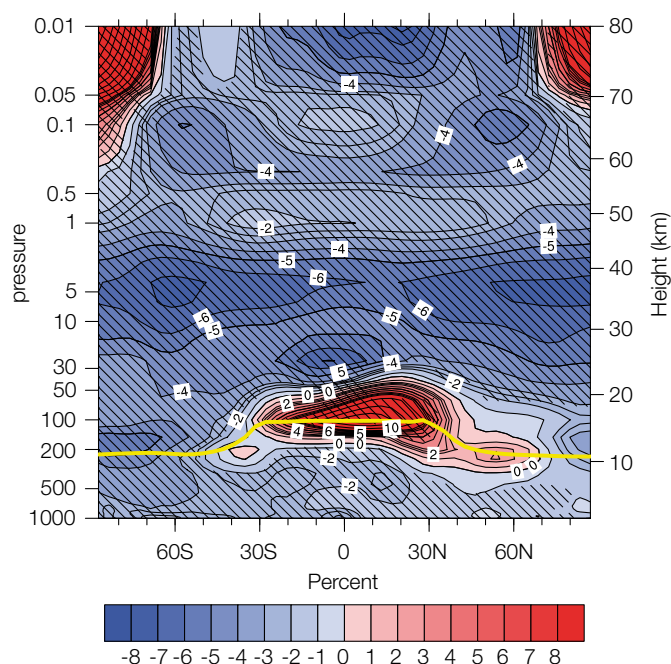


Figure 1. Latitude-height plot of the relative difference in ozone concentration between the reference simulation including all factors and the constant forcing simulation, averaged over the 1805–1825 period. Hatching shows significant differences with a 95% confidence level. The yellow line indicates the height of the WMO tropopause.

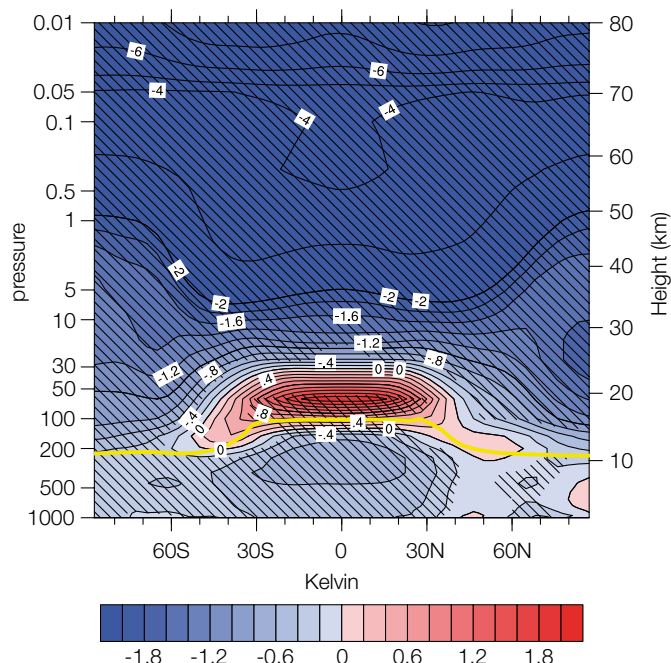


Figure 2. Same as in Fig 1, but for absolute differences in temperature.

References: Abreu J., Beer J., Ferriz-Mas A.: 2010, Past and future solar activity from cosmogenic radionuclides, in: SOHO-23: Understanding a Peculiar Solar Minimum, vol. 428, p. 287.

Shapiro A., et al.: 2011, A new approach to the long-term reconstruction of the solar irradiance leads to large historical solar forcing, A&A, 529.

Development of the Sulfate Aerosol Module for the CCM SOCOL

Eugene Rozanov in collaboration with J. Sheng and T. Peter, IAC ETH, Zurich

The SNF-supported IASSA project aims to assess sulphate aerosol behaviour after proposed geo-engineering by injection of sulphur containing gases. In the second phase of the project we have improved our coupled aerosol-CCM model (AER-SOCOL) and performed simulations under background aerosol conditions. The results are in agreement with the measurements and similar models.

The IASSA project aims to investigate the future climate and ozone evolution assuming different geo-engineering scenarios with a reasonable level of certainty using a coupled aerosol-chemistry-climate model taking into account the main components of the climate system (atmosphere, clouds, land surface, ocean, sea ice, chemical species, and sulphate aerosol) and their interactions.

We introduced a size-dependent composition scheme for sulphuric acid droplets. This novel scheme improved the aerosol module resulting in a decrease in the number of particles in the smallest size bins due to a considerably higher H₂SO₄ vapor pressure. We implemented the emission of sulphur containing gases into our coupled model AER-SOCOL. The emissions include IPCC historic emission and scenario data for SO₂ (anthropogenic, biomass burning, ships). DMS emissions are calculated in the model from its sea concentration. OCS, CS₂ and H₂S boundary conditions are adapted from the AER 2-D model (Weisenstein et al., 1997).

With the new model version we simulated the background aerosol distribution without volcanic eruptions. Figure 1 illustrates the calculated vertical profiles of primary sulphur compounds H₂SO₄, OCS and SO₂ under the background aerosol conditions. The simulated OCS volume mixing ratio agrees with measurements at ground level and above 20 km. The OCS mixing ratio decreases sharply above 20 km due to photolysis in agreement with measurements (not shown). SO₂ near the tropopause is also consistent with the measurements. H₂SO₄ reaches its minimum in the lower stratosphere where homogenous nucleation is most likely to occur. The resulting aerosol layer due to the microphysics is shown in Figure 2.

Figure 2 shows zonal mean aerosol sulphate volume mixing ratio during boreal summer (JJA). The stratospheric aerosol layer is clearly visible in the lower to middle stratosphere reaching maximum values at 20 hPa in the tropics. The results agree well with the ECHAM-SAM model simulation by Hommel et al. (2011) and also with observational data. We are simulating the Pinatubo eruption using the fully coupled AER-SOCOL for further validations.

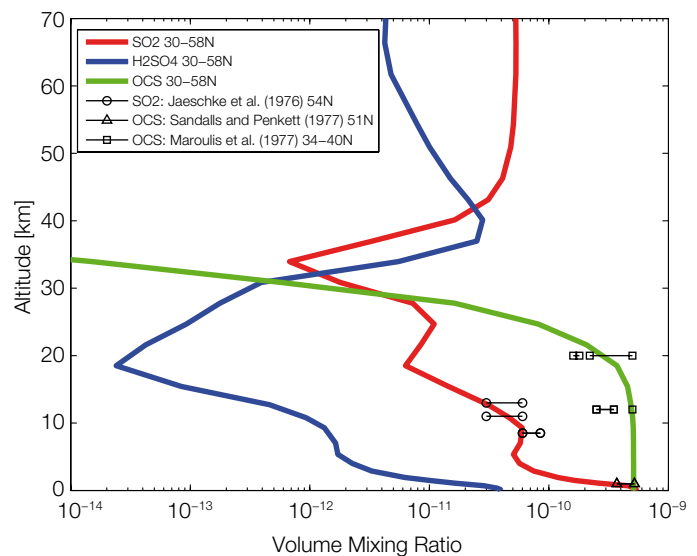


Figure 1. Mixing ratio (mol/mol) of the primary gaseous sulfur compounds H₂SO₄ (blue), SO₂ (red) and OCS (green) simulated by AER-SOCOL. The black data points are the observations.

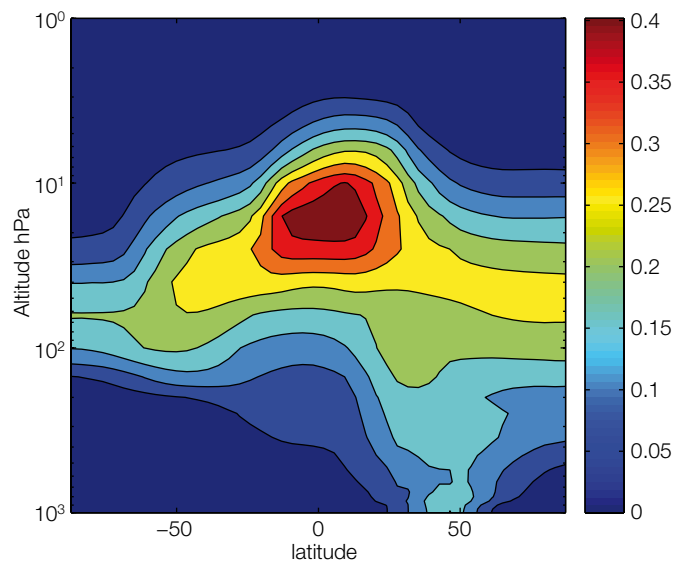


Figure 2. Zonal mean aerosol sulphate volume mixing ratio simulated by the AER-SOCOL for boreal summer (JJA).

References: Hommel R., Timmreck C., Graf H.F.: 2011, The global middle-atmosphere aerosol model MAECHAM5-SAM2: comparison with satellite and in-situ observations, *Geosci. Model Dev.*, 4, 809–834.

Weisenstein D.K., Yue G.K., Ko M.K., Sze N.D., Rodriguez J.M., Scott C.J.: 1997, A two-dimensional model of sulfur species and aerosols. *Journal of Geophysical Research*, 102(D11), 13019–13.

Assessment of the Lifetime of Halogen Source Gases

Eugene Rozanov in collaboration with Andrea Stenke, Fiona Tummon, and Thomas Peter (IAC ETHZ)

We participated in the SPARC Lifetime of Halogen Source Gases Activity, producing and analyzing output from the chemistry-climate model (CCM) SOCOL. Results from the study have been used to make new model lifetime estimates from 1960–2100.

The SPARC Lifetime of Halogen Source Gases activity aims to reduce the uncertainty associated with estimates of the lifetimes of ozone depleting substances (ODSs). As a contribution to this activity, model simulations with CCM SOCOL (Stenke et al., 2012) were carried out for the chapter focusing on global model lifetime estimates.

Species	WMO (2011)	SOCOL 2000	SOCOL 2100
CFC-11	45	52.2	50.7
CFC-12	100	86.4	84.2
CFC-113	85	82.8	81.3
CFC-114	190	173	176
CFC-115*	1020	627	632
N ₂ O	114	110	110
CCl ₄	35	42.6	41.3
CH ₄	12	7.3	8.1
HCFC-22	11.9	9.1	9.9
HCFC-141b	9.2	7.7	7.8
HCFC-142b	17.2	13.6	15.2

Table 1. Lifetimes (in years) of several ozone-depleting substances from the WMO 2011 Ozone Assessment and from SOCOL for 2000 and 2100. *The results for CFC-115 can largely be ignored (see text for details).

Initial results from this work indicate that the lifetimes of certain halogen species under present atmospheric conditions (2000) are currently under- or overestimated (see Table 1). For example, SOCOL simulates CFC-11 and CCl₄ lifetimes that are between 15–20% longer than those given by WMO (2011). Other models participating in the study exhibit similar results. On the other hand, the SOCOL lifetimes of HCFC-141b and HCFC-142b are between 17–22% shorter than proposed by WMO (2011). Again, results are similar for all participating models, suggesting that the WMO lifetime estimates will most likely need to be updated.

During this study, it was found that SOCOL, together with another participating model ULAQ, used reaction rate coefficients for the reaction CFC-115 + O(1D) that were three times higher than those used by the two other models which included this species. This error is likely the main reason for the much shorter CFC-115 lifetime exhibited by SOCOL (see Table 1), and will be corrected in future studies.

In terms of future lifetimes, SOCOL results indicate that the lifetimes of most CFC species will decrease by 2100, largely because of the reduction in anthropogenic ODS species and the resultant decrease in atmospheric concentrations.

Future ozone changes averaged between 80–15hPa are shown in Figure 1. In the tropics, SOCOL suggests a small decrease in ozone (<5%), a feature seen in many models and attributed to an enhancement of the Brewer-Dobson circulation (e.g. Eyring et al., 2007; Oman et al., 2010). In the mid- and high-latitudes SOCOL simulates substantial increases in ozone, which are greater in the southern hemisphere than in the northern hemisphere. These increases are the result of two factors, namely, the reduction in anthropogenic ODS species resulting in less ozone destruction, as well as increased transport of ozone-rich air from the tropics to the mid- and higher latitudes through the enhanced Brewer-Dobson circulation.

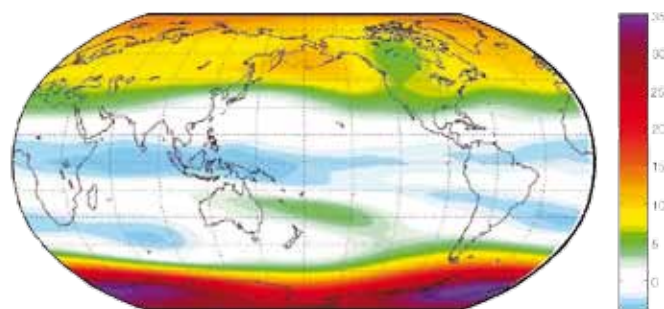


Figure 1. Annual average global ozone change from 2000 to 2100 (in %) averaged between 80–15 hPa and for all years simulated.

- References:
- Eyring V., Waugh D.W., Bodeker G.E., Cordero E., et al.: 2007, Multimodel projections of stratospheric ozone in the 21st century, *J. Geophys. Res.*, 112, doi: 10.1029/2006JD008332.
 - Oman L.D., Plummer D.A., Waugh D.W., Austin J., et al.: 2010, Multimodel assessment of the factors driving stratospheric ozone evolution over the 21st century, *J. Geophys. Res.*, 115, doi: 10.1029/2010JD014362.
 - Stenke A., Schraner M., Rozanov E., Egorova T., Luo B., Peter T.: 2012, The SOCOL version 3.0 chemistry-climate model: description, evaluation, and implications from an advanced transport algorithm, *Geosci. Model Dev. Discuss.*, 5, 3419–3467.
 - WMO, 2011: Scientific Assessment of Ozone Depletion: 2010, Global Ozone Research and Monitoring Project-Report No. 52, 516 pp., Geneva, Switzerland.

Influence of a Carrington-Like Event on Atmospheric Chemistry, Temperature and Climate

Eugene Rozanov in collaboration with Marco Calisto (ISSI, Bern, Switzerland), Ilya Usoskin (Oulu Univ., Finland) and Thomas Peter (IAC ETHZ, Switzerland)

We investigate the effects of a major solar proton event (SPE), similar to the Carrington event which took place in 1859, using the chemistry-climate model (CCM) SOCOL v2.0 and new ionization rate data. The results reveal significant changes of NO_x, HO_x, ozone and surface air temperature mostly over high latitudes. These results suggest that similar events in the future could have a major impact on atmospheric chemistry and the climate.

We have already studied the effects of strong solar proton events (SPE) on the future chemistry and climate (Calisto et al., 2012). However, it was suggested that the particle energy spectrum of the Carrington event should be substantially harder than that considered in this paper and the applied method for the ionization rate calculations does not account for nuclear cascade formation caused by highly (more than 500 MeV) energetic particles. These facts inspired us to revisit the problem.

For this study we have implemented the new ionization rates calculated with the CRAC-CRIL model (Usoskin et al., 2010) for the energy spectrum of the Carrington event retrieved from the scaled data obtained for the 1956 SPE. The new ionization rates properly include nuclear cascade formation and reproduce a Forbush decrease which is typical of such strong SPE events. Using these ionization rates we carried out two 9-month long 10-members ensemble runs with CCM SOCOL v2.0 (Schranner et al., 2008) for the year 2020 conditions. The control run is driven by background ionization rates, while for the experiment we include the ionization rates from the SPE event.

Figure 1 illustrates the response of the reactive nitrogen (NO_x=NO+NO₂) calculated as the relative difference between the experiment and reference runs. The obtained results reveal more substantial changes in NO_x from the mesosphere down to the troposphere in comparison to Calisto et al. (2012) followed by ozone depletion of up to 60%. These changes in the atmospheric state induced by the ozone changes also have an influence on the surface air temperature.

Figure 2 demonstrates the response of the January mean surface air temperature calculated as the absolute difference between the experiment and control runs. It shows that the extreme SPE may lead to a statistically significant winter-time warming of more than 5 K over Europe and Russia.

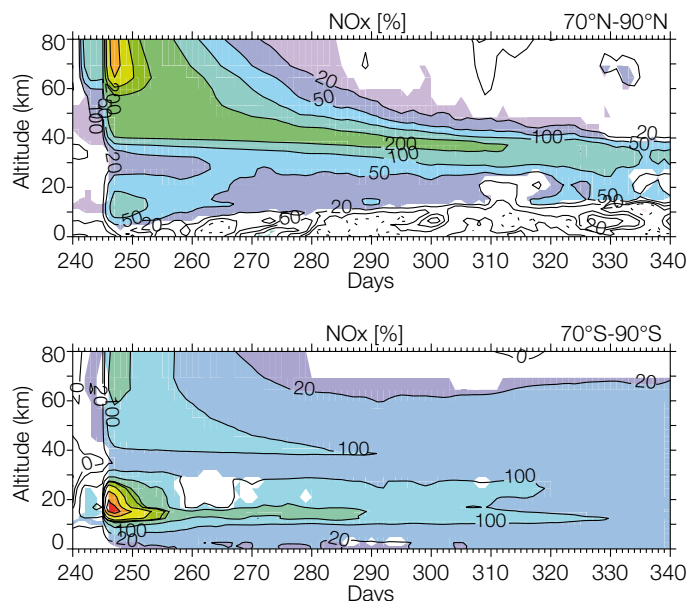


Figure 1. Upper/lower panel shows the changes (%) in zonal mean NO_x mixing ratio profile in the northern/southern Polar Regions (70°–90°). Colors indicate areas with at least 95% statistical significance.

SAT Carrington Usoskin Arctica 1956 January

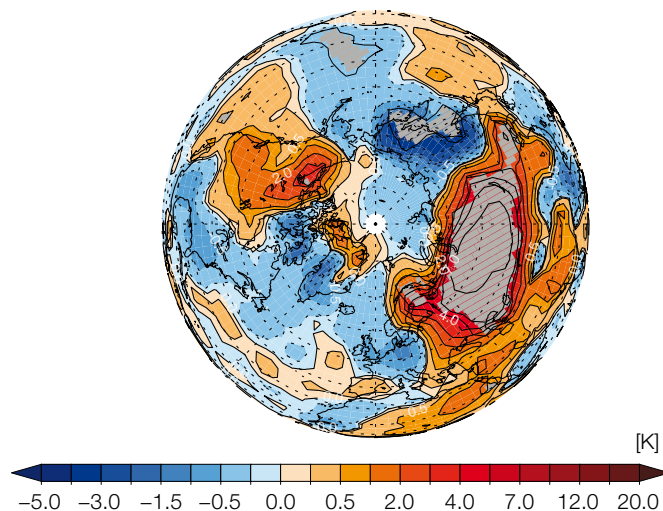


Figure 2. Response of the surface air temperature (K) to the major solar proton event for January. Colors indicate areas with at least 95% statistical significance.

References: Calisto M., Verronen P.T., Rozanov E., Peter T.: 2012, Influence of a Carrington-like event on the atmospheric chemistry, temperature and dynamics, *Atmos. Chem. Phys.*, 12, 8679–8686, doi:10.5194/acp-12-8679-2012.

Schranner M., et al.: 2008, Technical Note: Chemistry-climate model SOCOL: version 2.0 with improved transport and chemistry/microphysics schemes, *Atmos. Chem. Phys.*, 8, 5957–5974.

Usoskin I.G., Kovaltsov G.A., Mironova I.A.: 2010, Cosmic ray induced ionization model CRAC:CRIL: An extension to the upper atmosphere, *J. Geophys. Res.*, 115, D10302.

Stratospheric Circulation under the Montreal Protocol Restrictions

Tatiana Egorova, Eugene Rozanov, and Werner Schmutz

We present an on-going analysis of the simulations performed using the chemistry-climate model (CCM) SOCOL with and without Montreal Protocol and its Amendments (MPA) restrictions. Here we show that the absence of MPA would lead not only to global ozone loss but also to substantial dynamical changes in the stratosphere.

Ozone depletion caused by the absence of MPA (noMPA case), described in Egorova et al. (2012), affects stratospheric temperature and circulation patterns. The changes of the winter-time stratospheric jets in the Northern (NH) and Southern (SH) hemispheres are illustrated in Figure 1 using the zonal wind speed and latitude of the jet maxima. The impact of the greenhouse gases strengthens the jets and slightly extends their upper flanks in a vertical direction. These changes are more pronounced for the noMPA case due to additional cooling in the extra-tropical lower stratosphere.

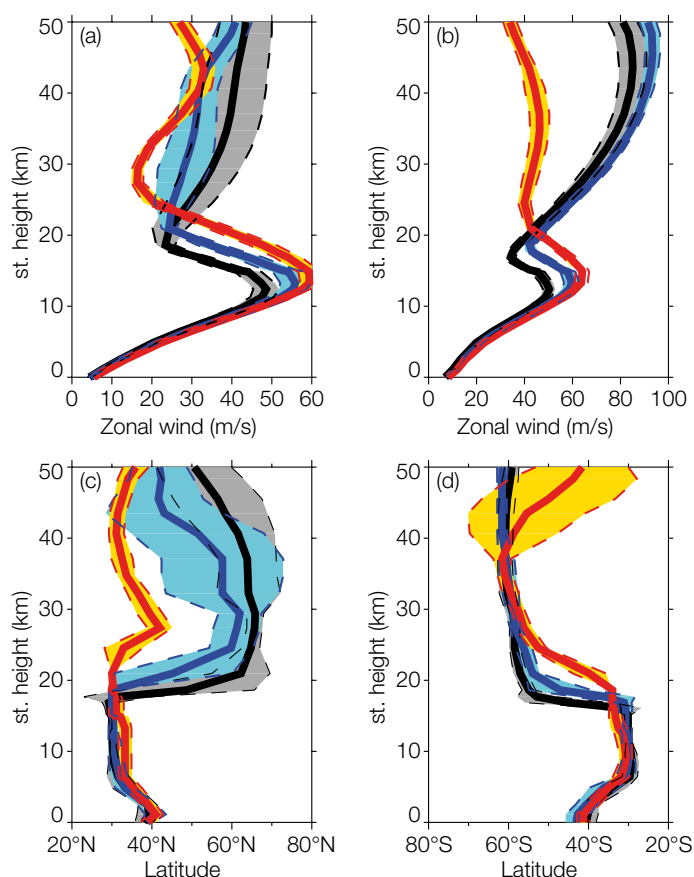


Figure 1. Zonal wind speed (a, b) and latitude of the jet maxima (c, d) for the boreal winter in the NH (a, c) and austral winter in the SH (b, d). The results are for the years 1987–2012 (black lines) and 2090–2100 (blue lines) of the reference run and for the years 2090–2100 of the noMPA run (red lines). The shading indicates standard deviations.

In the NH, some deceleration of the jet is visible between 25 and 45 km, while the latitude of the jet maxima is shifted by about 20° toward the equator. The opposite effects are observed in

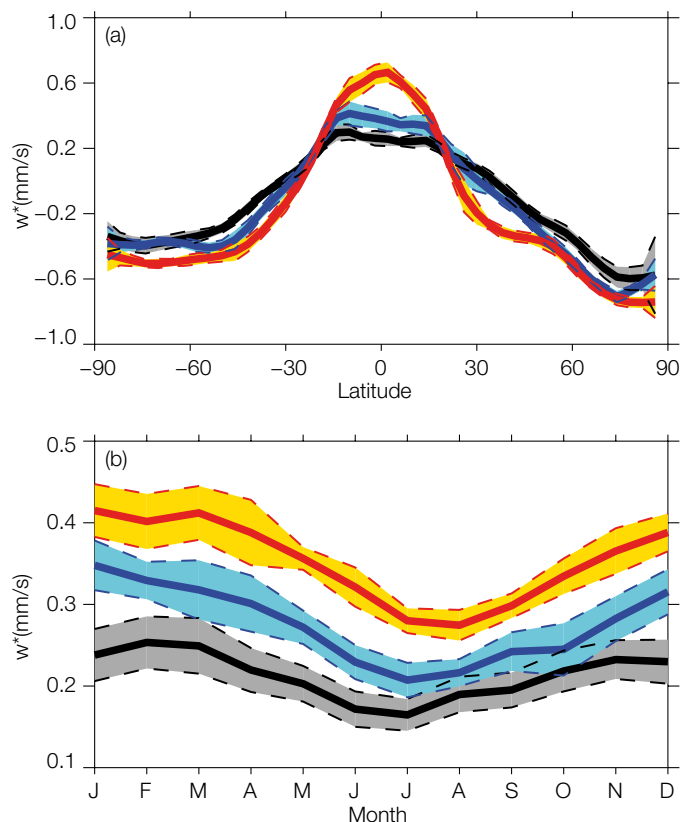


Figure 2. Annual mean (a) and monthly mean (b) residual vertical velocities at 50 hPa averaged over 30°S–30°N. The results are for the years 1987–2012 (black lines) and 2090–2100 (blue lines) of the reference run and for the years 2090–2100 of the noMPA run (red lines). The shading indicates standard deviations.

the SH where the latitude of the jet core moves only slightly equator-ward in the lower and upper stratosphere, while the jet strength reduces by up to 40 m/s. These changes are explained by the strong cooling in the equatorial stratosphere followed by the decrease of the equator-to-pole temperature gradient.

The variations in the wind distribution affect the wave-driven Brewer-Dobson circulation (BDC). The residual vertical velocities (w^*) are presented in Figure 2. The annual mean w^* (Figure 2a) show significant (almost 100%) increases in the tropical area in noMPA case and consistent increases of the downwelling velocities between 30° and 60° in the NH and from 50° and 70° in the SH. The seasonal cycle of the residual vertical velocities in the tropical lower stratosphere (see Figure 2b) shows that the intensification of the tropical upwelling velocities occurs during all months but reaches its maxima during boreal winter. Acceleration and vertical shift of the subtropical jets, and overall weakening and displacement of the polar vortices cause the changes in the BDC.

References: Egorova T., Rozanov E., Groebner J., Hauser M., Schmutz W.: 2012, Montreal Protocol benefits simulated with CCM SOCOL, Atmos. Chem. Phys. Discuss., 12, 17001–17030, www.atmos-chem-phys-discuss.net/12/17001/2012 doi: 10.5194/acpd-12-17001-2012.

Ground-Based Aerosol Optical Depth Time-Series at Three Swiss Sites

Stephan Nyeki, with the collaboration of MeteoSwiss, and Dept. Meteorology, University of Reading, England

Ground-based aerosol optical depth (AOD) time-series at two low-altitude sites in Switzerland (Locarno and Payerne) are updated and re-calibrated for the periods 1994–2013 and 2001–2013, respectively.

Sun-photometer measurements have been continuously conducted at four MeteoSwiss sites in Switzerland as part of the national SACRaM network (Swiss Alpine Climate Radiation Monitoring). Time-series go back as far as the early 1990s, and have recently been reported for the two high-altitude stations at Jungfraujoch (3580 m; 46.55°N, 7.98°E) and Davos (1590 m; 46.82°N, 9.85°E) (Ruckstuhl et al., 2008; Nyeki et al., 2012). This study examines the updated and re-calibrated AOD time-series at the other two low-altitude sites at Locarno (366 m; 46.18°N, 8.78°E) and Payerne (491 m; 46.82°N, 6.94°E).

AOD measurements began in Payerne with the SPM2000 sun-photometer (16 wavelengths in the 368–1024 nm range). These were replaced with precision filter radiometers (PFR) towards the end of 2000 which were then also installed at Locarno. As part of the MeteoSwiss PFR calibration programme, instruments are ‘rotated’ from low to high-altitude sites to allow Langley calibrations to be conducted at the latter. Six PFRs (standard WMO wavelengths: 368, 412, 500 and 862 nm) were calibrated over the 1994 – 2013 period using: 1) the Langley method at the Jungfraujoch and, 2) calibration against reference PFRs at Davos. AOD was determined using WORCC algorithms developed for our GAW-PFR (Global Atmosphere Watch, WMO) network of international PFRs.

The combined uncertainty related to instruments and retrieval algorithms is estimated to result in an AOD uncertainty <0.010 at $\lambda = 500$ nm.

The monthly AOD time-series at Locarno and Payerne are shown in Figure 1a-b, and exhibit weak seasonal cycles. This is more evident when compared to the Davos time-series in Figure 1c which has a distinct cycle. The large number of high AOD events at Locarno and Payerne is typical of sites close to anthropogenic sources as well as sites within the planetary boundary layer. A detailed trend analysis of the 1995 – 2013 Davos time-series gave a statistically non-significant trend (95 % confidence level) of $+0.002/\text{decade}$. In a similar manner to the analysis of the Jungfraujoch and Davos time-series (Nyeki et al., 2012), several rigorous statistical tests (seasonal Kendall test, Sen’s slope estimator, homogeneity tests, trend change tests) will be applied to the Locarno and Payerne data sets in order to establish whether any significant trends in AOD have occurred.

References: Nyeki S., Halios C., Baum W., Eleftheriadis K., Flentje H., Gröbner J., Vuilleumier L., Wehri C.: 2012, Ground-based aerosol optical depth trends at three high-altitude sites in Switzerland and southern Germany from 1995–2010, *J. Geophys. Res.*, 117, D18202, doi: 10.1029/2012JD017493.

Ruckstuhl C., Philipona R., Behrens K., Collaud Coen M., Dürr B., Heimo A., Mätzler C., Nyeki S., Ohmura A., Vuilleumier L., Weller M., Wehri C., Zelenka A.: 2008, Aerosol and cloud effects on solar brightening and the recent rapid warming, *Geophys. Res. Lett.*, 35, L12708, doi: 10.1029/2008GL034228.

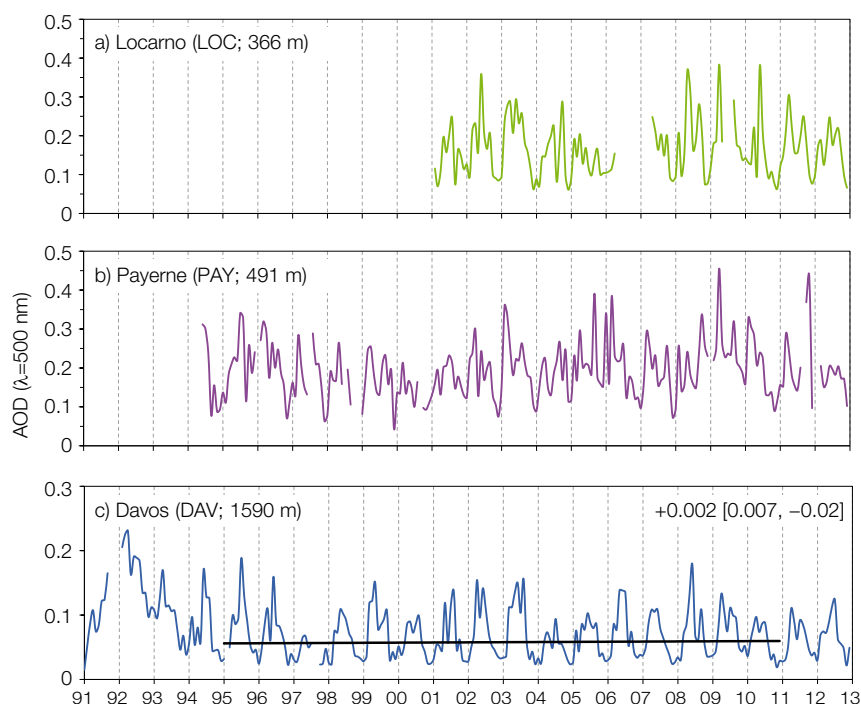


Figure 1. Time-series of monthly AOD average values at MeteoSwiss stations: a) Locarno, b) Payerne, and c) Davos. Trends in AOD units are shown per decade only at Davos as of 1995 when the influence of the 1991 Pinatubo volcanic eruption had diminished to background stratospheric levels. Square brackets denote the 95 % confidence interval.

Spectral Aerosol Optical Depth from a Precision Spectroradiometer

Natalia Kouremeti and Julian Gröbner

Spectral direct solar irradiance from the prototype Precision Spectroradiometer (PSR) was used to retrieve spectral aerosol optical depth which is in good agreement with the measurements from the collocated World AOD reference triad at PMOD/WRC in Davos.

The PSR is designed to measure spectral aerosol optical depth in the 320–1040nm spectral range with a wavelength depending resolution of 1.5 to 3nm. The instrument was operated from April to May 2012 and continuously from October 2012 onwards to measure solar spectra every minute. Between June and September 2012, the PSR participated in the Direct Normal Incidence Field Campaign organised at Payerne, Switzerland in the frame of COST ES 1002.

The standard air mass extrapolation technique (Langley-plot) was used on several clear sky days to retrieve a reference solar spectrum to be used for the retrieval of spectral aerosol optical depth. Figure 1 shows an example of spectral AOD retrieval from the PSR where the absorption of several atmospheric trace gases is highlighted. These absorption features can in turn be used to retrieve their concentrations, as is currently being investigated.

The spectral AOD measured by the PSR at 368nm, 412nm, 500nm, and 862nm was compared with co-located PFR Triad measurements at PMOD/WRC. As shown in Figure 2, the AOD retrieved by the PSR is consistent with the reference values, having a correlation better than 0.995, an absolute agreement ± 0.01 and a root-AOD mean-square error (rmse) less than 0.004. The comparison results fulfill the required WMO criterion for atmospheric AOD determination.

As a next step, we are currently investigating the retrieval of atmospheric column ozone using the Chappuis band (500 to 700nm), and by comparing it to the total column ozone retrieved in the ultraviolet by reference spectroradiometers such as the Brewer spectrophotometer.

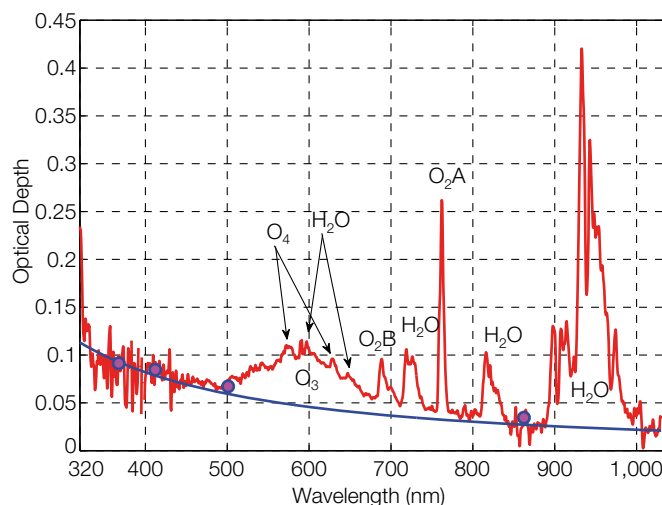


Figure 1. Spectral optical depth from the PSR (red curve) and the retrieved Ångström fit (blue curve) for measurements on 2 May 2012 at Davos, Switzerland. The magenta dots are the aerosol optical depth measurements from the collocated PFR-Triad. The absorption features from several atmospheric trace gases were not subtracted to demonstrate the possibility of using appropriate retrieval procedures to determine their atmospheric concentration.

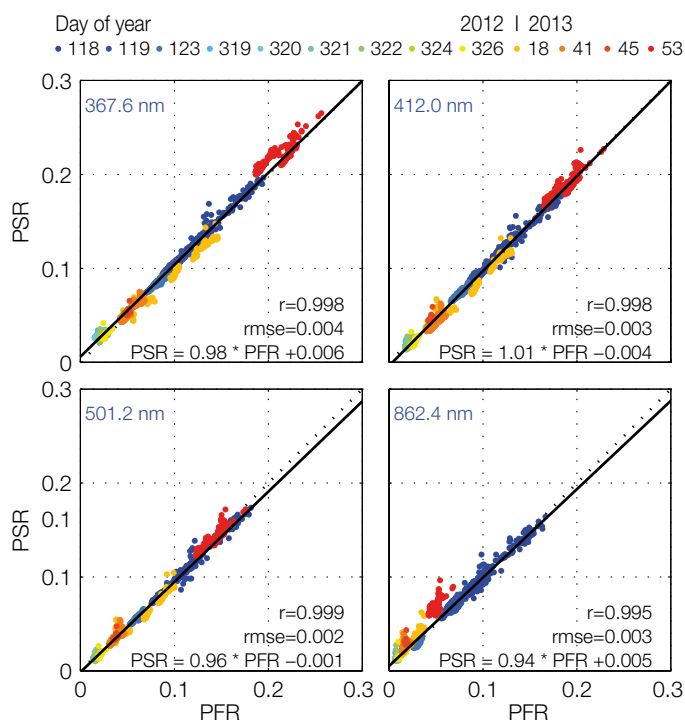


Figure 2. Comparison of AOD measurements between the PSR and the PFR Triad, evaluated at the common PFR wavelengths at the common wavelengths of 368nm, 412nm, 500nm, and 862nm. The different colors represent different days (see legend at top of figure) and the black solid line represents the AOD linear fit. The dashed line represents the ideal case.

Global Dimming and Brightening Trends at Davos

Daniel Lachat and Christoph Wehrli

Atmospheric transmission over Davos derived from pyrhelimeter measurements has shown small but significant trends during Global Dimming and Brightening periods (Lachat and Wehrli, 2012). A pronounced trend of Global Dimming and Brightening was found (Ohmura, 2009) in the global radiation record in the Global Energy Balance Archive (GEBA) for Davos. Here we analyze the relative contribution of transmission and cloudiness towards trends in global radiation.

The amount of solar radiation received at the Earth's surface depends on atmospheric transmission and on total cloud cover. By comparing the global radiation flux under all-weather to clear-sky conditions, the relative contribution of these effects can be quantified.

We estimated the global radiation flux under clear-sky conditions as the sum of the clear-sky direct and diffuse flux component. The direct flux component is derived from daily direct irradiance measurements at the PMOD. The diffuse flux component was simulated using the SMARTS2 radiative transfer model.

The trend periods of Global Dimming from 1953 to 1989 and Global Brightening from 1990 onward are shown in Figure 1 for clear-sky global radiation (upper panel) and all-weather global radiation from the GEBA record (lower panel).

The Dimming period shows a large decrease in all-weather global radiation of -16.7 W/m^2 , of which only -0.9 W/m^2 are explained by the transmission effect reflected in the clear-sky global radiation trend. This suggests changes in cloudiness as a cause.

In contrast, the increase in all-weather global radiation of $+5.5 \text{ W/m}^2$ during the Brightening period is almost entirely explained by changes in transmission reflected by an increase of $+4.7 \text{ W/m}^2$ in clear-sky global radiation. This is particularly interesting, as the record of apparent aerosol transmission over Davos presented in our 2011 annual report suggests a turn-around from the Brightening period to renewed Dimming in 2003. This turn-around is most likely to show up in global radiation as well since the trends in global radiation are dominated by changes in transmission.

References: Lachat D., Wehrli C.: 2012, A century of apparent atmospheric transmission over Davos, Switzerland, *Theoretical and Applied Climatology*, Springer, Vol. 110 Issue 4, 539–547.

Ohmura A.: 2009, Observed decadal variations in surface solar radiation and their causes, *J. Geophys. Res.*, 114, D00D05.

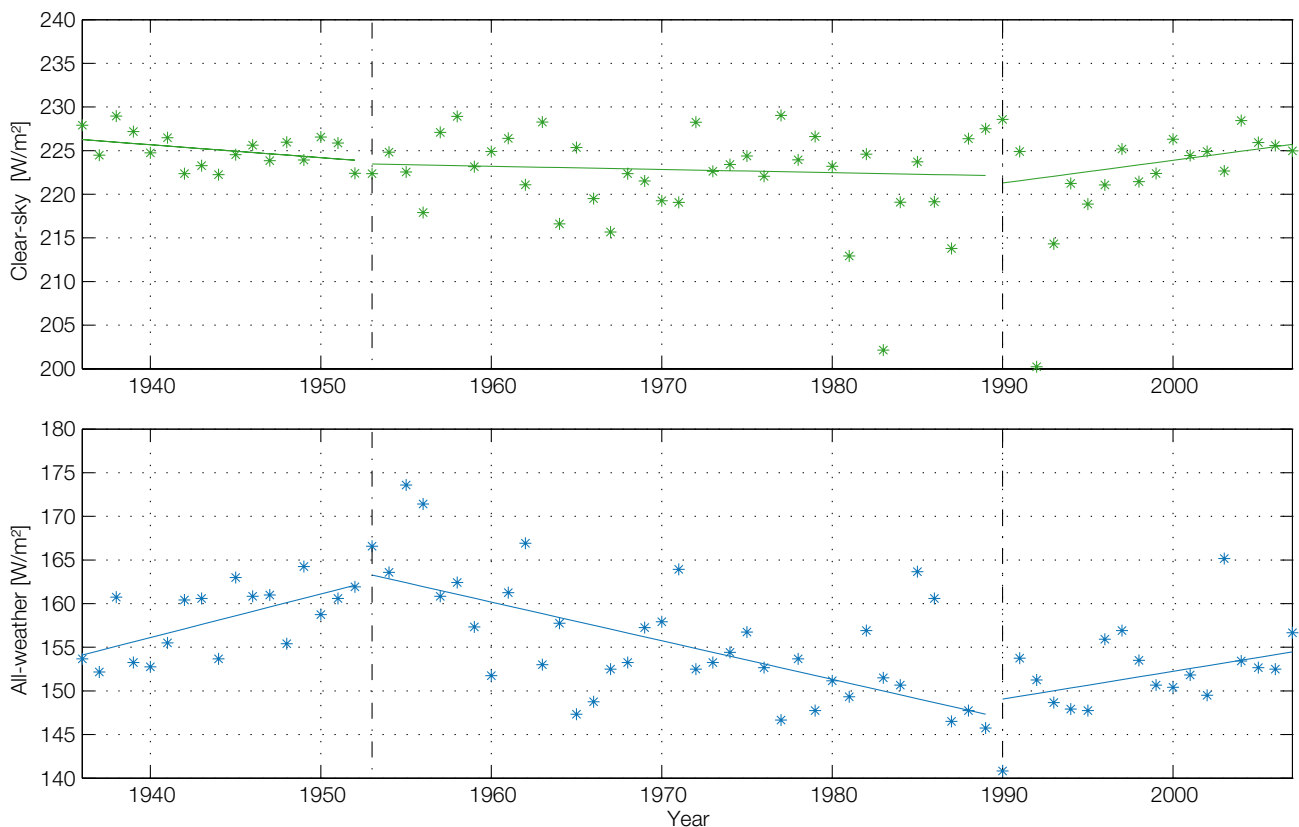


Figure 1. Annual means of clear-sky global radiation reconstructed from measured direct and calculated diffuse radiation (top panel), and measured All-weather global radiation (bottom panel) with trend lines for specified periods of Dimming and Brightening.

Development of a New High Resolution Extraterrestrial Spectrum

Luca Egli, Julian Gröbner, and Alexander Shapiro in collaboration with Medical University, Innsbruck, Austria and ARPA, Aosta, Italy

We present a new high resolution extraterrestrial spectrum (ET) to improve the modeling of solar UV irradiance at the Earth's surface with radiative transfer simulations. The new ET is based on measured and modeled high resolution spectra and was corrected with satellite-based measurements exhibiting a low absolute uncertainty. Validation with 4 different absolutely calibrated ground-based spectroradiometers revealed a similar structure of the deviation in the 296–500 nm wavelength range, which allows the new ET to be readjusted.

High resolution extraterrestrial spectra (ET) are necessary as input to radiative transfer models (e.g. Libradtran, Mayer and Killing 2005) for modeling solar spectra at the Earth's surface using different parameters such as total atmospheric ozone, aerosol optical depth and effective albedo. For this reason we developed an improved ET spectrum covering the 296–1080 nm wavelength range with an increment of 0.01 nm and a slit width resolution of 0.05 nm. The new ET was created by combining different available extraterrestrial and ground-based measurements and model results. First, we used the high resolution ground-based 'Kitt Peak' (KP) spectrum (Kurucz 1994) available for the 296–600 nm wavelength range. Second, to cover the 600–1080 nm wavelength range the spectral lines were modelled at PMOD/WRC with the physically-based code for Solar Irradiance (COSI, Shapiro et al. 2010). Both, the measured and modelled spectra are assumed to correctly display the small-scale structure of spectral lines at a high resolution. However, the absolute irradiance value of the combined ET (KP-COSI) may diverge compared to observed ET. A satellite-based spectrum created by Thuillier et al. (2003) with a low absolute uncertainty was therefore used to adjust KP-COSI to the absolute value of the 'Thuillier' spectrum. Since 'Thuillier' was measured at a relatively low spectral resolution and a bandwidth of about 0.5–1.0 nm, the correction of the KP-COSI spectrum was applied after a convolution of KP-COSI with a constant triangular slit function with a full width half maximum of 1 nm.

The resulting new ET based on 'KP', 'COSI' and 'Thuillier' was validated with 4 different ground-based spectroradiometers at 3 different locations:

1. At PMOD/WRC, Davos Switzerland with the QASUME solar UV reference instrument and the BREWER double monochromator.
2. At ARPA, Aosta, Italy, with a Bentham DTM300 double monochromator.
3. At Jungfraujoch with a Bentham DTM300 double monochromator from the Medical Univ. of Innsbruck.

Both, the global solar UV measurements under clear sky conditions in Davos and Aosta were compared to modeled global irradiance using the Libradtran (Mayer and Kylling 2005) radiative transfer model with the newly created ET as an input.

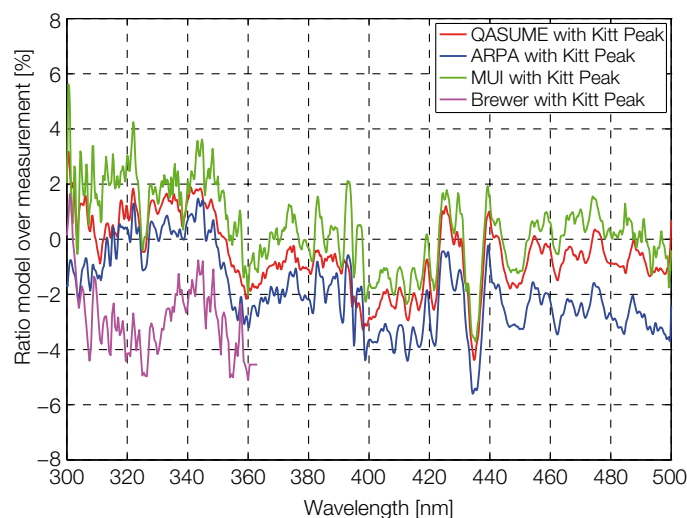


Figure 1. Ratio between modeled spectra using the newly created extraterrestrial (ET) spectrum and ground-based measured spectra with 4 instruments at 3 locations. The ratio is smoothed with a running mean over 3 nm to reduce small scale variations. The comparison shows a similar structure of the fractional deviation for all methods.

The observations at Jungfraujoch were direct sun measurements under clear sky conditions compared with model calculations. The validation revealed that all 4 instruments at all 3 locations showed a similar structure in the fractional deviation from the model calculation to the measurements in the 296–500 nm wavelength range (Figure 1). Remarkably the same structure can be observed when using the 'COSI' spectra only instead of 'KP' and therefore the new ET can be created for the Libradtran model application with only COSI and 'Thuillier'.

The validation results further indicate that the new ET exhibits a reproducible structure for all instruments and locations. This may lead to an additional correction of the new ET in particular for the significant biases in the wavelength regions around 350 and 430 nm. This adjustment could improve the uncertainty of modelled solar UV spectra on earth's surface.

Acknowledgement: The work leading to this study was partly funded by the EMRP ENV03 Project 'Traceability for surface spectral solar ultraviolet radiation'. The EMRP is jointly funded by the EMRP participating countries within EURAMET and the European Union.

References: Mayer B., Kylling A.: 2005, ACP,5,1855–1877.

Kurucz, R.L.: 1994, IAU Symp. 154.

Shapiro A.I., Schmutz W., Schoell M., Haberleiter M., Rozanov E.: 2010, A&A 517, A48; Doi: 10.1051/0004-6361/200913987.

Thuillier G., Hersé M., Labs D., Foujols T., Peetermans W., Gillotay D., Simon P. C., Mandel H.: 2003, Sol. Phys., 224, 1–22.

UV Measurements at Mountain Sites

Gregor Hülsen with the collaboration of Medical Univ. of Innsbruck, and ARPA Aosta

UV data from 4 mountain and 3 valley stations in the Alps was analyzed. The maximum UV index of 13 is present during the summer months on the mountain tops compared to a maximum of 10 in the mountain valleys.

Solar UV measurements are recorded at many mountain sites across the world. These measurements deliver important information for climatology and environmental studies. Because of the increase of mountaineering activities at remote mountain locations and skiing activities in the mountains, UV measurements also serve as an important health indicator.

Solar UV measurements from the European alpine stations at Davos in Switzerland, the Italian Valle d'Aosta region and the Austrian UV measurement network are distributed across the Alps. The selected measurement sites are representative of alpine resorts and cities with many activities both in summer and winter.

Here, we analyze UV data from seven stations in the European Alps for the years 2007 to 2012. High altitude stations include: Weissfluhjoch (Davos, Switzerland, 2540 m a.s.l.), Plateau Rosa (Valle de Aosta, Italy, 3500 m), Sonnblick (Austria, 3106 m) and Hafelekar (Innsbruck, Austria, 2275 m). In addition, data from three alpine valley stations was investigated: Davos (Switzerland, 1610 m), Aosta (Italy, 569 m) and Innsbruck (Austria, 577 m).

The UV levels reach values up to 13 in the Alps at high altitudes compared to 10 in the low valleys (see Figures 1–3). Of special interest are the touristic summer months for mountaineering in the Alps in July–September. The high season for skiing activities in the Alps is from December till April, where the high reflectivity of snow increases additionally the human UV exposure. At the high altitude sites the skiing extends into the summer season. At the end of April, the UV Index can be as high as 11 at altitudes above 2000 m a.s.l. and 8 in the valleys. In the summer season, the UV Index is around 8 in the low valleys and goes up to 13 on the top of the mountains.

Outlook: In the future, data from the Andes mountain range will be analyzed. In the southern hemisphere, UV networks in Argentina and Peru provide measurements across the Andes. Marcapomacocha is the highest UV-B station in Peru at 4500 m, with Arequipa at 2300 m and Cusco at 3400 m. Another representative Andes station is La Quiaca, which is the highest Argentinian UV station (3459 m) located at the border between Argentina, Bolivia and Chile (see <http://gaw.empa.ch/gawsis/reports.asp?StationID=202>). The erythemal weighted UV data will be converted to a Vitamin D weighted dataset. This analysis will enable mountaineers to weigh-up the beneficial and harmful effects of UV radiation.

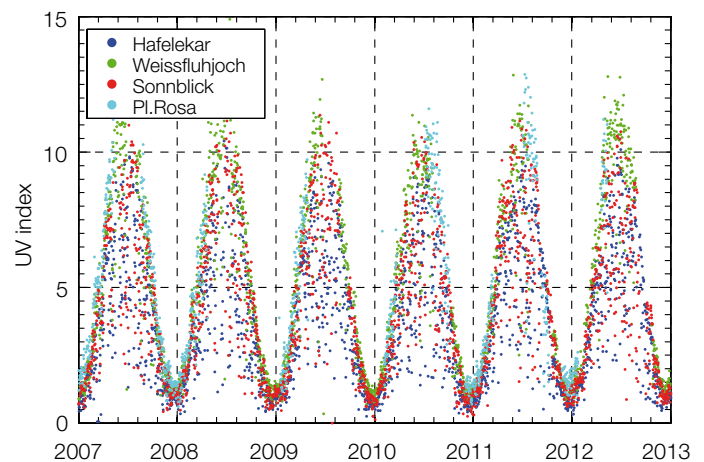


Figure 1. UV index for 4 high altitude stations: Weissfluhjoch, Plateau Rosa, Sonnblick and Hafelekar. Plotted are the daily maxima.

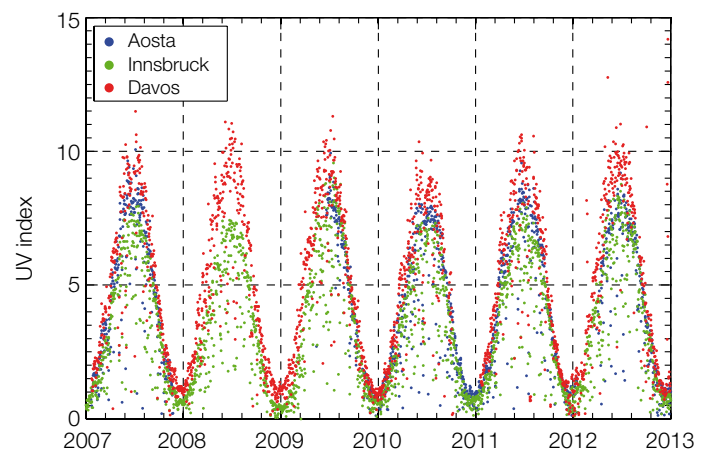


Figure 2. UV index for 3 alpine valley stations: Davos, Aosta and Innsbruck. The daily maxima are plotted.

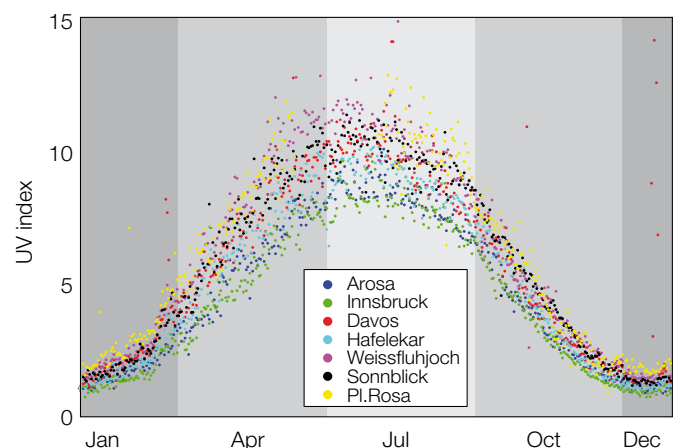


Figure 3. UV index for all stations listed in Figure 1 and 2. Maxima in the years 2007 to 2012 are plotted.

Determination of Fractional Cloud Cover and Cloud Type Using Sky Cameras

Stefan Wacker and Julian Gröbner

Hemispherical sky cameras were installed at four Swiss sites to calculate fractional cloud cover and to determine cloud type on a routine basis with a high temporal resolution during daytime. Cloud type is correctly classified at a mean score of 90% when one unique cloud class occurs in the image. Otherwise the overall performance of the cloud type algorithm decreases and is between 40 and 60%.

Clouds greatly impact the Earth's radiation budget and hence the climate. However, clouds and their feedbacks on climate remain the largest source of uncertainty in the simulation of climate changes. These uncertainties mainly emerge from insufficient cloud observations due to the absence of an automated observing system designed to monitor changes in cloud type and cover. Meanwhile, cloudiness is regarded as a priority 2 Essential Climate Variable (ECV) by the WMO which means that there is consensus that continuous observations of this climate variable are essential to study climate change. Various national weather services are currently evaluating which methods are most suitable for replacing human cloud observations.

In order to test novel and cost effective methods, we installed four hemispherical sky cameras over the last two years at Payerne, Zimmerwald, Davos and Jungfrauoch. The camera system allows the fractional cloud cover to be calculated with a 1-minute resolution. This is accomplished by calculating the ratios of the blue to the green channel and blue to the red channel for each pixel which are then compared to a reference value. Cloud cover can be reliably calculated with an uncertainty of about 5%.

We have also tested an algorithm to classify the images into seven different cloud classes (see Heinle et al., 2010): cirrus-cirrostratus (ci-cs), cirrocumulus-altocumulus (cc-ac), stratus-altostratus (st-as), cumulus (cu), stratocumulus (sc), cumulonimbus-nimbostratus (cb-ns) and cloud-free (cf). The cloud type classification algorithm is based on a set of statistical features describing the color and the texture of an image. We generated a training sample from the Payerne data set by visual inspection of the images. In order to train the algorithm, the images of the training set contain only one single cloud class. The training set contains 200 pictures for each cloud class. The performance of the algorithm is illustrated in Figure 2: The score of correctly classified images is over 80% for all cloud types except for cirrocumulus-altocumulus: The algorithm recognizes only 50% of the images containing cirrocumulus and altocumulus while it misclassifies 30% and 10% of these images as cumulus and cirrus-cirrusstratus/stratocumulus, respectively.



Figure 1. Hemispherical sky image taken on the 10/8/2012 at Jungfrauoch.

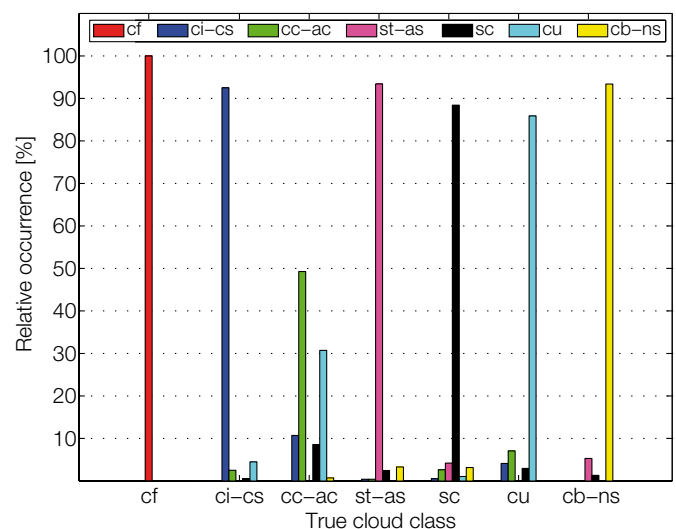


Figure 2. Scores of correct and incorrect cloud type classification for the Payerne training set. The y-axis represents the relative occurrences of the predicted cloud types for the respective true cloud classes. The true cloud class in an image was determined by human observers. The training set contains approximately 1400 images or 200 images for each cloud class.

We have also tested the cloud type algorithm using independent test samples at all four stations which contain images not necessarily showing one unique cloud class as the training sample does. The mean score of the correctly classified images substantially decreases and is typically between 40 and 60%. While the score of a correct classification for cumulonimbus-nimbostratus and cloud-free conditions is between 60 and 100%, the classification of the other cloud classes is more problematic.

References: Heinle A., Macke A., Srivastav A.: 2010, Automatic cloud classification of whole sky images, Atmospheric Measurement Techniques, 3, doi: 10.5194/amt-3-557-2010.

Correlation of Spectral with Total Solar Irradiance on VIRGO

Christoph Wehrli, Werner Schmutz, and Alexander Shapiro

We have analysed Spectral Solar Irradiance measurements with SPM-B on VIRGO and found a robust, positive correlation of spectral with total irradiance in monthly data since 2002. Annual averages of these data show weak negative correlations in the 862 nm and 402 nm channels, but the 500 nm remains positively correlated with Total Solar Irradiance (TSI).

The variability of Solar Spectral Irradiance (SSI) over the rotational period and its trend over the solar activity cycle are important for understanding the Sun – Earth connection as well as for observational constraints for solar models. Recently, the SIM experiment on SORCE has published an anti-correlation with TSI on the 11-year cycle for the visual spectral range (Harder et al., 2009). This result was unexpected for the solar community, and if true, has impact on the understanding of solar influence on the climate.

VIRGO has measured TSI and SSI at three wavelengths (862, 500, and 402 nm) since January 1996. This long time-series is analysed in order to verify whether the anti-correlated SIM/SORCE trend in the visual spectral range is confirmed by independent VIRGO observations.

The challenge of all space experiments in observing the Sun is a change in sensor sensitivity due to exposure to intense UV and particulate radiation. The measurements thus represent the product of solar variability and instrumental degradation that is difficult to factorize.

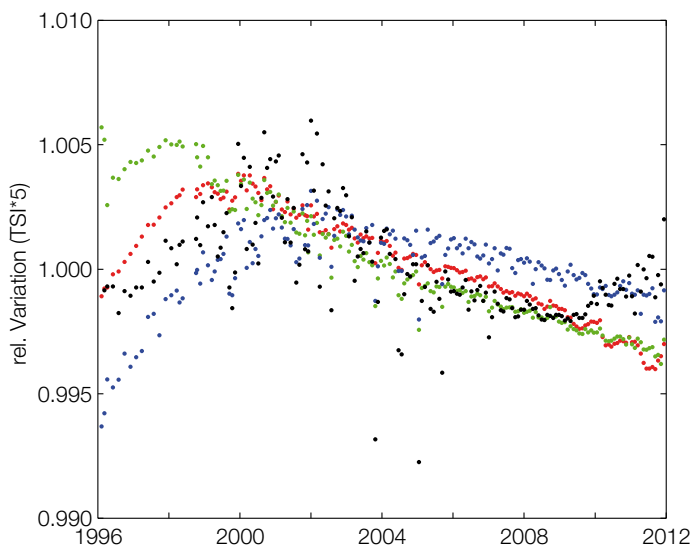


Figure 1. Variations relative to mean of uncorrected VIRGO SSI (red, green, and blue) measurements. Corresponding TSI variations (black) are fully corrected for instrumental drift and expanded by a factor of 5.

The rarely exposed (every 30 days) backup instrument SPM-B has maintained more than 99% of its initial sensitivity over the SOHO mission. As its relative variations (Fig. 1) are about 5 times larger than the corresponding TSI variations we conclude that these variations are dominated by instrumental effects. Ignoring VIRGO data prior 2002, we approximate the instrumental degradation since 2002 by a linear regression and correlate linearly detrended SSI data with the variability of corresponding TSI measurements.

	SSI-862	SSI-500	SSI-402
TSI 30 d	0.25 [0.08, 0.41]	0.87 [0.83, 0.91]	0.48 [0.33, 0.60]
TSI 1 y	-0.58 [-0.88, 0.03]	0.91 [0.68, 0.98]	-0.43 [-0.82, 0.23]

Table 1. Correlation coefficients for relative variations in TSI and SSI channels with 95% uncertainties in brackets. Results for monthly snapshot values in 1st row, for annual means in 2nd row.

Due to the 30-day sampling rate, the correlation for spectral backup data may represent a mixture of solar cycle and solar rotation activity. While annual average correlations at 862 nm and 402 nm are negative, though not significant at the 2 σ level, that at 500 nm remains significantly positive. This finding is corroborated by a robust linear regression between TSI and SSI variations, shown in Fig. 2.

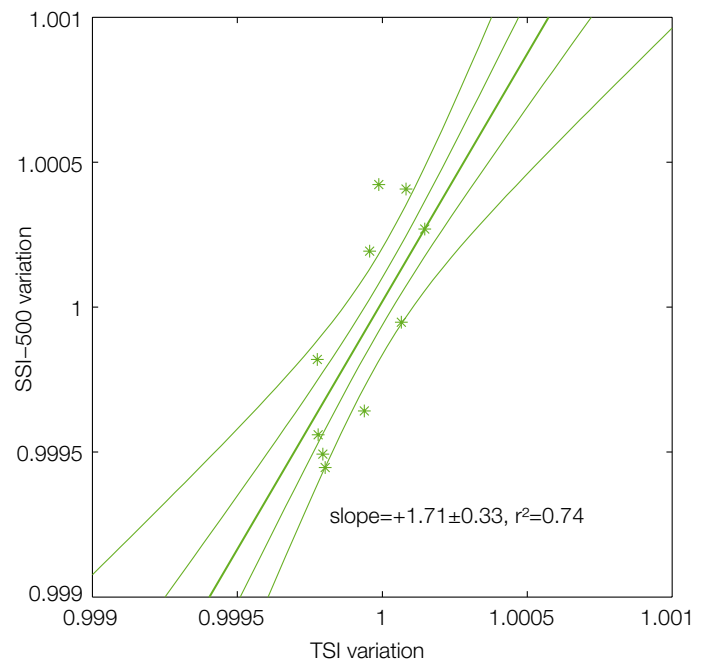


Figure 2. VIRGO SSI-500 nm versus TSI variations based on annual means from 2002 to 2012. Solid lines indicate the robust linear regression, the dash dot and dashed lines show 1 σ and 2 σ uncertainties.

References: Harder J.W., Fontenla J.M., Pilewskie P., Richard E.C., Wood T.N.: 2009, Trends in solar spectral irradiance variability in the visible and infrared, *Geophys. Res. Lett.*, 36, L07801.

Spectral Solar Irradiance as Observed by PREMOS/PICARD

Gaël Cessateur, Werner Schmutz, Alexander Shapiro in collaboration with CNES, Paris, France

The PREMOS instrument onboard the French PICARD mission measures Spectral Solar Irradiance (SSI) in five spectral channels. We present here the first results from the solar spectral radiometer. Degradation for the continuous exposed channels is severe but head B preserves its sensitivity.

PREMOS was launched in June 2010, and has been measuring solar irradiance continuously since the 6 September 2010. The solar spectral radiometer observes the irradiance at six different wavelengths as given in Table 1.

Head A	Head B	Head C
210 nm	215 nm	210 nm
535 nm	607 nm	535 nm
782 nm	215 nm	782 nm
266 nm	607 nm	266 nm

Table 1. Wavelength characteristics of the PREMOS filter radiometers.

The optical and near IR filters are identical to the filters of the PICARD SODISM instrument as well as the 215 nm filter, while the 210 nm filter was chosen to match the Herzberg filter implemented on the LYRA/PROBA2 instrument (Hochedez et al, 2006). The PREMOS filter radiometer therefore covers an important part of the spectral range.

PREMOS is composed of 12 channels i.e. three 4-channel instruments, where a redundancy strategy was established in order to estimate sensitivity loss due to sunlight exposure. One channel (Head A) is operated continuously (six measurements per minute with an integration time of 9.911 seconds for the normal mode), while its back-up channel (Head C) is exposed only once per day for 3 minutes. Finally, the Head B channel is a self-consistent system with twice the same channels; the first pair is exposed every fourth orbit for one minute, while the second pair is exposed once per week for about 2 minutes.

Head A has experienced a pronounced degradation since we have lost more than 99% of the signal for both UV channels and about 45% for the visible channel while more than 86% of the signal remains for the near IR channel. This degradation has most probably been induced by the polymerization of surface contaminants on filters under the solar UV exposure. However, the degradation is not a linear function of time in the visible and near-infrared channels, which complicates our ability to determine the solar variability for those spectral ranges. This problem is currently under investigation. The back-up Head C has also experienced a loss of sensitivity of about 15% in the UV channels.

The back-up channel from Head B has only been exposed less than 4 hours, and is thus a powerful tool for assessing the degradation of all UV and visible channels. Figure 1 represents a direct comparison between the 215 nm PREMOS Head B channel and SOLSTICE/SORCE measurements. Both curves have been corrected independently, and show a good correlation. In addition, PREMOS measurements give us more precise information about the 13.5 day modulation, which is critical for climate modeling.

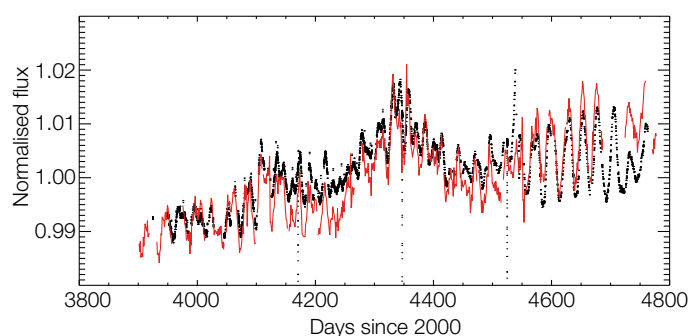


Figure 1. Normalized time-series for PREMOS (in black) and SOLSTICE (in red) at 215 nm from September 2010 to February 2013.

References: Hochedez J.-F., Schmutz W., Stockman Y., et al.: 2006, LYRA, a solar UV radiometer on Proba2 Advances in Space Research, 37, 303–312.

The PREMOS/PICARD Total Solar Irradiance (TSI) Time-Series

André Fehlmann, Werner Schmutz, and Wolfgang Finsterle

After more than two years in space the PREMOS absolute radiometers on the French PICARD satellite still work perfectly. The primary instrument PREMOS A is continuously measuring the Total Solar Irradiance (TSI). The back-up instrument PREMOS B records data in a bi-weekly interval for 90 minutes in order to track the sensitivity degradation of the primary radiometer. Correcting for the sensitivity degradation and removing otherwise distorted data yields the PREMOS TSI time series.

Although the orbit of the PICARD satellite has been selected to maximize the visibility of the Sun, there are periods where the Sun is either occulted by the Earth or the instruments observe the Sun through the Earth's atmosphere. During eclipses the PREMOS radiometers are normally set to night-mode where the instruments are protected by a front cover. However, TSI values measured through the atmosphere are lower due to absorption. The PICARD data center provides an orbit event file indicating the periods where the Sun is observed through the atmosphere. The same file also contains information about lunar eclipses, passages through the South Atlantic Anomaly (SAA) and stellar pointings where the satellite is pointed to a star rather than the Sun for calibration purposes. We exclude all these data to obtain a clean raw PREMOS/PICARD TSI time-series.

The ratio of PREMOS A/B (c. f. Figure 1) can then be used to correct for the sensitivity degradation of the primary radiometer A. During the first few days of exposure, the sensitivity of our radiometers increased linearly rather than decreased. An analysis showed that this increase can be considered identical for both instruments. After the increase, we found a stable plateau phase where the sensitivity of PREMOS A does not change. The third distinct phase is the ongoing decrease of sensitivity. We use a linear fit to the PREMOS A/B ratio during the increasing and the plateau phases. For the decreasing phase, we apply a piecewise cubic spline interpolation to describe the sensitivity change. Figure 2 shows the full PREMOS TSI time-series as well as the PREMOS/PICARD to TIM/SORCE ratio which shows no significant trend over the two-year operation period of PREMOS.

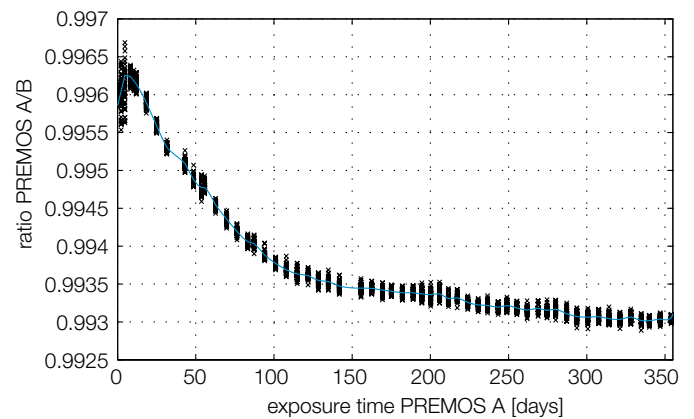


Figure 1. Ratio of the PREMOS radiometers A to B. The continuing degradation of the PREMOS A instrument cannot be described by an analytical function. We use a piecewise cubic spline interpolation to determine the sensitivity change correction. This technique also considers the apparent bumps in the ratio, e.g. after 55 or 80 days of exposure.

The standard deviation of the PREMOS to TIM ratio is 35 parts per million.

We use a linear fit to the PREMOS A/B ratio during the increasing and the plateau phases. For the decreasing phase, we apply a piecewise cubic spline interpolation to describe the sensitivity change. Attempts to fit an exponential or double exponential function to the decreasing phase yielded very poor results. Although it has no physical basis, the cubic spline interpolation thus provides the best correction function. Figure 2 shows the full PREMOS TSI time-series as well as the PREMOS/PICARD to TIM/SORCE ratio which shows no significant trend over the two-year operation period of PREMOS.

References: Fehlmann A.: 2012, Metrology of Solar Irradiance, PhD Thesis, University of Zürich.

Fehlmann A., Kopp G., Schmutz W., Winkler R., Finsterle, W., Fox N.: 2012, Fourth World Radiometric Reference to SI radiometric scale comparison and implications for on-orbit measurements of the total solar irradiance, Metrologia 49, 34.

Schmutz W., Fehlmann A., Hülsen G., et al.: 2009, The PREMOS/PICARD instrument calibration, Metrologia 46, S202.

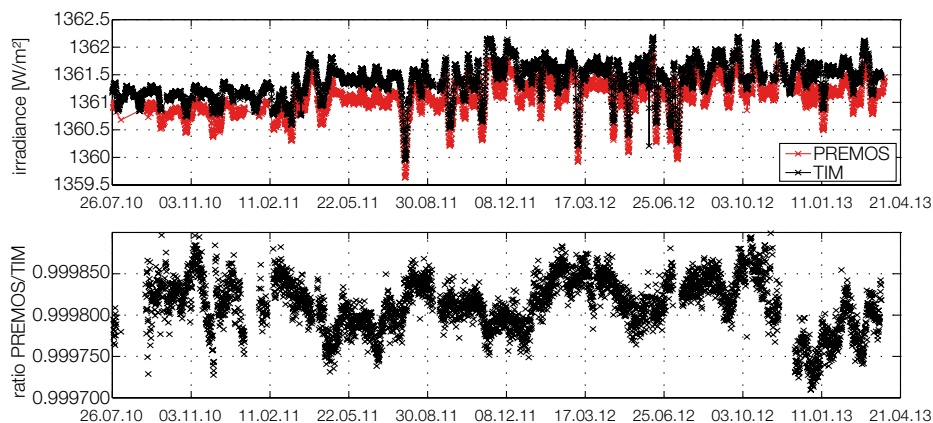


Figure 2. Upper panel: The measured 6-hourly mean PREMOS and TIM TSI values. Lower panel: The ratio of PREMOS/PICARD and TIM/SORCE shows no significant trend.

Modeling of the Spectral Solar Irradiance

Gaël Cessateur, Alexander Shapiro, Werner Schmutz in collaboration with MPI, Lindau, Germany

PREMOS measurements constitute an excellent opportunity for solar modeling purposes. By using HMI/SDO data in order to determine the filling factors for different features, we are able to reproduce the level of variability of the solar irradiance by using generic spectra provided by the COSI code.

In order to compare the Solar Spectral Irradiance (SSI) as observed by PREMOS to modeled irradiance variations, we decompose HMI/SDO data in different activity regions. The main assumption of our model is that the variability in SSI is directly connected to the solar magnetic surface evolution (Fligge, Solanki and Unruh, 2000). A specific radiance is associated with each different feature, such as plages, sunspots, the quiet Sun, or network. The total sum is assumed to represent the variability in solar irradiance at a specific wavelength. A synthetic spectra is then calculated for each feature with the COSI model (Shapiro et al, 2010).

In order to discriminate the filling factor for each feature, we use the HMI/SDO data as provided by N. Krivova, S. Solanki and K.L. Yeo from the MPI, Lindau, Germany. A first attempt has been made at 215 nm, as displayed in Figure 1. There is a very good correlation between the PREMOS data and our model. We also compare the PREMOS data to the SORCE measurement. The correlation is not as good as with our model. Because of instrumental degradation, the deviation of the SORCE measurement is today very high, which complicates merely the use of the SORCE data for solar physics purposes. Same results have been obtained for the 607 nm channel: the solar modulation induced by the rotation is very well reproduced. Further studies such as a direct comparison of our measurement with the SOLSPEC data are planned in order to more carefully assess the degradation of PREMOS.

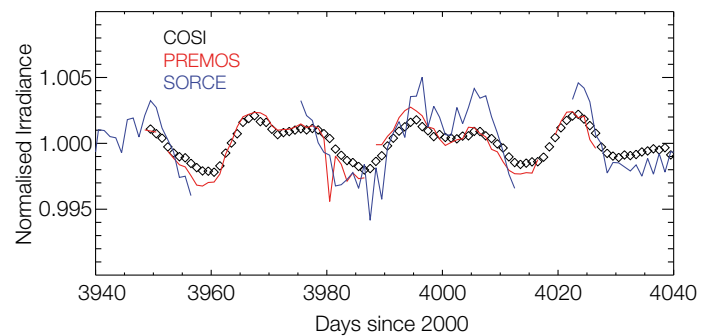


Figure 1. Daily Spectral Solar Irradiance comparison at 215 nm from PREMOS (red thick line), from SORCE/SOLSTICE (in blue), and the COSI model (black diamond) over three months (September–December 2010).

- References:
- Fligge M., Solanki S.K., Unruh Y.C.: 2000, Modelling irradiance variations from the surface distribution of the solar magnetic field. *A&A*, 353, 380–388.
 - Shapiro A.I., Schmutz W., Schoell M., Haberreiter M., Rozanov E.: 2010, NLTE solar irradiance modeling with the COSI code. *A&A*, 517, A48.

Modeling of Variations in the EUV Spectral Irradiance

Margit Haberreiter in collaboration with the Royal Observatory Belgium

Variations of the solar spectral irradiance in the EUV spectral range have an important impact on the terrestrial ionospheric density and temperature. Here we discuss latest improvements of our approach to model the EUV.

Solar EUV radiation is emitted from a wide range of layers in the solar atmosphere, i.e. the chromosphere, transition region and corona. Therefore, to model the solar EUV variation correctly, models of the different regimes are required. For the reconstruction of the EUV we use the approach presented by Haberreiter (2011, 2012), employing the Solar Modeling (SolMod) code. Furthermore, the chromospheric and transition region models by Fontenla et al. (2009) are used along with coronal models presented by Haberreiter (2012).

For understanding the variations originating in the corona, we analyze images taken by the Extreme UV Imaging Telescope (Delaboudinière et al. 1995) onboard SOHO. Currently, the identification of the features in the corona is based on a 3-component model, i.e. accounting for the quiet Sun, active regions and coronal holes. Figure 1 shows the reconstruction of the SOHO/SEM spectral range from 26 to 34 nm based on two data sets, the Barra et al. (2009) study, denoted as ‘SolMod - B2009’, and for further testing the analysis carried out by Verbeeck et al. (2013), denoted as ‘SolMod - V2013’. The latter analysis is derived from a combination of two spectral EIT channels (the 171 and 195 Å) which explains the lower solar cycle variation in the reconstruction.

Figure 2 shows a 2-month close-up of a detailed reconstruction study. The comparison shows that the overall variation of the observations is captured reasonably well with the SolMod reconstruction, however, the variation is partly overestimated. The reason for this is that with the 3-component model the active regions are represented too coarsely, leading to an overestimation of the bright areas.

In collaboration with the Royal Observatory in Belgium, further developments are made regarding the identification of up to six coronal features. This will be improved within the recently started FP7 Space Project SOLID. Also, within SOLID we will employ images taken with the Precision Solar Photometric Telescope (PSPT) located in Rome and Hawaii to model the variability of the underlying chromosphere and transition region. This approach is expected to improve the final reconstruction.

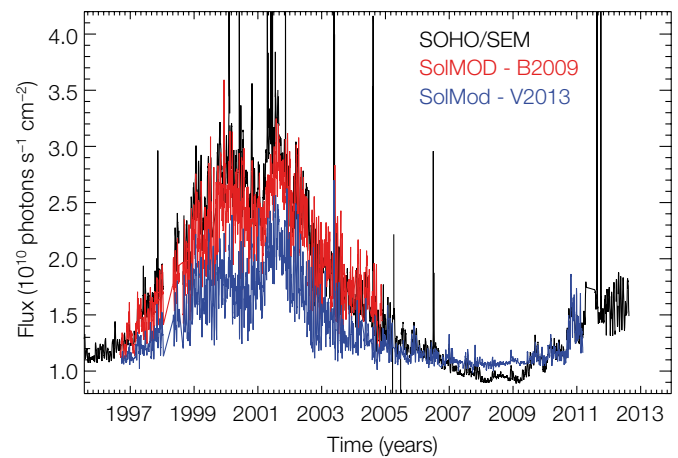


Figure 1. Reconstruction of the EUV based on two segmentation analyses, B2009 and V2013. The number of features identified from the solar corona will be improved in future SOLID studies.

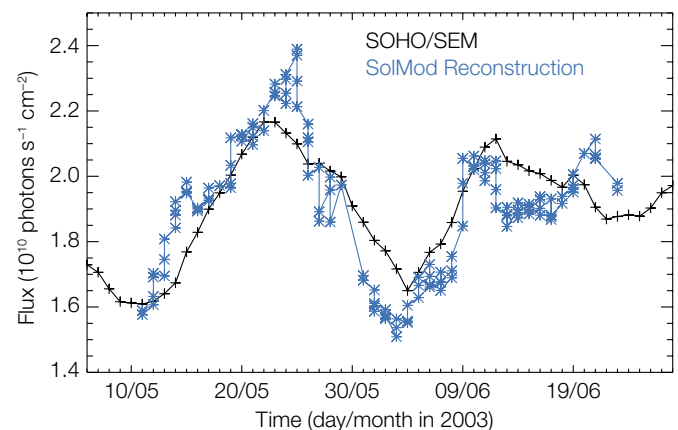


Figure 2. Close-up for the period of two months of the SolMod reconstruction time-series for May–June 2003 based on the Verbeeck et al. (2013) analysis (V2013) and the observed EUV variation. The solar rotation variation is reproduced well, however it is partly overestimated. The reconstruction has been scaled by a factor of 1.2.

Acknowledgement: MH acknowledges support by the Holcim Science Foundation along with the FP7 Project SOLID No. 313188.

- References:**
- Barra V., Delouille V., Kretzschmar M., Hochedez J.: 2009, *A&A*, 505, 361.
 - Delaboudinière J.-P., Artzner G.E., Brunaud J. et al.: 1995, *Solar Phys.*, 162, 291.
 - Fontenla J.M., Curdt W., Haberreiter M., Harder J., Tian H.: 2009, *ApJ*, 707, 482.
 - Haberreiter M.: 2011, *Solar Physics*, 274, 473–479.
 - Haberreiter M.: 2012, *Proceedings IAU Symposium* 286.
 - Verbeeck, et al: 2013, submitted to *A&A*.

Physical Understanding of the Solar Irradiance at Radio Wavelengths

Rinat Tagirov, Alexander Shapiro, Gaël Cessateur, and Werner Schmutz

We are developing the theoretical basis for a method of nowcasting the solar spectrum which is based on the idea of decomposing the solar radio spectrum into components corresponding to quiet Sun and active regions (e.g. sunspots, plage, network etc). Combined with ground based radio observations the method will allow the solar spectrum to be nowcast in real time.

The observed solar spectrum at each moment of time can be thought of as a combination of the spectra originating from the quiet Sun and active components on the solar surface. We can calculate theoretical spectra corresponding to the quiet Sun and the active components and then find their linear combination yielding the best agreement between the observations and theory in a given range. The coefficients of this linear combination are filling factors. Assuming the latter do not depend on wavelength we can state that the overall theoretical solar spectrum can be obtained by constructing the linear combination of the overall theoretical spectra corresponding to the quiet Sun and active components with the obtained set of filling factors. It is reasonable to choose radio wavelengths as the spectral range for reconciling observations and theory because the observations in this range can be obtained using ground based instrumentation. Fig. 1 displays the general idea of the method for radio range. Hence following this idea we can use real-time solar radio spectrum observations to nowcast overall solar spectrum.

We now discuss the theoretical modeling of solar spectra corresponding to active components using COde for Solar Irradiance (COSI) developed at the Physical Meteorological Observatory Davos.

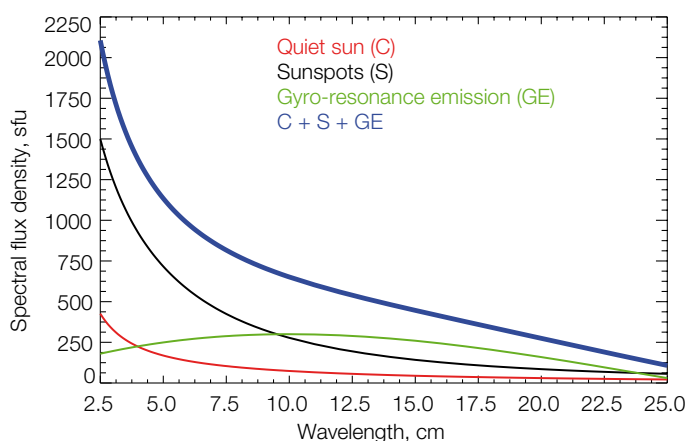


Figure 1. The principal idea of solar radio spectrum decomposition. The sum (blue curve) of three components is presented. Red curve corresponds to quiet Sun, black - to sunspots (models C and S in our analysis respectively) and green - to gyro-resonance emission (GE) which significantly contributes to the solar radio spectrum. Red and black curves were calculated with COSI. Green curve has been kindly provided by K. Tapping (private communication) and is used here only for demonstration purposes. The proper treatment of gyro-resonance emission will be carried out in our further analysis.

As the code was originally designed for modeling the ultraviolet spectral range our current objective is to upgrade COSI routines for proper calculations of solar spectrum in radio wavelengths and achieve a reasonable agreement of these calculations with existing radio observations available in the literature (e.g. Benz 2009 and references therein). As a part of this activity we implemented a new algorithm for computing Gaunt factors (Janicki 1990) because the old one did not work for radio range. For calculation of solar spectra corresponding to the quiet Sun and various activity manifestations we use FAL99 models of solar atmosphere structure (Fontenla et al. 1999) as COSI input. Fig. 2 shows the preliminary results of our calculations for six of the aforementioned models: C – average supergranule cell interior, A – faint supergranule cell interior, E – average network, F – bright network/faint plage, P – bright plage, S – sunspot umbra. As seen from the figure our calculations are in reasonable agreement with observations. The cause of the discrepancy longward 15 cm is currently under investigation.

References: Benz A.: 2009, Quiet and slowly varying radio emissions of the Sun, Landolt-Boernstein LB VI/4b 4.1.1.6.

Janicki C.: 1990, A computer program for the free-free and bound-free Gaunt factors of Rydberg systems, Comp. Phys. Comm., vol. 60, pp. 281 – 296.

Fontenla et. al: 1999, Calculation of solar irradiances. I. synthesis of the solar spectrum, The Astrophysical Journal, vol. 518, pp. 480 – 499.

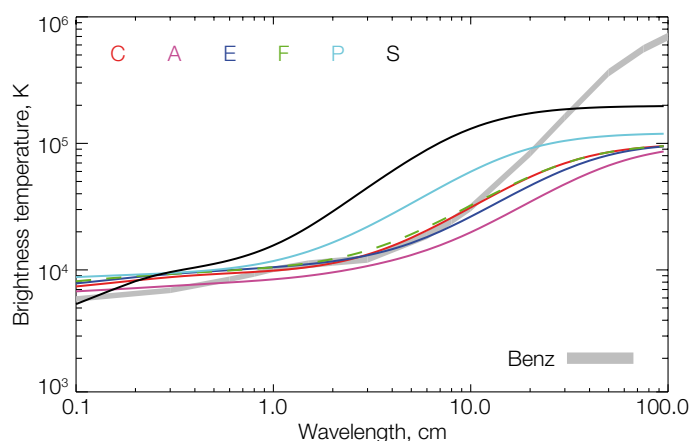


Figure 2. Theoretical solar radio spectra calculated with COSI using FAL99 models against the observational data provided by Benz (2009) and represented as a strip of values confined by the error bars given. The dependency of the brightness temperature at the solar disc center on wavelength was chosen as a spectral characteristic for the purposes of convenience. Brightness temperature is directly related to the spectral flux density.

Modeling the Variability of Sun-Like Stars

Alexander Shapiro, Werner Schmutz in collaboration with MPI, Lindau, Germany and Blackett Lab. Imperial College London, U.K.

We present a model which attributes the variability of the stellar radiative energy flux to the imbalance between the contributions from dark starspots and bright faculae. Our approach allows us to model the stellar photometric variability as a function of an activity index and reproduce the transition from faculae-dominated to spot-dominated regimes of variability.

The present consensus is that variability of the solar spectral irradiance (SSI) is caused by the magnetic features on the solar surface. The available physically based models (see, Ermolli et al. 2012) calculate the variable solar spectrum by weighting the spectra of the individual components of the solar atmosphere (e.g. quiet Sun, sunspot, faculae, or active network) with their filling factors (i.e. surface area coverage).

There is an empirical dependency between annually averaged solar facular and spot filling factors and Ca S-index of the chromospheric activity (see definition in Radick et al. 1998). While the facular filling factor linearly depends on the S-index, the spot dependency is quadratic (Solanki & Unruh 2013), so the relative contribution of spots increases with activity. We extrapolate the solar dependencies of filling factors on the S-index to stars with different levels of chromospheric activity. This allows us to calculate facular and spot filling factors for the stars. Assuming that the contrasts between quiet and active regions are the same for the Sun and Sun-like stars we calculate stellar variability as a function of chromospheric activity.

Figure 1 shows the dependency of stellar variability on the chromospheric activity (characterized via $\log R'_{\text{HK}}$ value, which is a function of S-index, see Radick et al. 1998 for the detailed discussion). The calculations are performed assuming solar distribution of the active regions on the surface, i.e. sunspot bands between 5° and 30° and facular bands between 5° and 40° . The minimum of the variability around $\log R'_{\text{HK}} = -4.85$ is due to compensation effect of spot and facular contributions. For less active stars the variability is dominated by faculae, for more active by spots.

Figure 2 illustrates the transition from a direct (faculae-dominated regime) to inverse (spot-dominated regime) correlation of activity and photometric flux. There is strong evidence that for the fast rotating stars the active regions emerge not at the equatorial belts as for the Sun but at the polar caps (Schussler & Solanki 1992). To take this into account we also performed calculations, assuming a polar cap (North and South caps latitude $> 45^\circ$) distribution of the active regions. One can see that most of the stars in Fig. 2 are located between these two extreme cases.

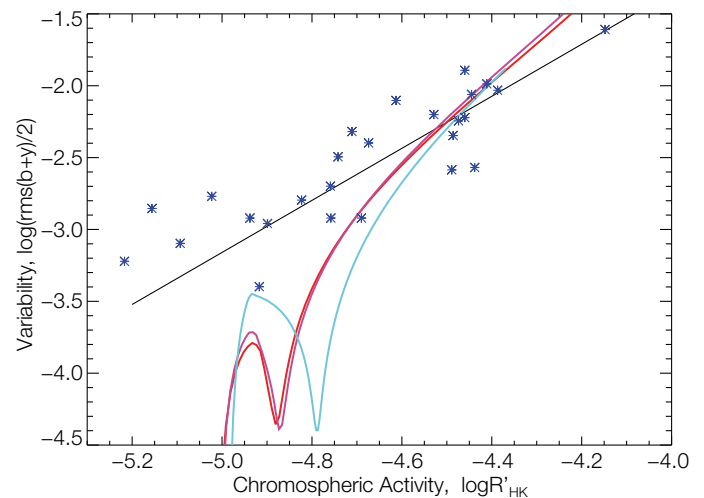


Figure 1. Photometric variability versus chromospheric activity. The blue stars indicate stars from Lockwood et al. (2007). Colour curves are theoretical dependencies between variability and activity calculated for three different angles between the direction to the observer and stellar rotational axis: 90° (red curve, star is observed from the equator), 57° (magenta curve), and 0° (cyan curve, star is observed from the pole).

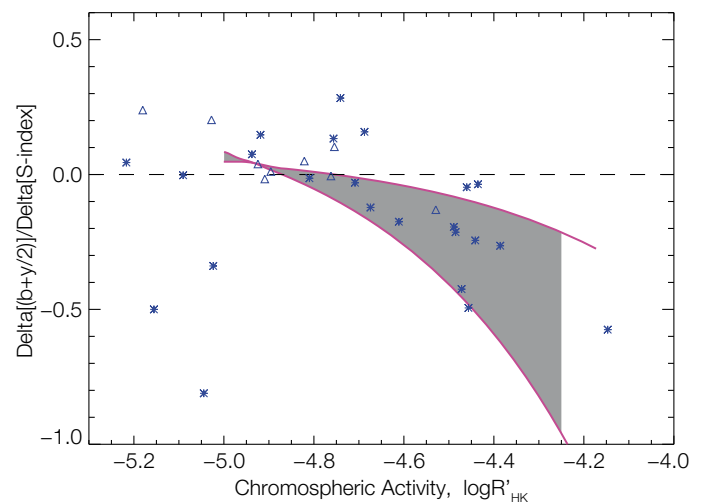


Figure 2. Slope of the regression of photometric brightness variation on S-index. The blue stars and triangles indicate values observed by Lockwood et al. (2007). Upper and lower curves are calculated assuming polar caps and equatorial band distribution of active regions, respectively.

- References:
- Ermolli I., Matthes K., Dudokde Wit T., et al.: 2012, Atmos. Chem. Phys. Discuss., 12, 24557.
 - Lockwood G.W., Skiff B.A., Henry G.W., et al.: 2007, ApJS, 171, 260.
 - Radick R.R., Lockwood G.W., Skiff B.A., Baliunas S.L.: 1998, ApJS, 118, 239.
 - Schussler M., Solanki S.K.: 1992, A&A 264, L13.
 - Solanki S.K., Unruh Y.C.: 2013, Astron. Nachr., 1/2, 145–150.

Comparison of Stellar and Solar Variabilities

Alexander Shapiro, Werner Schmutz, Gaël Cessateur, and Eugene Rozanov

We present a comparison of the available photometric records of Sun-like stars with reconstructions of the solar irradiance over the last 9000 years. We show that stellar photometric data provide a way to constrain the historical solar irradiance variability.

Monitoring of the photometric and chromospheric HK emission data series of stars similar to the Sun in age and average activity level showed that there is an empirical relationship between the stellar average chromospheric activity level and photometric variability (Lockwood et al. 2007, Hall et al. 2009). Interestingly the Sun appears to be significantly less variable than indicated by the empirical relationship (see Figure 1).

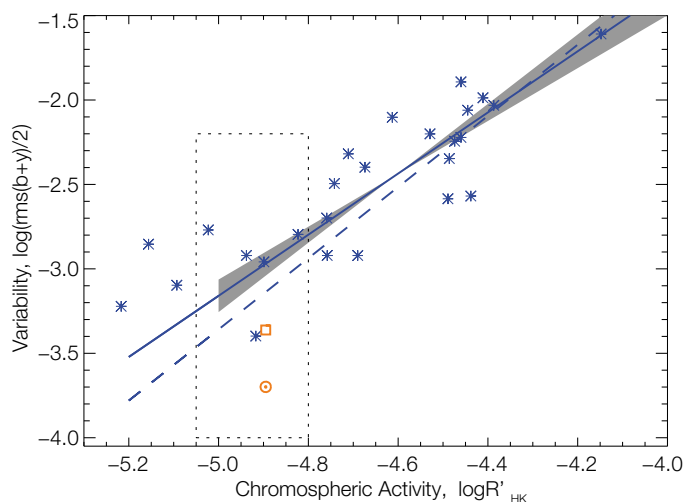


Figure 1. Photometric variability versus chromospheric activity. The blue stars indicate stars with observed variability from Lockwood et al. (2007). The solid and dashed lines are regression lines calculated excluding and including stars with unconfirmed variability, respectively. The shaded area corresponds to the one-sigma uncertainty. The orange symbols denote the position of the present Sun: according to modern reconstructions (solar symbol, corresponds to the mean of Lean (2005), Krivova et al. (2010), and Shapiro et al. (2011) values) and according to an estimate by Lockwood et al. (2007) (square symbol).

We show that the position of the Sun on the diagram of photometric variability versus chromospheric activity changes with time. The present solar position is different from its temporal mean position as the satellite era of continuous solar irradiance measurements has accidentally coincided with a period of unusually high and stable solar activity. Therefore, instead of using present solar variability for the comparison with Sun-like stars, one should use the temporal mean of the variability over a time interval sufficiently long to reveal the entire range of solar variability.

We calculate the trajectories of the Sun on the Variability vs. Activity diagram over the last 9000 years as a function of two parameters: V_{11} , which is the RMS variability of solar annual Stroemgren (b+y)/2 fluxes during cycles 21 and 22 (1976–1996 period) and V_{LT} , which is the relative change of Stroemgren (b+y)/2 flux between 22/23 and the Maunder minima.

Figure 2 shows the example of the solar trajectory over the last 9000 years in the photometric variability versus chromospheric activity diagram for one set of the V_{11} and V_{LT} parameters.

By assuming that the temporary mean Sun obeys the activity versus regression correlation we estimate the magnitude of the secular component in the solar variability. While the currently available stellar data yield a relatively large amplitude of the secular component, careful estimation of the involved uncertainties yields that a 0.17% decrease in the solar flux in the Stroemgren (b+y)/2 filters during the Maunder minimum relative to the present value is within 95% confidence level. This corresponds to 1.9–2.7 W/m² TSI change.

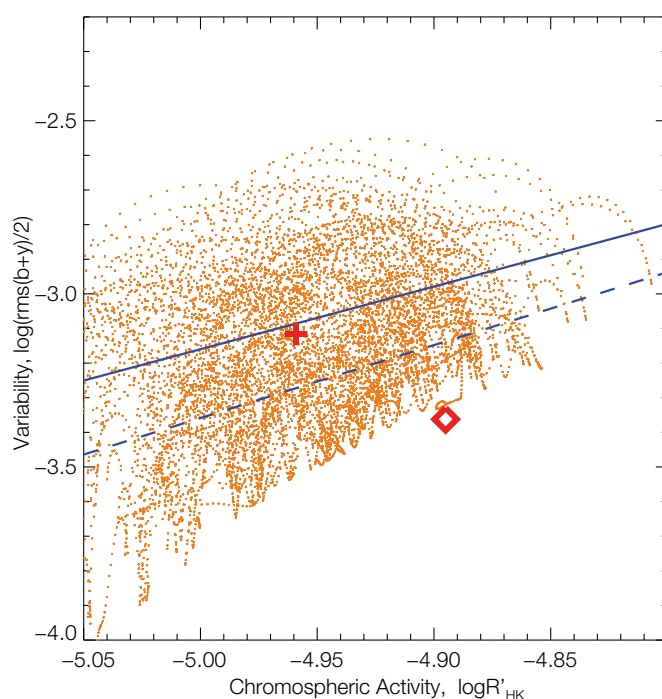


Figure 2. The same as Figure 1 but with trajectories of the Sun over the last 9000 years (orange dots) for $V_{LT} = 0.5\%$ and $V_{11} = 0.00044$ mag. The red square and cross symbols indicate the positions of the present and 'mean' Sun.

References: Hall J.C., Henry G.W., Lockwood G.W., Skiff B.A., Saar S.H.: 2009, *AJ*, 138, 312.

Krivova N.A., Vieira L.E.A., Solanki S.K.: 2010, *Journal of Geophysical Research (Space Physics)*, 115, 12112.

Lean J., Rottman G., Harder J., Kopp G.: 2005, *Sol. Phys.*, 230, 27.

Lockwood G.W., Skiff B.A., Henry G.W., et al.: 2007, *ApJS*, 171, 260.

Shapiro A.I., Schmutz W., Rozanov E., et al.: 2011, *Astron. Astrophys.*, 529, A67.

Shapiro A.I., Schmutz W., Cessateur G., Rozanov E., et al.: 2013, *Astron. Astrophys.*, in press.

FP7 Space Project SOLID – First European Comprehensive SOLar Irradiance Data Exploitation

Margit Haberreiter and Werner Schmutz in collaboration with CNRS, France; Royal Observatory Belgium; University of Bradford, UK; Universität Bremen, Germany; Imperial College London, UK; MPS, Germany; INAF, Italy; University of Cambridge, UK; University of Thessaloniki, Greece

The FP7 SOLID Project is tailored to provide a complete and consistent time-series of solar spectral radiation incident on the Earth's atmosphere from the XUV/EUV to the radio wavelength regions. This will be achieved by combining all existing space observations of the solar spectral irradiance and complementing them by state-of-the-art irradiance modelling.

Variations in solar radiation incident on the Earth's atmosphere are the most important natural factor in the terrestrial climate. Therefore, the time-dependent spectral solar irradiance (SSI) is a crucial input to any climate model. However, the main difficulty is that observations of the spectral radiation incident at the top of the Earth's atmosphere to date only exist in numerous diverse data sets (see Figure 1). SOLID will make an important contribution, as the major objective of the project is to analyse and merge existing European irradiance observations, complemented by non-European space data. In addition, modelling results will be used to bridge observational gaps in wavelength and time. This will allow the SOLID team to reduce the uncertainties in the irradiance time-series and to provide a consistent data set focusing on the period from the beginning of the space era to the present but also including the pre-space era.

Most importantly, the irradiance product will contain a detailed uncertainty analysis, which is an essential requirement by the user communities. Besides the climate community, further users of the SSI data product are expected to be the stellar, planetary, and lunar communities, as well as modellers of the Earth's ionosphere. The SOLID-consortium includes representatives from all European solar space experiments; European teams specialized in multi-wavelength solar image processing, as well as European experts in irradiance modelling. Finally, representatives from the climate community, who will accompany the project with wide dissemination activities, complement the SOLID team. Further details can be found on the SOLID webpage <http://projects.pmodwrc.ch/solid/>.

SOLID in short

Starting Date:	01/12/2012
Duration:	36 months
EU Contribution:	€ 1.994.373,60
Estimated total cost:	€ 2.579.598,40
Coordinator :	PMOD/WRC

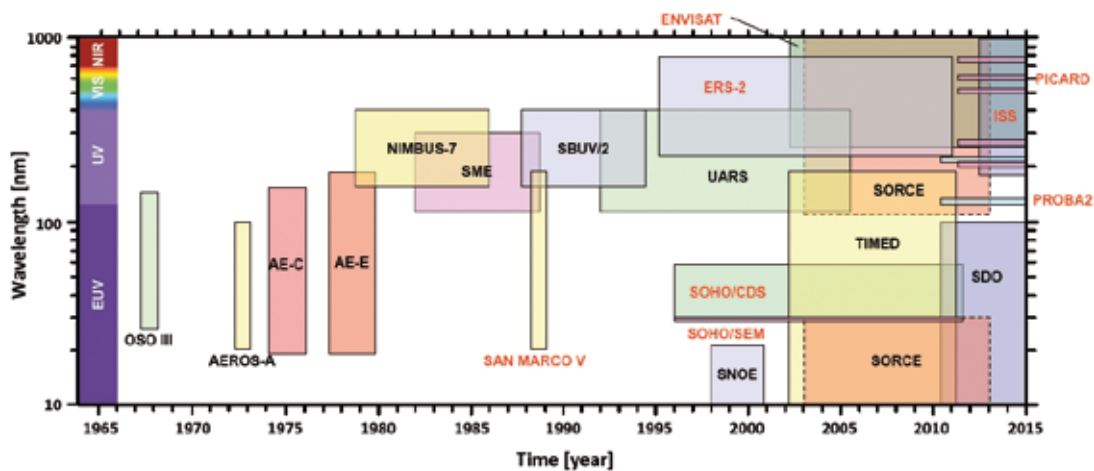


Figure 1. Space observations of the solar spectral irradiance since 1965 as a function of wavelength. European missions are indicated as red text. The goal of SOLID is to fill the substantial gaps (white area) in wavelength and time, and provide a consistent time-series with realistic uncertainty estimates. Figure courtesy T. Dudok de Wit.

- Anton M., Sorribas M., Bennouna Y., Vilaplana J.M., Cachorro V.E., Gröbner J., Alados-Arboledas L.: 2012, Effects of an extreme desert dust event on the spectral ultraviolet irradiance at El Arenosillo (Spain), *J. Geophys. Res.*, 117, D03205, 9 pp., doi: 10.1029/2011JD016645.
- Broomhall A.-M., Chaplin W.J., Elsworth Y., Simoniello R.: 2012, Quasi-biennial variations in helioseismic frequencies: can the source of the variation be localized?, *Mon. Not. Royal Astron. Soc.*, 420, 1405-1414, doi: 10.1111/j.1365-2966.2011.20123.x.
- Calisto M., Verronen P., Rozanov E., Peter T.: 2012, Influence of a Carrington-like event on the atmospheric chemistry, temperature and dynamics, *Atmos. Chem. Phys.*, 12, 8679-8686, doi: 10.5194/acp-12-8679-2012.
- Dolla L., Marqué C., Seaton D.B., Van Doorselaere T., Dominique M., Berghmans D., Cabanas C., De Groof A., Schmutz W., Verdini A., West M.J., Zender J., Zhukov A.N.: 2012, Time Delays in Quasi-periodic Pulsations Observed during the X2.2 Solar Flare on 2011 February 15, *Astrophys. J. Letters*, 749, L16, 7 pp., doi: 10.1088/2041-8205/749/1/L16.
- Egorova T., Rozanov E., Shapiro A.V., Schmutz W.: 2012, Principal Possibility of the Successful Nowcast and Short-Term Forecast in the Middle Atmosphere Based on the Observed UV Irradiance, *International Journal of Geophysics*, vol. 2012, Article ID 298431, 7 pp., doi: 10.1155/2012/298431.
- Fehlmann A., Kopp G., Schmutz W., Winkler R., Finsterle W., Fox N.: 2012, Fourth World Radiometric Reference to SI radiometric scale comparison and implications for on-orbit measurements of the total solar irradiance, *Metrologia* 49, S34–S38, doi: 10.1088/0026-1394/49/2/S34.
- Fröhlich C.: 2012, Total Solar Irradiance Observations, *Surveys in Geophysics*, Vol. 33, 453-473, doi: 10.1007/s10712-011-9168-5.
- Gröbner J.: 2012, A Transfer Standard Radiometer for atmospheric longwave irradiance measurements, *Metrologia*, 49, S105-S111, doi: 10.1088/0026-1394/49/2/S105.
- Halios C.H., Helmis C.G., Flocas H.A., Nyeki S., Assimakopoulos D.N.: 2012, On the variability of the surface environment response to synoptic forcing over complex terrain: a multivariate data analysis approach, *Meteorology and Atmospheric Physics*, 118, 107-115, doi: 10.1007/s00703-012-0209-5.
- Judge P.G., Lockwood G.W., Radick R.R., Henry G.W., Shapiro A.I., Schmutz W., Lindsey C.: 2012, Confronting a solar irradiance reconstruction with solar and stellar data, *Astron. Astrophys.*, 544, A88, 6 pp, doi: 10.1051/0004-6361/201218903.
- Junk J., Feister U., Helbig A., Gørgen K., Rozanov E., Krzyściński J., Hoffmann L.: 2012, The benefit of modeled ozone data for the reconstruction of a 99-year UV radiation time series, *J. Geophys. Res.*, 117, D16102, 10 pp., doi: 10.1029/2012JD017659.
- Kohlhepp R., Ruhnke R., Chipperfield M., De Maziere M., Notholt J., Barthlott S., Batchelor R., Blatherwick R., Blumenstock T., Coffey M., Demoulin P., Fast H., Feng W., Goldman A., Griffith D., Hamann K., Hannigan J., Hase F., Jones N., Kagawa A., Kaiser I., Kasai Y., Kirner O., Kouker W., Lindenmaier R., Mahieu E., Mittermeier R., Monge-Sanz B., Morino I., Murata I., Nakajima H., Palm M., Paton-Walsh C., Raffalski U., Reddmann T., Rettinger M., Rinsland C., Rozanov E., Schneider M., Senten C., Servais C., Sinnhuber B.-M., Smale D., Strong K., Sussmann R., Taylor J., Vanhaelewyn G., Warneke T., Whaley C., Wiehle M., Wood S.: 2012, Observed and simulated time evolution of HCl, ClONO₂, and HF total column abundances, *Atmos. Chem. Phys.*, 12, 3527-3556, doi: 10.5194/acp-12-3527-2012.
- Kopp G., Fehlmann A., Finsterle W., Harder D., Heuerman K.: 2012, Total solar irradiance data record accuracy and consistency improvements, *Metrologia* 49, S29–S33, doi: 10.1088/0026-1394/49/2/S29.
- Lachat D., Wehrli C.: 2012, A Century of apparent Atmospheric Transmission over Davos, Switzerland, *Theoretical and Applied Climatology*, 110, 539-547, doi: 10.1007/s00704-012-0685-z.
- Mitchell D.M., Charlton-Perez A., Gray L., Akiyoshi H., Butchart N., Hardiman S., Morgenstern O., Nakamura T., Rozanov E., Shibata K., Smale D., Yamashita T.: 2012, The nature of Arctic polar vortices in chemistry–climate models, *Q. J. R. Meteorol. Soc.*, 138, 1681-1691, doi: 10.1002/qj.1909.
- Nezval E.I., Chubarova N.E., Gröbner J., Omura A.: 2012, *Izvestiya RAN. Fizika Atmosfery i Okeana*, 48, 682–690.
- Nyeki S., Halios C.H., Baum W., Eleftheriadis K., Flentje H., Gröbner J., Vuilleumier L., Wehrli C.: 2012, Ground-based aerosol optical depth trends at three high-altitude sites in Switzerland and southern Germany from 1995 to 2010, *J. Geophys. Res.*, 117, D18202, 7 pp., doi: 10.1029/2012JD017493.

Refereed Publications

- Petkov B., Vitale V., Gröbner J., Hülsen G., De Simone S., Gallo V., Tomasi C., Busetto M., Lonar Barth V., Lanconelli C., Mazzola M.: 2012, Short-term variations in surface UV-B irradiance and total column ozone at Ny-Ålesund during the QAARC campaign, *Atm. Env.*, 108, 9-18, doi: 10.1016/j.atmosres.2012.01.006.
- Revell L.E., Bodeker G., Huck P., Williamson B., Rozanov E.: 2012, The sensitivity of stratospheric ozone changes through the 21st century to N₂O and CH₄, *Atmos. Chem. Phys.*, 12, 11309–11317, doi: 10.5194/acp-12-11309-2012.
- Revell L.E., Bodeker G., Smale D., Lehmann R., Huck P., Williamson B., Rozanov E., Struthers H.: 2012, The effectiveness of N₂O in depleting stratospheric ozone, *Geophys. Res. Lett.*, 39, L15806, 6 pp., doi: 10.1029/2012GL052143.
- Rozanov E., Calisto M., Egorova T., Peter T., Schmutz W.: 2012, Influence of the Precipitating Energetic Particles on Atmospheric Chemistry and Climate, *Surveys in Geophysics*, 33, 483-501, doi: 10.1007/s10712-012-9192-0.
- Scaife A., Spanghel T., Fereday D., Cubasch U., Langematz U., Akiyoshi H., Bekki S., Braesicke P., Butchart N., Chipperfield M., Gettelman A., Hardiman S.C., Michou M., Rozanov E., Shepherd T.: 2012, Climate change projections and stratosphere–troposphere Interaction, *Clim. Dyn.*, 38, 2089–2097, doi: 10.1007/s00382-011-1080-7.
- Shapiro A.V., Rozanov E., Shapiro A.I., Wang S., Egorova T., Schmutz W., Peter T.: 2012, Signature of the 27-day solar rotation cycle in mesospheric OH and H₂O observed by the Aura Microwave Limb Sounder, *Atmos. Chem. Phys.*, 12, 3181-3188, doi: 10.5194/acp-12-3181-2012.
- Simoniello R., Finsterle W., Salabert D., García R. A., Turck-Chièze S., Jiménez A., Roth M.: 2012, The quasi-biennial periodicity (QBP) in velocity and intensity helioseismic observations. The seismic QBP over solar cycle 23, *Astron. Astrophys.* 539, A135, 9 pp., doi: 10.1051/0004-6361/201118057.
- Simoniello R., Jain K., Tripathy S.C., Turck-Chièze S., Finsterle W., Roth M.: 2012, Seismic comparison of the 11- and 2-year cycle signatures in the Sun, *Astronomische Nachrichten* 333, 1018-1021, doi: 10.1002/asna.201211813.
- Skinner S.L., Zhekov S.A., Güdel M., Schmutz W., Sokal K.R.: 2012, New X-Ray Detections of WNL Stars, *Astron. J.*, 143, 116, 8 pp., doi: 10.1088/0004-6256/143/5/116.
- Thuillier G., Deland J., Shapiro A., Schmutz W., Bolsée D., Melo S.M.L.: 2012, The Solar Spectral Irradiance as a Function of the MgII Index for Atmosphere and Climate Modelling, *Sol. Phys.* 277, 245–266, doi: 10.1007/s11207-011-9912-5.
- Toledano C., Cachorro V.E., Gausa M., Stebel K., Aaltonen V., Berjón A., Ortiz de Galisteo J.P., de Frutos A.M., Bennouna Y., Blindheim S., Myhre C.L., Zibordi G., Wehrli C., Kratzer S., Hakansson B., Carlund T., de Leeuw G., Herber A., Torres B.: 2012, Overview of sun photometer measurements of aerosol properties in Scandinavia and Svalbard, *Atmosph. Env.*, 52, 18-28, doi: 10.1016/j.atmosenv.2011.10.022.

Other Publications

- Brugnara Y., Brönnimann S., Luterbacher J., Rozanov E.: 2012, Influence of the sunspot cycle on the Northern Hemisphere wintertime circulation from long upper-air data sets, *Atmos. Chem. Phys. Discuss.*, 12, 30371–30407, doi: 10.1029/2011JD016645.
- Cessateur G., Shapiro A.I., Dominique M., Kretzschmar M., Krivova N., Shapiro A.V., Schmutz W., Schoell M., Solanki S., Tagirov R., Thuillier G., Wehrli C., Yeo K.L.: 2012, Solar Spectral Irradiance as observed by LYRA/PROBA2 and PREMOS/PICARD, EGU General Assembly Conf. Abstracts 14, 8254.
- Egorova T., Rozanov E., Gröbner J., Hauser M., Schmutz W.: 2012, Montreal Protocol benefits simulated with CCM SOCOL, *Atmos. Chem. Phys. Discuss.*, 12, 17001-17030, doi:10.5194/acpd-12-17001-2012.
- Ermolli I., Matthes K., Dudok de Wit T., Krivova N.A., Tourpali K., Weber M., Unruh Y.C., Gray L., Langematz U., Pilewskie P., Rozanov E., Schmutz W., Shapiro A., Solanki S.K., Thuillier G., Woods T.N.: 2012, Recent variability of the solar spectral irradiance and its impact on climate modelling, *Atmos. Chem. Phys. Discuss.*, 12, 24557-24642, doi:10.5194/acpd-12-24557-2012.
- Haberreiter M.: 2012, Towards the reconstruction of the EUV irradiance for solar Cycle 23, In: C.H. Mandrini and D.F. Webb (eds.), *Comparative Magnetic Minima: Characterizing quiet times in the Sun and Stars*, IAU Symp. 286, p. 97-100, doi: 10.1017/S174392131200470X.
- Halain J.-P., Rochus P., Renotte E., Appourchaux T., Berghmans D., Harra L., Schühle U., Schmutz W., Auchère F., Zhukov A., Dumesnil C., Delmotte F., Kennedy T., Mercier R., Pfiffner D., Rossi L., Tandy J., BenMoussa A., Smith P.: 2012, The EUV instrument on board the Solar Orbiter mission: From bread-board and proto-types to instrument model validation. In: *Society of Photo-Optical Instrumentation Engineers (SPIE) Conference Series 8443*, id. 844307, doi: 10.1117/12.924343.
- Rozanov E.V., Egorova T.A., Shapiro A.I., Schmutz W.K.: 2012, Modeling of the atmospheric response to a strong decrease of the solar activity. In: C.H. Mandrini and D.F. Webb (eds.), *Comparative Magnetic Minima: Characterizing quiet times in the Sun and Star*, IAU Symp. 286, p. 215–224, doi: 10.1017/S1743921312004863.
- Stenke A., Schraner M., Rozanov E., Egorova T., Luo B.-P., Peter T.: 2012, The SOCOL version 3.0 chemistry-1 climate model: description, evaluation, and implications from an advanced transport algorithm, *Geosci. Model Dev. Discuss.*, 5, 3419–3467.
- Suter M., Finsterle W., Kopp G.: 2012, WRR to SI comparison with DARA, WMO-TECO 2012, Bruxelles, Conference Proceeding.
- Tsagouri I., Belehaki A., Bergeot N., Cid C., Egorova T., Kutiev I., Mikhailov A., Nunez M., Pietrella M., Potapov A., Qahwaji R., Tulunay Y., Velinov P., Viljanen A.: 2012, Progress in space weather modeling in an operational environment (SG1.3 report), COST Action ES0803 Workshop on Final Results, Prague, 13-14 March 2012.
- Thuillier G., Bolsée D., DeLand M., Melo S.M.L., Schmutz W., Shapiro A.: 2012, A New Solar Spectral Irradiance Reconstruction based on MGII and Neutral Monitoring Indices for Use in Climate Modelling, EGU General Assembly Conf. Abstracts 14, 8248.
- Wacker S., Gröbner J., Vuilleumier L.: 2013, Trends in Surface Radiation And Cloud Radiative Effect Over Switzerland. In: *The Past 15 Years*, AIP Conference Proceedings.
- Zubov V., Rozanov E., Egorova T., Karol I., Schmutz W.: 2012, Role of external factors in the evolution of the ozone layer and stratospheric circulation in 21st century, *Atmos. Chem. Phys. Discuss.*, 12, 28467-28492, doi: 10.5194/acpd-12-28467-2012.

Personnel Department

Sandra Kissling and Werner Schmutz

2012 was a year of profound changes.

In the first semester of 2012 most PMOD/WRC staff were still working in the Holland House building. However, by August we finally moved back into our newly renovated 'old school house'. It was a relief but nevertheless hard work to organize everything. Many thanks to all who packed, organized, gave a hand and helped so that we were able to move in on 17th August. From then on we quickly returned to normal every-day business. On 27th October we had an Open Day which was prepared during a one-day meeting at the Schatzalp, Davos. The Open Day was a great success and many visitors were able to gain vivid impressions of many aspects of our day-to-day work. Thanks to all the helping hands on this day.

As in every year, several staff left our institute. During the first half of the year Micha Schöll and Rosaria Simoniello left for new challenges. Both of them did a great job and supported the science department with their efforts. Daniel Bühlmann left the technical department in June. We would like to thank him for his support and commitment.

In October Sonja Degli Esposti left our institute to pursue her career as Head of Personnel at the AFIAA Investment AG in Zürich. Since 1998 she was the stable backbone of the administration/HR and supported the institute wherever she could. We all appreciated her devotion and strong loyalty to our institute. No thank you will ever be enough for her outstanding contribution.

The second long term supporting mainstay of the administration department was Stephanie Ebert. After having worked long at the PMOD/WRC, she also decided to continue her career in Zürich. Her absence also left a gap which takes time to fill. Claudia Casanova was hired to take over from Stephanie Ebert and started in August but left us in December. The administration department had therefore lost, quite by coincidence, its core staff over a short time period.

However, time is passing and new staff arrived. Valeria Büchel, a mechanical engineer, joined the technical group in August. Since then she provides her team with enthusiastic and professional support. We are glad to have her at PMOD/WRC.

A new electronics apprentice also joined the technical department. Andri Morandi started work in August. We are proud to have such a determined and successful young person in our team. We wish him all the best in the next few years.

Our new scientist Dr. Natalia Kouremeti started her work in September. After being here in early Spring she decided to take on the job after having previously worked at the University of Thessaloniki, Greece. Since then she has become an active team member of the WRC-WORCC group. We are happy to have her here and wish her all the best in the future.

Sandra Kissling started as the head of administration/HR in December. Taking over this job after Sonja Degli Esposti was not an easy task to start with, but the administration department is running well and is once again the backbone of the institute.

Two PhD students successfully finished their thesis and obtained a Doctorate in 2012: Anna Shapiro and Daniel Lachat successfully passed their exams. Marcel Spescha finished his degree in Java application development with the best mark possible and Ricco Soder successfully finished his Bachelor of Science FHO in Telecommunication majoring in 'Applied Electrical Engineering'. Congratulations to all of them.

Throughout the year we also have had great support from numerous civilian conscripts who did an excellent job in helping wherever help was needed. Thanks to all of them.

Scientific Personnel

Prof. Dr. Werner Schmutz	Director, physicist
Dr. Gaël Cessateur	Postdoc, solar physics group, physicist
Dr. Luca Egli	Scientist EUVC section, physicist
Dr. Tatiana Egorova	Scientist, climate group, meteorologist
Dr. André Fehlmann	Postdoc, solar physics group, physicist
Dr. Wolfgang Finsterle	Head WRC-section solar radiometry, physicist
Dr. Julian Gröbner	Head WRC-sections IR radiometry, WORCC and WUVCC, physicist
Dr. Margit Haberleiter	Scientist, solar physics group, physicist
Dr. Gregor Hülsen	EUVC scientist, physicist
Dr. Natalia Kouremeti	Postdoc, WORCC Section, physicist (since 10.09.2012)
Dr. Stephan Nyeki	WORCC and IR scientist, physicist
Dr. Eugene Rozanov	Scientist, climate group, physicist
Dr. Alexander Shapiro	Postdoc, solar physics group, physicist
Dr. Rosaria Simoniello	Postdoc, solar physics group, physicist (until 31.03.2012)
Dr. Micha Schöll	Postdoc, solar physics group, physicist (until 31.01.2012)
Dr. Stefan Wacker	Postdoc, IR section, physicist
Dr. Christoph Wehrli	WORCC scientist, physicist
Dr. Daniel Lachat	PhD student, UNIBE (until 31.12.2012) Postdoc, WRC-WORCC group, physicist (since 01.01.2013)
Dr. Anna Shapiro	PhD student, ETHZ (until 30.09.2012) Postdoc, solar physics group, physicist (since 01.10.2012)
Markus Suter	PhD student, UNIZH
Rinat Tagirov	PhD student, ETHZ

Technical Personnel

Manfred Gyo	Head technical department, electronic engineer, Quality System manager
Valeria Büchel	Mechanical engineer and part time project manager space experiments (since 15.08.2012)
Daniel Bühlmann	Technician (until 30.06.2012)
Etienne de Coulon	Software development engineer
Fabian Dürig	Mechanical engineer
Daniel Pfiffner	Project manager space experiments, deputy head technical department and Quality System, electronic engineer
Marco Senft	Software developer
Ricco Soder	Research engineer
Marcel Spescha	Technician
Christian Thomann	Technician
Diego Wasser	Electronic technician
Thierry Hartmann	Electronics apprentice, 2 nd /3 rd year
Andri Morandi	Electronics apprentice, 1 st year (since 01.08.2012)

Administration

Sonja Degli Esposti	Head administration/Human Resources (until 30.11.2012)
Sandra Kissling	Head administration/Human Resources (since 01.12.2012)
Stephanie Ebert	Administration, book-keeping (until 31.12.2012)
Claudia Casanova	Administration, book-keeping (from 06.08.2012 until 31.12.2012)
Irene Keller	Administration, import/export
Eliane Tobler	Administration apprentice, 1 st /2 nd year

DACA-13 (Project-Staff)

Anja Schilling Project manager DACA-13 conference

Caretaker

Stana Petrovic General caretaker, cleaning (until 30.11.2012)
 Maria Sofia Ferreira Pinto General caretaker, cleaning (since 01.12.2012)

Civilian Service Conscripts

Marcel Knupfer 02.01. – 31.05.2012
 Flavio Lanfranchoni 09.01. – 30.03.2012
 Florian Schwarz 02.04. – 25.05.2012
 Dario Eberhard 04.06. – 12.09.2012
 Samuel Nüesch 11.06. – 09.09.2012
 Claudio Dellagiacoma 03.09. – 05.10.2012
 Stephan Kälin 17.09. – 29.12.2012
 Laurin Diener 08.10. – 04.01.2013

Meeting Organisation

CCMVal Davos Congress Center, 21–24 May, 2012
 Theme: 'Process-oriented evaluation and analysis of troposphere-stratosphere chemistry-climate models'

PAGES-FUPSOL Meeting Davos PMOD/WRC, 5–7 September, 2012

Public Seminars

30/03/2012	Pia Zacharias, ISSI Bern, 3D MHD modeling of the solar Corona	31/08/2012	Giovanni Privitera, Istituto Ricerche Solari Locarno, Reduction and Analysis of Spectropolarimetric Data
07/05/2012	Marina Battaglia, Institut for 4D Technologien, X-ray and EUV observations of solar flares as diagnostic of chromospheric and coronal plasma parameters		Demidov Mikhail, Istituto Ricerche Solari Locarno, Dignostics of Solar Magnetic Field Properties by Comparison of Observations in Different Spectral Lines
			Michele Bianda, Istituto Richerche Solari Locarno, Installing a ZIMPOL-3 system on GREGOR in Tenerif

Course of Lectures, Participation in Commissions

Werner Schmutz	<p>Course of lecture Astronomie, HS 2012, ETH-ZH</p> <p>Examination expert in astronomy, BSc ETH-ZH, PhD sci. nat. ETH-ZH, and PhD Uni ZH</p> <p>Vice president of the International Radiation Commission (IRS, IAMAS)</p> <p>Comité consultatif de photométrie et radiométrie (CCPR, OICM)</p> <p>Science Programme Committee, ESA</p> <p>Expert group on space weather of the UN Committee on the Peaceful Uses of Outer Space</p> <p>Swiss representative in the Committee on Space Research (COSPAR)</p> <p>Swiss Management Committee delegate to the COST action ES00803 (ECF)</p> <p>Swiss Management Committee delegate to the COST action ES01005 (ECF)</p> <p>President of the national Committee on Space Research, Commission of SCNAT</p> <p>Member of the Commission for Astronomy, SCNAT</p> <p>GAW-CH working group (MeteoSwiss)</p>
Wolfgang Finsterle	<p>Member of: CIMO ET Standardization</p> <p>Chairman of: ISO/TC180 SC1 (Solar Energy, Climate-Measurement and Data)</p>
Julian Gröbner	<p>Course of lecture Solar Ultraviolet Radiation WS 2012, ETH-ZH</p> <p>GAW-CH Working group (Meteoswiss)</p> <p>NEWRAD Scientific committee member – chair elect</p> <p>Chairman of Infrared Working group of Baseline Surface Radiation Network (BSRN)</p> <p>Member IAMAS International Radiation Commission</p> <p>Member of the CIMO expert team on New In-Situ Technologies</p>
Margit Haberreiter	<p>Swiss Management Committee substitute delegate to the COST action ES1005 (ECF), Leader of WP1.1</p> <p>Co-Investigator of EUJ and SPICE onboard Solar Orbiter</p> <p>Review Service for Astronomy and Astrophysics, Advances in Space Research</p> <p>Member of the SPICE Science Steering Committee</p> <p>Member of the Programme Committee for the Alpach Summer School 2013</p> <p>Member of the Inter-Division IAU Working Group ‘Impact of Magnetic Activity on Solar and Stellar Environments’</p>
Eugene Rozanov	<p>International Commission on the Middle Atmosphere (ICMA, IAMAS)</p> <p>Swiss Management Committee delegate to the COST action ES01005 (ECF)</p>
Christoph Wehrli	<p>Aerosol Optical Depth course at GAWTEC</p> <p>GAW-CH Working group (Meteo Swiss)</p> <p>Scientific Advisory Group Aerosol (WMO/GAW)</p>

Modernization and Renovation of the PMOD/WRC Institute Building

Stephan Nyeki and Werner Schmutz

Indoor installation and decorative work continued throughout 2012. As the main building phase for the ground-floor had finished towards the end of 2011, the Technical department was able to move back into the Institute in early 2012. Offices and laboratories had been renovated to keep features of the former School-House such as wood paneling and floors but had been modernized with better lighting and white-washed walls. Along with new furniture and a working coffee machine, the new working environment was welcomed by all. Work on the upper floors, however, continued until summer 2012 which meant that the Administration and Science departments had to remain in the Holland House building for several more months. The geothermal heating system was installed during this period. This was the final major building phase as it consisted of drilling numerous bore-holes into the bedrock surrounding the institute. The car-park had once again become a big building site as heavy machinery had to be used. An array of solar heating panels and a bicycle shed were also constructed during this time. After the car-park was asphalted, outdoor work on the Institute building was finally finished (see Figure 1).

The 17th August 2012 was eventually set as our 'moving-in day'. It took several days to clear the halls of the numerous pallets loaded up high with furniture, books, and instruments but life slowly returned to a working rhythm. All staff were at last under one roof.

Despite the 2-year period it took to renovate and modernize the institute building, the wait was well worth the while. Some of the main improvements to the new building include:

- A new multi-media auditorium for scientific and public meetings with a 100+ seating capacity was built on the top floor under the sloping roof. The carefully renovated wooden roof-beams give the large room a suitable setting for scientific and public meetings.
- The institute building is now solely heated by a geothermal heating system in combination with solar heating panels. Heat is extracted from the surrounding bed-rock through numerous bore-holes which are about 200 meters deep. The solar heating panels have several functions. They provide: 1) hot water, 2) help to heat the building, and 3) if enough heat is left, it is pumped into the bedrock to be stored.
- An entire extra floor of office space is now available on the 2nd floor.
- The basement has been completely renovated and comprises: 1) A completely new optical laboratory, 2) the refurbished old optical laboratory now with air-conditioning, and 3) a new clean-room next to laboratories and a vacuum test facility.
- A new roof-platform for calibrating instruments and long-term monitoring measurements.



Figure 1. The newly renovated PMOD/WRC building.

PMOD/WRC Open Day Event

Stephan Nyeki and Werner Schmutz

Our Open Day event was held on Saturday 27th October. The public were invited to meet PMOD/WRC staff and to view the newly renovated building. Despite the cool temperatures and occasional flurry of snow, visitors of all ages came throughout the day. Many different events were held to give the public a glimpse into the day-to-day working life at the PMOD/WRC. Some of the events are pictured below.

Figure 1. Christoph Wehrli explaining how early radiation monitoring instruments worked which can be seen in the glass case.



Figure 2. Ricco Soder (on the right) describing the inner workings of an engraving machine. Youngsters were able to engrave their names onto key-tags.



Figure 3. A popular attraction during Open Day was the hand-painted caricatures drawn by Michaela Maria Drux, a cabaret artist. Children and adults queued for ages to have their pictures drawn.



Figure 4. The new measurement platform for radiation, ozone and meteorological instruments on the Institute roof is being shown by Julian Gröbner (on the right). The roof-platform has enough room for major campaigns to be conducted.



Figure 5. Wolfgang Finsterle during a slide-show presentation in the new auditorium, giving the public an overview of the different scientific fields covered by the PMOD/WRC.



Figure 6. Banner in the streets of Davos advertising the Open Day to the public.

Bilanz 2012 inklusive Drittmittel

Aktiven	31.12.2012
	CHF
Flüssige Mittel	2'772'234.19
Wertschriften	278'528.00
Forderungen	102'970.72
Aktive Rechnungsabgrenzungen	494'379.77
	<u>3'648'112.68</u>
Passiven	
Verbindlichkeiten	155'213.40
Kontokorrent Stiftung	9'567.60
Passive Rechnungsabgrenzungen	2'052'116.58
Rückstellungen	1'213'394.74
Eigenkapital	217'820.36
	<u>3'648'112.68</u>

Erfolgsrechnung 2012 inklusive Drittmittel

Ertrag	CHF
Beitrag Bund Betrieb WRC	1'366'896.00
Beitrag Bund (BBL), Umbau PMOD/WRC	2'195'467.00
Beitrag Kanton Graubünden	452'088.00
Beitrag Gemeinde Davos	589'555.00
Beitrag Gemeinde Davos, Mieterlass	154'614.00
Overhead SNF	151'413.95
Instrumentenverkäufe	150'560.00
Kalibrationen	192'290.15
Übriger Ertrag	83'095.70
Finanzertrag	19'003.70
Ausserordentlicher Ertrag	3'788.28
Auflösung Rückstellungen	46'933.45
Drittmittel	2'323'820.71
	<u>7'729'525.94</u>
Aufwand	
Personalaufwand	3'716'962.50
Investitionen	961'478.88
Unterhalt	77'828.64
Verbrauchsmaterial	57'727.90
Verbrauch Commercial	110'038.45
Reisen, Kongresse, Kurse	186'108.50
Raumaufwand/Energieaufwand	225'060.30
Verwaltungsaufwand	144'858.05
Finanzaufwand	7'501.70
Übriger Betriebsaufwand	47'156.72
BBL, Umbau PMOD/WRC	2'195'467.00
	<u>7'730'188.64</u>
Ergebnis 2012	<u>-662.70</u>
	<u>7'729'525.94</u>

AERONET	Aerosol Robotic Network, GSFC
AOD	Aerosol Optical Depth
ASRB	Alpine Surface Radiation Budget
BIPM	Bureau International des Poids et Mesures, Paris, F
BISON	Birmingham Solar Oscillation Network
BOLD	Blind to Optical Light Detector
BOS	Bolometric Sensor, Belgium instrument on the mission PICARD
BSRN	Baseline Surface Radiation Network of the WCRP
BUSOC	Belgian User Support and Operation Centre of ESA
CCM	Chemistry-Climate Model
CAS	Commission for Atmospheric Sciences, Commission of WMO
CCPR	Comité Consultatif de Photométrie et Radiométrie, BIPM
CIE	Commission Internationale de l'Eclairage
CIPM	Comité International des Poids et Mesures
CIMO	Commission for Instruments and Methods of Observation of WMO, Geneva
CMC	Calibration and Measurement Capabilities
CNES	Centre National d'Etudes Spatiales, Paris, F
CNRS	Centre National de la Recherche Scientifique, Service d'Aéronomie Paris
Col	Co-Investigator of an Experiment/Instrument/Project
COSI	Code for Solar Irradiance – Solar Atmosphere Radiation Transport Code developed at PMOD/WRC
COSPAR	Commission of Space Application and Research of ICSU, Paris, F
CSAR	Cryogenic Solar Absolute Radiometer
CSL	Centre Spatial de Liège
CTM	Chemical Transport Model
CUCF	Central UV Calibration Facility, NOAA, Boulder, USA
DARA	Digital Absolute Radiometer
DIARAD	Dual Irradiance Absolute Radiometer of IRMB
DLR	Deutsche Luft und Raumfahrt
ESA	European Space Agency
ESF	European Science Foundation
ESTEC	European Space Research and Technology Center, Noordwijk, NL
ETH	Eidgenössische Technische Hochschule (Z: Zürich, L: Lausanne)
EUI	Extrem Ultraviolet Imager, Experiment on Solar Orbiter, to be launched 2017
EURECA	European Retrievable Carrier, flown August 1992–June 1993 with SOVA Experiment of PMOD/WRC
EUSAAR	FP6 project: European Supersites for Atmospheric Aerosol Research
EUV	Extreme Ultraviolet Radiation
EUVC	European Ultraviolet Calibration Center at PMOD/WRC
FMI	Finnish Meteorological Institute
FP7	European Framework Program of the European Commission
FRC-III	Third Filter Radiometer Comparison
FSI	Full Sun Imager
GAW	Global Atmosphere Watch, an Observational Program of WMO
GAWTEX	GAW Training & Education Center
GCM	General Circulation Model
GHG	Greenhouse Gases
GOLF	Global Oscillations at Low Frequencies, Experiment on SOHO
GSFC	Goddard Space Flight Center, Greenbelt, MD, USA
HRI	High Resolution Imagers
IACETH	Institute for Climate Research of the ETHZ
IAMAS	International Association of Meteorology and Atmospheric Sciences of IUGG
IAPS	Intensified Active Pixel Sensor
IAS	Institut d'Astrophysique Spatiale
IAU	International Astronomical Union of ICSU, Paris, F
ICSU	International Council of Scientific Unions, Paris, F
IO	Institut d'Optique
IPC	International Pyrheliometer Comparisons
IR	Infrared
IRC	International Radiation Commission, Commission of IAMAS
IRIS	Infrared Integrating Sphere Radiometer
IRMB	Institut Royal Météorologique de Belgique, Brussel, B
IRS	International Radiation Symposium of the Radiation Commission of IAMAS
IRSOL	Istituto Ricerche Solari Locarno
ISO/IEC	International Organisation for Standardization/International Electrotechnical Commission
ISS	International Space Station
IUGG	International Union of Geodesy and Geophysics of ISCU
JRC	Joint Research Center of the European Commission in Ispra, I
KIS	Kiepenheuer-Institut für Sonnenphysik, Freiburg i.Br., D
LATMOS	Laboratoire Atmosphères, Milieux, Observations Spatiales, French research institution
LVPS	Low Voltage Power Supply
LYRA	Lyman-alpha Radiometer, Experiment on PROBA 2, built by PMOD/WRC
METAS	Federal Office of Metrology

MGO	Main Geophysical Observatory, St. Petersburg, RUS
MITRA	Monitor to Determine the Integrated Transmittance
MPS	Max Planck Institute for Solar System Research
MSSL	UCL Mullard Space Science Laboratory
NASA	National Aeronautics and Space Administration, Washington DC, USA
NEWRAD	New Developments and Applications in Optical Radiometry
NILU	Norwegian Institute for Air Research
NIST	National Institute of Standards and Technology, Gaithersburg, MD, USA
NOAA	National Oceanographic and Atmospheric Administration, Washington DC, USA
NPL	National Physical Laboratory, Teddington, UK
NRI	Near Infrared
NRL	Naval Research Laboratory, Washington DC, USA
NREL	National Renewable Energy Lab, Golden, CO, USA
ODS	Ozone Destroying Substances
PFR	Precision Filter Radiometer
PI	Principle Investigator, Leader of an Experiment/Instrument/Project
PICARD	French Space Experiment to Measure the Solar Diameter, launched 2010
PMOD	Physikalisch-Meteorologisches Observatorium Davos
PMO6	PMO6 Type Radiometer
PREMOS	Precision Monitoring of Solar Variability, PMOD/WRC Experiment on PICARD, to be launched 2010
PROBA 2	ESA Technology Demonstration Space Mission, launched 2 December 2009
PRODEX	Program for the Development of Experiments, ESA
PTB	Physikalisch-Technische Bundesanstalt, Braunschweig & Berlin, D
RBCC-E	Regional Brewer Calibration Center for Europe, Izaña Observatory
ROB	Royal Observatory of Belgium
QASUME	Quality Assurance of Spectral Ultraviolet Measurements in Europe
QMS	Quality Management System
RA	Regional Association of WMO
RMO	Regional Metrology Organisation
ROB	Royal Observatory of Belgium
SCNAT	Swiss Academy of Sciences
SCOPE5	Scientific Collaboration between Eastern Europe and Switzerland, Grant of the SNSF
SLF	Schnee und Lawinenforschungsinstitut, Davos
SFI	Schweiz. Forschungsinstitut für Hochgebirgsklima und Medizin, Davos
SI	International System of Units
SIAF	Schweiz. Institut für Allergie- und Asthma-Forschung, Davos
SMHI	Swedish Meteorological and Hydrological Institute
SNSF	Swiss National Science Foundation
SOCOL	Combined GCM and CTM Computer Model, developed at PMOD/WRC
SOHO	Solar and Heliospheric Observatory, Space Mission of ESA/NASA
SOLAR	Experiment Platform on the ISS
SORCE	Space Mission of NASA
SOTERIA	Solar-Terrestrial Investigations and Archives
SOVA	Solar Variability Experiment on EURECA
SOVIM	Solar Variability and Irradiance Monitoring, PMOD/WRC Experiment on the International Space Station Alpha, 2008
SPICE	Spectral Imaging of the Coronal Environment, Experiment on Solar Orbiter, to be launched 2017
STEP	Solar Terrestrial Energy Program of SCOSTEP/ICSU
SuMo	Sun Monitor
SUSIM	Solar Ultraviolet Spectral Irradiance Monitor on Board UARS
TSI	Total Solar Irradiance
TVLS	Toroidal Variable-Line-Space
UARS	Upper Atmosphere Research Satellite of NASA
UCL	University College London
UV	Ultraviolet
UVA	UV Radiation in the Range of 315–400nm
UVB	UV Radiation in the Range of 280–315nm
VIRGO	Variability of Solar Irradiance and Gravity Oscillations, PMOD/WRC Experiment on SOHO, launched December 1995
WCRP	World Climate Research Program
WDCA	World Data Center for Aerosols, Ispra, I
WIGOS	WMO Integrated Global Observing System
WIS	WMO Information System
WISG	World Infrared Standard Group of Pyrgeometer, maintained by WRC
WMO	World Meteorological Organization, a United Nations Specialized Agency, Geneva
WRC	World Radiation Center, Davos
WRC-IRS	Infrared Radiometry Section of WRC
WRC-SRS	Solar Radiometry Section of WRC
WRC-WORCC	World Optical Depth Research and Calibration Center, WRC Section
WRDC	World Radiation Data Center, St. Petersburg, RUS
WRR	World Radiometric Reference
WSG	World Standard Group, realizing the WRR, maintained by WRC
WWW	World Weather Watch, an Observational Program of WMO

Annual Report 2012

Editors: Werner Schmutz and Stephanie Ebert
Publication by PMOD/WRC

Edition: 650, printed 2013

PMOD/WRC, Davos, Switzerland



*Dorfstrasse 33, 7260 Davos Dorf, Switzerland
Phone +41 81 417 51 11, Fax +41 81 417 51 00
www.pmodwrc.ch*